UNIVERSITEIT GENT

FACULTEIT PSYCHOLOGIE EN PEDAGOGISCHE WETENSCHAPPEN

Dynamics and network structure in neuroimaging data

Margarita Papadopoulou

Promotor: Prof. Daniele Marinazzo
Copromotor: Prof. Karl Friston

Proefschrift ingediend tot het behalen van de academische graad van Doctor in de Psychologie

2015

Contents

Abbreviations

A

AMPA	α-amino-3-hydroxy-5-methyl-4-isoxazolepropionic acid

B

BMS	Bayesian Model Selection
BOLD	Blood Oxygen-Level-Dependent

C

CNS	Central Nervous System
CMC	Canonical Microcircuit
CSD	Cross Spectral Density

D

DCM	Dynamic Causal Modelling
DCMs	Dynamic Causal Models
DTF	Directed Transfer Function
dDTF	directed DTF

E

ECD	Equivalent Current Dipole
ECoG	Electrocorticographic
ED	Edge Density
EEG	Electroencephalograph
ERP	Event Related Potential

F

FFT	Fast Fourier Transform
fMRI	functional Magnetic Resonance Imaging

G

GABA gamma-aminobutyric acid

I

ICA Independent Component Analysis

iEEG intracranial Electroencephalography

K

KA Kainic Acid

L

LIF Leaky Integrate-and-Fire

LFP Local Field Potentials

LH Left Hippocampus

M

MRI Magnetic Resonance Imaging

MEG Magneto-Encephalography

MSV Maximum Singular Value

N

NMDA N-methyl-D-aspartate

P

PC Pyramidal Cell

PET Positron emission tomography

PDC Partial Directed Coherence

R

RH Right Hippocampus

RS Reconstructed Sources

S

SEEG	Stereo Electroencephalograph
SNR	Signal-to-Noise Ratio
SVD	Singular Value Decomposition
SSCs	Spiny Stellate Cell
SOZ	Seizure Onset Zone

T

TF	Time Frequency
TE	Transfer Entropy

Acknowledgements

After four years that admittedly passed in the blink of an eye, this PhD comes to an end. I am deeply grateful to have had so many wonderful people supporting me throughout this period of my life.

Daniele, I would like to thank you first. Thank you for trusting me to be your very first PhD student, for challenging me and giving me the opportunity to grow. It was a bumpy road but it was worth it.

Professor Friston, I will always be grateful for the trust you showed me, for your help and guidance, for introducing me to the beautiful DCM world. Thank you for your kindness and generosity. I am honoured to have worked with you.

Professor Lemieux, thank you for always being there to help and hosting me in your lab twice. Working with you has been a great pleasure.

Marco, I still remember the first day at the FIL and how welcoming you were. Thank you for the million of things you taught me and for being such a great colleague and friend.

A special thanks as well to all those nice people who were always eager to help whenever I was flooding them with questions related to their expertise. Pieter, it was great working with you; we did make the best party team in the conferences. Gerald, I was lucky enough to have finally met you even in the last months of this PhD. Chapter 4 of this thesis would not be there without your help. Thank you for your patience and your eagerness to share your knowledge. Umair, thank you for all the nice things you taught me, for letting me be there during the data acquisition and making me actually see the story behind the data I receive for

analysis; thanks for passing on to me your passion for what you do - seeing you work with your patients was a true inspiration. I do hope our scientific roads will cross again. Gregor, thank you for your input in Chapter 5 and for the nice songs we have been exchanging during our breaks.

Professor Vonck, thank you for providing us with data and for always being willing to help.

I would also like to thank my guidance committee and Professor De Soete who greatly contributed to the smooth completion of this PhD thesis.

Colleagues and friends in Ghent, thank you for being there in the good and bad moments that life had in store for me in the past four years.

Roma, thank you for being the one to celebrate good news with me, and share my concerns with when times got tricky.

Han, Sanne and Wouter you were the best office mates I could have wished for. I am grateful for the nice memories, for your continuous support, for treating me in such a unique way. Without you these years would not have been the same. You will be truly missed.

New and older members of the team, Alessandro, Caroline, Elena, Enrico, Frederik, Hannelore thank you each one separately for your support throughout this time.

Guorong, even you are part of the team I would like to say a special thanks to. It is because our arrival in Ghent was synchronous and we thus shared – in what I'll call an amalgamation of English, Greek and Chinese - our ambitions, fears and dreams for the future. You are a great colleague and a precious friend.

Jasmina, I couldn't thank you enough. We walked through this PhD path together from the very beginning and I will certainly never forget how supportive and caring you have been. I'm looking forward to seeing all the nice things we dreamt of coming true!

Celine and Tom, I always felt I had a second family in Belgium. Thank you for being there for me, for supporting me and for taking such a great care of me.

I would also like to thank all the good friends back in Greece and the others spread around the world, who spent hours on Skype talking to me, who visited me in Ghent and who have always been around for the past many years.

To Maggie and Sofia for always believing in me. To Iris, Michalis, Aurelie, Olga, Melin and Maria. To Sofia and Thanos. To my dearest Chrysanthi and Dimitris from the north. To Marie in London, Teresa in Portugal, Lucia in Italy.

I would finally like to thank all my extended family back in Greece. Yorgo, Stella, Lefkothea, Yanni and Charis, beloved aunties Athanasia and Agni, uncle Yorgos. Your love and support is invaluable. My heart bursts each time I think of our reunions.

To my brother, Kyriakos, for his love and for his - sometimes over-exaggerated - concerns.

Dad and mom I am not sure how I can express my gratitude and how blessed I feel to have you. Mum, thank you for the endless Skype calls and your precious advice during this - not always easy -PhD period. Thank you for being able to be so strong with everything, always ready to support us. Dad, you are my hero. Thank you for everything you did for me but especially for what you managed to do the past year, for

being able to fight headfirst and win. You impersonate the human spirit. All nice moments lie ahead of us.

Finally, I would like to thank Asteris with whom I have been sharing my life for the past 10 years. Mor, we made it through the good and thorny parts that a PhD life involves and it's been a fantastic journey. As I have always told you in the past 10 years, the best is yet to come and in the end it always does.

Ghent, June 2015

Preface

In the past decade, concepts and methodologies initially developed for use by information theory and mathematical physics have found high applicability in the modelling and interpreting of neuroimaging data, which are characterized by complex dynamics and rich connectivity. Adopting a network perspective on the relationship between brain anatomy and function can provide fundamental insights into the means by which simple elements are organized into dynamic patterns. Recent studies on functional and structural brain connectivity have revealed that specific properties of complex brain networks support information segregation and integration during high cognitive processes. Alterations of these network properties, encountered during development, aging or neurological disease, have important clinical consequences. Furthermore, investigating the paths and directionality of information flow through the brain permits the inference of a hierarchical organization, such as top-down control and bottom-up modulation, at different scales in the brain. The last decade has witnessed a continuous rise in studies of complex networks and their associated paradigms. Although initial efforts focused on disentangling the intricate topological properties of complex networks, interest has now shifted towards the study of dynamic processes at different temporal and spatial scales, and the co-evolution of network structures with those processes.

One of the biggest challenges to date has been the understanding the non-trivial topological organization of the brain at the structural/anatomical and functional levels. Aside from structural connectivity, which typically corresponds to white matter tracts, several methods have been employed to infer connectivity in the brain. Functional

connectivity is usually inferred on the basis of correlations among neural activity, and defined as statistical dependencies among remote neurophysiological events. Another important family of methods aims to reveal directed information transfer between brain regions (effective connectivity). In recent years, many approaches have been proposed, including structural equation modelling, dynamic causal models (DCMs), Granger Causality or Transfer Entropy. Of course, networks obtained from these measures are intrinsically different, both between themselves and with respect to the structural network. There is furthermore a strong variability between subjects, and the reproducibility of the network structure in time has not been extensively explored. In order to maximize the information regarding brain function that can be extracted from the data, it is important to study in detail both the differences between these networks and their common features**.**

Taking into consideration all the above, the main focus of this thesis was to investigate the modulations of dynamic networks as a tool for understanding brain function. To this end, epilepsy, a chronic neurological disorder that is characterized by recurrent seizures and affects around 1% of the world population, was a convenient benchmark for this work for two main reasons: the network perspective we adopt to study the brain and the modifications to the dynamics of this network. During a seizure there is an abnormal manifestation of neuronal activity in the brain, involving dynamical changes that span across multiple spatiotemporal scales. Understanding these mechanisms will then imply considering a wide range dynamical repertoire. The body of this thesis is structured as follows:

In **Chapter 1**, the reader will be introduced to all the terminology, measures and methods that will be expounded upon in the following chapters.

We start by giving a brief description of human brain components spanning from the most basic (neurons and their physiology) to distinct large cortical regions. We then briefly summarise the most widely used techniques for studying brain activity, with emphasis on electrophysiology and electrophysiological data, which are the sole data collection methods used in the thesis. We continue with a brief description of networks and their attributes, and how these are applied when studying the human brain. Finally, we give a short introduction of the techniques we used in the thesis to infer and model dynamic connectivity in the brain, addressing separately the data driven or model free methods (e.g., directed transfer function) and a model method, namely DCM.

Chapter 2 is divided in two main parts. In the first part, the reader can find a short review on the main functional connectivity methods used in the literature to study information flow on a diseased brain network (epileptic in our case).

The second part comprises our application of both invasive and scalp electroencephalograph (EEG) recordings of a patient with epilepsy. We restrict ourselves to frequency domain measures (e.g., coherence, directed transfer function and partial directed coherence). Computing information transfer between brain regions allows us to explore their dynamic connections. With this in mind, we use the resulting dynamical networks to map the underlying brain activity and possibly to indicate a transition to the ictal phase. Chapter 2 is published as:

M. Papadopoulou, K. Vonck, P. Boon, D. Marinazzo., 2012, “Mapping the epileptic brain with EEG dynamical connectivity: established methods and novel approaches”, European Physics Journal Plus, 127.

In **Chapter 3** we are interested in investigating the modulations of a diseased brain network at the synaptic level, with phenomena varying on a scale of seconds. To achieve this, we have used a biologically informed method (DCM) the basic principles of which are discussed in the introductory Chapter 1. Our main goal is to identify key synaptic parameters or connections that cause observed signals using invasive recordings from three seizures in one patient with epilepsy. We consider a network of two sources covering two regions of interest. Chapter 3 is published as:

M. Papadopoulou, M. Leite, P. Van Mierlo, K. Vonck, L. Lemieux, K.J. Friston, D. Marinazzo, 2015, “Tracking slow modulations in synaptic gain using Dynamic Causal Modelling: validation in epilepsy”, NeuroImage, 107.

In **Chapter 4** we expand the study presented in Chapter 3 by advancing the methodology used. Using DCM we now adopt a Bayesian update scheme, which allows for a clear understanding of how neuronal variables fluctuate over separable timescales. For this study we use local field potentials (LFPs) recorded from 3 rats with induced epileptic seizures. Our main focus is on characterising the pathophysiology of seizure onset (shortly after the lesion) in terms of physiologically plausible variables such as changes in synaptic efficacy and rate constants. Using Bayesian model comparison, we investigate whether the parametric changes were limited to intrinsic connectivity among the neuronal populations (and their time constants), the spectral form of endogenous (afferent) neuronal input, or both.

In **Chapter 5**, we compare directed transfer function (DTF) and effective connectivity measures (DCM) based on (invasive) electrocorticographic (ECoG) activity and reconstructed responses at the same locations based on simultaneous (non-invasive) scalp (EEG) data. These multimodal recordings were obtained from a macaque monkey under three different conditions: resting state, anaesthesia and recovery. Our interest is twofold; we first establish the connectivity architecture between two sources of interest (a frontal and parietal source) and investigate how their coupling changes over different conditions. We then evaluate the consistency of the connectivity results, when analyzing sources recorded from invasive data (128 implanted ECoG sources) and source activity reconstructed from scalp recordings (19 EEG sensors). Chapter 5 is published as:

Papadopoulou, M., Friston, K., Marinazzo, D., 2015, "Estimating directed connectivity from cortical recordings and reconstructed sources", Brain Topograpy, In Press. First online 9 September 2015.

Finally, in **Chapter 6**, we summarize our findings across chapters and discuss implications for future research.

Chapter 1
Introduction

Brain activity: What it's made of and how we measure it

The neuron: General functioning

The brain is one of the most complex and diversified organs of the human body, and is the central organ of the nervous system, located in the head and protected by the skull. The nervous system further includes the spinal cord, which together with the brain forms the central nervous system (CNS) and the ganglia of the peripheral nervous system. Neurons are the core components of the nervous system, its characteristic cells, and they transmit signals throughout the body. Signals are transmitted from a neuron to another via synapses. The human brain comprises an estimated number of 10^{11} neurons interconnected by approximately 10^{14} synapses. The role of neurons spans from sensing external/internal stimuli and processing information to directing muscular action. The general structure of a neuron can be seen in Figure 1. In their general form, each neuron

possesses a soma (cell body), dendrites and an axon. Dendrites are extensions of neurons, short and highly branched and they receive signals and conduct them to the cell body. The soma is where the signals from the dendrites are joined and passed on. The soma does not really have an active role in the transmission of the neural signal but it maintains the cell and keeps the neuron functional. Finally, the axons extend from the cell body to the terminal endings of neurons and conduct signals away from the cell body to other cells.

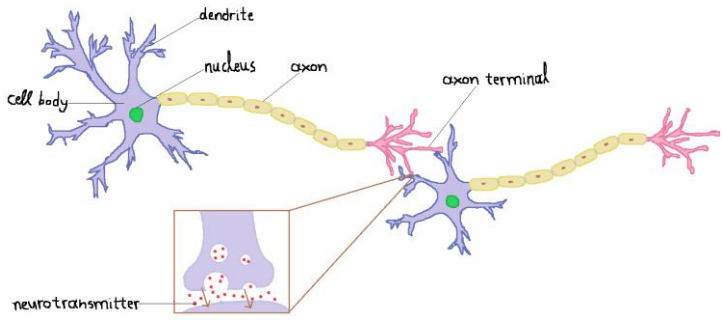

Figure 1. A typical neuron structure with branched dendrites, which receive signals at synapses with several hundred other neurons, and a single long axon that branches laterally and at its terminal. Typically, neurons have a single long axon extending from the cell body to the other end of the neuron. The message then moves through the axon to the other end of the neuron, then to the tips of the axon and then into the space between neurons. From there, the message can move to the next neuron.

Communication between neurons depends upon the properties of neuronal membranes. Neuronal membranes have embedded proteins that form ion channels through which some ions, such as sodium (Na+), chloride (Cl-), potassium (K+) and calcium (Ca2+) can diffuse. In order to maintain the cell membrane potential, cells keep a low concentration of Na+ and high levels of K+. Consequently, neurons at rest show a greater concentration of K+ inside the cell than outside and greater concentration of Na+, Cl-

and Ca2+ outside the cell than inside. This results in a resting potential of approximately -70 mV across the cell membrane. Any transient change in the permeability of the membrane will cause an inflow/outflow of these ions as the system attempts to eliminate the concentration gradient and establish equilibrium. In other words, when a neuron receives a signal, Na+ channels in the membrane are open and allow an influx of positive ions into the cell, which cause a reduction of the difference in charge across the membrane (depolarisation). The localised depolarisation also triggers neighbouring sodium channels to open up and depolarise the membrane nearby. This process can be continued along the axon without weakening, as the signal is continuously reamplified across the way.

At the synapse between two neurons, chemical or electrical conduction is used and synapses can be either excitatory or inhibitory, according to their effect on the afferent neurons. The chemical conduction between the presynaptic axon terminal and the postsynaptic dendrite is based on neurotransmitters such as dopamine, glutamate and gamma-aminobutyric acid (GABA). These neurotransmitters are contained in the axon terminals, and they are released into the synaptic cleft when the neuron has fired. For example, glutamate (the most common neurotrasmitter) opens postsynaptic Na+ channels. The influx of Na+ decreases the electrical potential at a channel's location. This local depolarization is known as an excitatory postsynaptic potential. Alternatively, GABA interacts with receptors to open Cl- and K+ channels. The inflow of Cl- or outflow of K+ results in an increase in the resting potential at a channel's location. This local hyperpolarization is referred to as an inhibitory postsynaptic potential.

Distinction of cortical neurons

Having given a general description of a neuron, it should be noted that several different types of neurons exist, and these can be classified according to their shape, the channel proteins at their synaptic junctions or a characteristic firing pattern (e.g., regular and fast spiking, continuous bursting, etc.). The latter classification reveals three distinct neurons in the neocortex: pyramidal cells (PCs), spiny stellate cell (SSCs) and inhibitory interneurons.

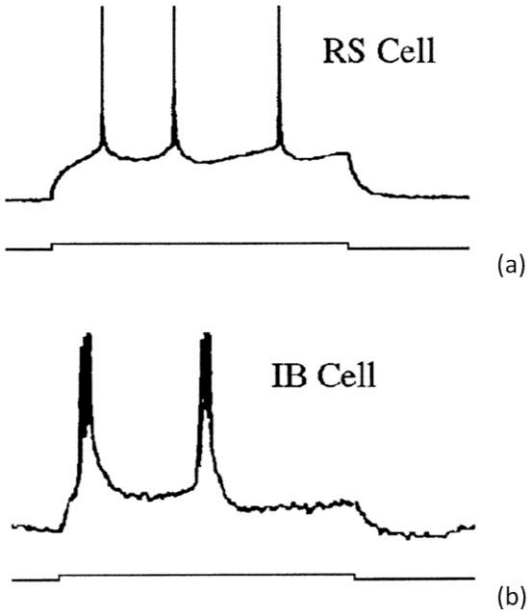

Figure 2. Typical spiking of pyramidal cells in (a) supragranular layers exhibiting regular spiking (b) infragranular layer exhibiting an intrinsic bursting type of signalling.

Pyramidal Cells are projection neurons of the neocortex, sending signals out to other brain areas. They also comprise the largest part of the neocortex's total number of neurons (about 65%). As we will see later, PCs can be found in both

supragranular and infragranular layers, with the difference between the two lying in the signalling type they exhibit under experimental conditions. The cells in supragranular layers exhibit a regular spiking type of behaviour, while cells in infragranular layers show an intrinsic bursting type of signalling (Figure 2).

Spiny stellate cells comprise 20% of the total number of neurons in the neocortex. SSCs are local interneurons found only in layer IV. However their axons project vertically to layer II.

Inhibitory neurons make up the last 15% of the total number of neurons in the neocortex. They are the main constituents of the family of so called interneurons, as their axons and dendrities are limited to a single brain area. This is in contrast to principal cells, which often have axonal projections outside the brain area where their cell bodies and dendrites are located. A general division of the interneurons in these layers is that between local and projection interneurons (Figure 3). The local interneurons differ from projection neurons and from the general model of a neuron described above in that they lack a conductile element, the axon, so that connections with other neurons are made directly by dendro-dendritic or dendro-somatic connections. However these neurons are still a minority of the neocortex, with the majority being neurons containing chemical synapses as described above. This 15% subdivides as follows:

- 7.5% is classified as Class I-GABAergic cells and they can be found in all six neocortex layers. They exhibit a fast spiking behaviour.

- 2.55% is classified as Class II-GABAergic, which are found in layers II-IV. They exhibit a low threshold spiking behaviour.
- 2.55% is classified as Class III inhibitory interneurons and they exhibit an irregular spiking behaviour.
- The remaining 2.4% of inhibitory interneurons do not have a specific classification; however their firing patterns would still possibly fall within one of the three classes mentioned above.

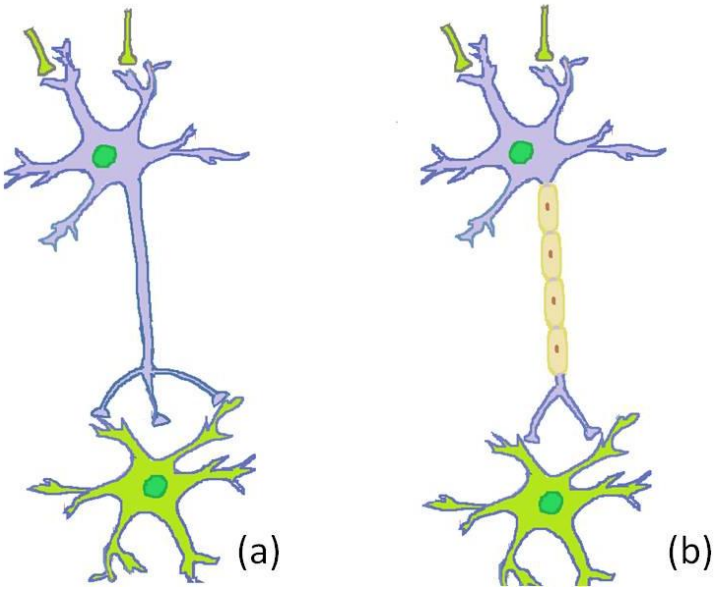

Figure 3. Types of neurons typically found in the neocortex: (a) The structure of a local interneuron, which lacks the conductile element - the axon; (b) Projection interneuron.

Cortical layers

The cerebral cortex consists of convoluted grey and white matter. The grey matter consists mainly of neuron cell bodies and capillaries, whereas the white matter conveys

fibers between the different parts of the cortex and from other parts of the CNS. The evolved cortex in mammals is called neocortex, which is a six layered structured covering more than the 90% of our total cortical area. The remaining 10% is covered by the so-called allocortex, which also includes the hippocampus structure.

Experimental evidence suggests that the neocortex is organised in columns, six-layered laminar structures that provide a higher level of detail. The neurons of different layers are connected vertically to form microcircuits, and neurons in a given column are highly interconnected, both structurally and dynamically. Each column is thought to be responsible for specific signal processing tasks; however, rather than being 'fixed,' these columns tend to be dynamic, with the cortical circuits being able to rewire their lateral connections in response to modulatory signals. So instead of fixed columns we consider groups of cells that are able to dynamically modulate the strength of their interconnections in order to form functional cell assemblies.

A brief description of the six neocortex layers, the type of neurons that each one comprises and their connectivity rules and hierarchies, is given below (see also Figure 4).

- *Layer I*, the molecular layer, is the outermost layer, only contains a few neurons (all inhibitory) and projects mainly to dendrites of neurons from the deeper layers.
- *Layer II*, the external granular cell layer, contains a mix of small pyramidal cells and some inhibitory neurons.
- *Layer III* contains almost all cell types that can be found in the neocortex except the excitatory spiny stellate cells, and cells found exclusively in layer I.

- Layers I-III are called *supragranular* layers are the primary origin and termination of intracortical connections
- *Layer IV* contains small excitatory cells called spiny stellate cells, found exclusively in this layer. It also contains a variety of inhibitory cells. It is suggested that layer IV is the main layer that receives input signals coming into the neocortex from the thalamus. Typically the neurons in layer IV are strongly intercoupled. Layer IV is also called *granular* layer.
- *Layer V* comprises large pyramidal cells and a smaller population of inhibitory cells.
- *Layer VI* is a multiform layer containing various neurons and blends gradually into the white matter. Layer VI comprises mainly large pyramidal cells that project their axons back to the thalamus and also a class of inhibitory neurons called Martinotti cells whose axonal outputs make long projections across all layers of the neocortex. The next second target of thalamic inputs to the neocortex (after layer IV) is layer VI.
- Layers V & VI are called *infragranular* layers, also known to connect the cerebral cortex with subcortical regions.

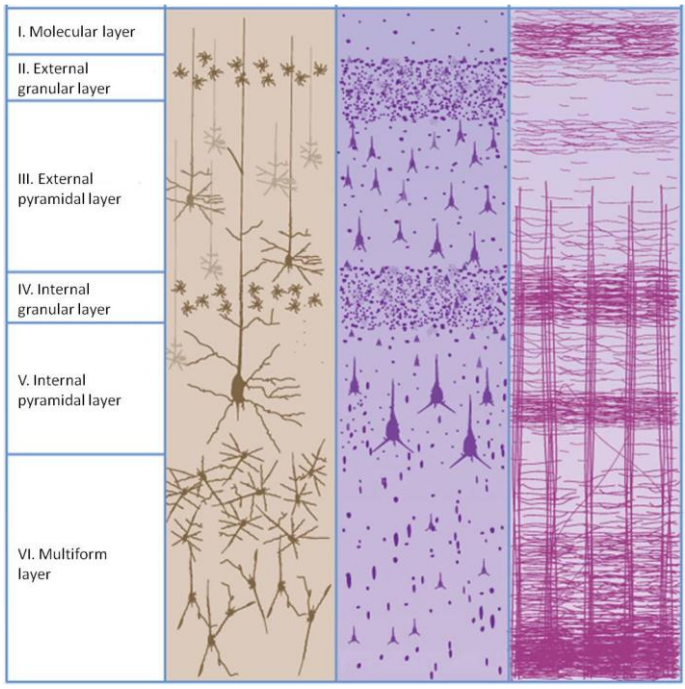

Figure 4. The six distinct layers of the cerebral cortex (image modified from (Berne et al. 2008)).

Macrostructure of the brain

Overall, the structure of the human brain does not differ much from that of other mammals. It comprises many specialized areas which collaborate: the *cortex* is the outermost layer of brain cells, the *brain stem* is between the spinal cord and the rest of the brain, and the *cerebellum* is at the base and the back of the brain.

The cerebral cortex is divided in macroregions known as lobes, each of them connected to different functions varying from reasoning to auditory perception (Figure 5). The *frontal lobe* is the most anterior, and some of the functions associated with it include conscious thought, reasoning and motor skills. The *parietal lobe*, located in the middle section of the brain, is associated mostly with integrating sensory

information from various senses. The *temporal lobe*, located at the bottom section of the brain, contains the primary auditory cortex and is associated with sound interpretation. This lobe is also associated with our memories as the hippocampus, a structure responsible for forming memories, is contained within. Finally, the *occipital lobe* is located at the back portion of the brain and it contains the brain's visual processing system, so it is mainly associated with interpreting visual stimuli and information.

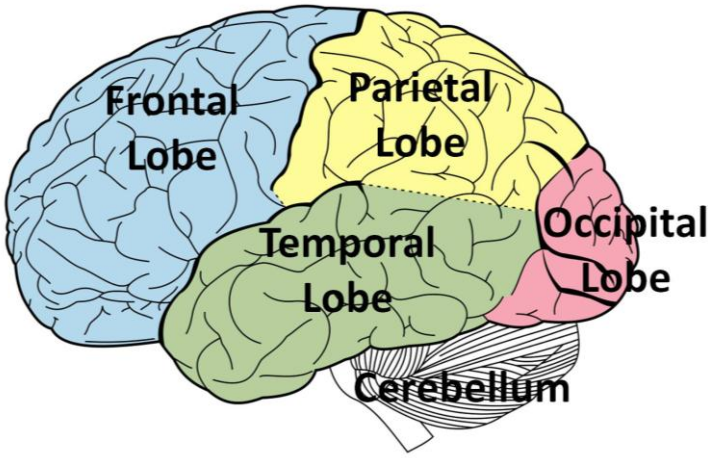

Figure 5. The 4 brain lobes (frontal, temporal, parietal and occipital).

Functional specialisation, integration, hierarchical structure and connectivity

Given the above, we conclude that the human brain seems to follow two principles of functional organisation, namely functional specialisation and functional integration (Friston, 2002). Undoubtedly, the functional role of each brain component, ranging from single neurons to large cortical areas, is determined by its connections. If some patterns appear continuously in the brain, one might think that their

presence is not random and perhaps should account for rules of connectivity. Functional segregation refers to the existence of these specialised components (e.g., neurons that are grouped together to form distinct cortical areas, or specialized cortical areas interacting with each other in a wide repertoire of tasks and conditions).

But what are the exact connectivity rules that apply to the neocortex layers? In other words, do we know the exact connections within and between the neurons of each layer? Strictly speaking the answer is no, as it is rather impossible to know the exact connections emerging from each neuron at any time. However, after numerous studies on the neocortex, it has been experimentally verified that there are indeed some rules to which cortical organisations adhere.

Several circuit models have been proposed for the cortex of both humans and animals (from macaque monkeys downwards) (White 1989; Felleman & Van Essen 1991; Bastos et al. 2012; Douglas et al. 1989). Even though it's impossible for them to capture the exact connections between any pair of neurons, there are good approximations of how the cortex is organised. We will briefly mention the anatomy and the physiology of these connections, as we will refer to them several times later on in this thesis. The first distinction is between *extrinsic* and *intrinsic* connections. Extrinsic connections couple different cortical areas, whereas intrinsic connections are restricted to a cortical column. The functional role of each of the cortico-cortical connections may differ, and it appears there is some hierarchical organisation that distinguishes *forward* and *backward* connections. This distinction primarily refers to which are the cortical layer of origin and termination for each connection. Forward connections originate from supragranular layers (I-III) and they mainly terminate in layer

IV. Backward connections originate from infragranular layers (V & VI) and terminate mainly in supragranular layers (I-III). Forward connections are thought to be driving, always eliciting a response, while backward connections are thought to modulate responsiveness of lower areas to inputs from higher or lower areas (Büchel & Friston 1997; (Friston 2002). In addition, forward connections mediate the postsynaptic effects with fast GABA and α-amino-3-hydroxy-5-methyl-4-isoxazolepropionic acid (AMPA) receptors, and backward connections with the remarkably slower N-methyl-D-aspartate (NMDA) receptor.

The notion of hierarchical organisation is nicely described in Felleman & Van Essen (1991), where the authors study the visual cortex of a macaque monkey, adopting the organisation found there to establish more general rules which can be then applied to several levels of different cortical areas.

What do we measure?

Techniques to study the brain

Neuroimaging techniques allow the investigation of where and when in the brain specific processes occur. We will briefly discuss the most widely used techniques, outlining the main advantages and disadvantages of each.

Single and multi-unit recordings

Information on the activity of individual neurons has been obtained over the past decades through in vivo single cell recordings on anesthetised or awake animals, or via in vitro recordings on extracted brain slices. This process allows a detailed observation of the electrical currents and potentials generated by the cells, offering at the same time a high

temporal and spatial resolution. Microelectrodes can be carefully placed within or close to the cell membrane, allowing an intracellular or extracellular recording. However, this is a highly invasive method not suitable for human studies. A representative paradigm of single cell recordings is that of (Hubel & Wiesel 1962), who studied the fundamental tuning properties of neurons in the visual cortex. As single-unit recording only provides information at the single-neuron level, an alternative would be a multi-unit recording which records electrophysiological activity from a cluster of cells at the same time.

LFP recordings

Local field potentials are signals recorded from extracellular electrodes that presumably reflect the integration of membrane currents in a local region of cortex.

Positron emission tomography

Positron emission tomography (PET) is based on the detection of positrons from radioactively labelled water injected into the body. Increased blood flow to active areas of the brain is indicated by increased positron detection. PET has a relatively good spatial resolution (5-100mm) but a very poor temporal resolution (30-60s).

Magnetic resonance imaging

In magnetic resonance imaging (MRI), radio waves are used to excite atoms in the brain, which produces magnetic changes that can be detected by a large magnet surrounding the body. MRI produces a very precise 3-D picture; however, it only gives us information on structure, not function.

Functional MRI (fMRI) measures the blood oxygen-level-dependent (BOLD) contrast signal. This is a distortion in the local magnetic field when oxyhaemoglobin is converted to deoxyhaemoglobin when neurons consume oxygen. fMRI has a very good spatial resolution (1mm) but not so good temporal resolution. In addition, the scanning sessions are quite tiring for the participants, and there are of course constraints to the types of tasks that can be used in the scanner.

Magneto-encephalography

Magneto-encephalography (MEG) uses a super-conducting quantum interference device to measure magnetic fields produced by electrical brain activity. MEG has excellent temporal resolution and very good spatial resolution. However, it's quite expensive, extremely sensitive to magnetic fields outside the brain, and requires accurate reconstruction of the activity at the source level.

Electroencephalography

We have already briefly discussed the way in which neuronal activity in the brain induces electric fields that extend to the surface of the head. These electric fields can be measured and give rise to characteristic spatial and temporal patterns that can be ascribed to different physiological and cognitive mechanisms. EEG is one of the most widely-used neuroimaging techniques, as it is able to capture human brain activity patterns noninvasively and with millisecond precision.

The different temporal and spatial resolutions of all the neuroimaging techniques described above can be seen in Figure 6.

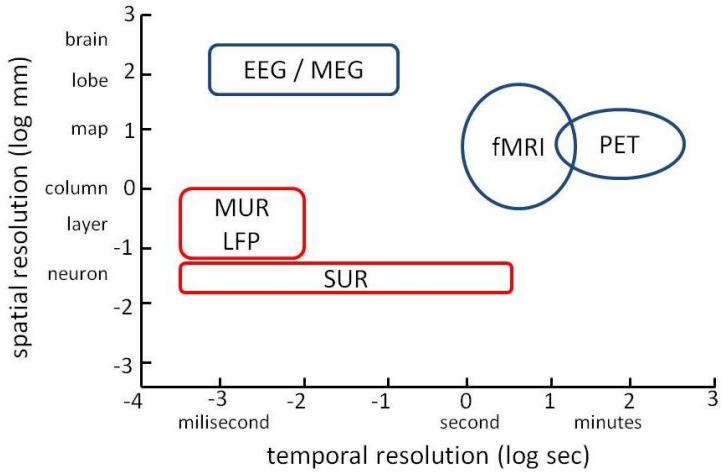

Figure 6. The spatial and temporal resolution of different functional neuroimaging methods.

How do we record EEG signals?

EEG brain activity is recorded using special sensors, called electrodes. Electrodes detect the movement of electrical charges that are a consequence of the activity of the brain cells. EEG can be recorded on the scalp (the common choice in human subjects), or from inside the skull (intracranial EEG).

Scalp EEG

Electrodes are usually placed on the scalp using the international 10-20 system where 10-20 refers to the fact that the differences between adjacent electrodes are either 10% or 20% of the total frontal back or right left distance of the scalp (Figure 7). Each electrode site has a letter to identify the lobe along with a number to identify the hemispheric location. The position of the electrodes is based on four anatomical landmarks, namely the nasion (point

between the forehead and the nose), the inion (lowest point of the skull from the back of the head), and the pre auricular points anterior to the ear. Other than the international 10-20 system, many other electrode systems exist for recording electric potentials on the scalp (e.g., 10-10, 10-5 systems).

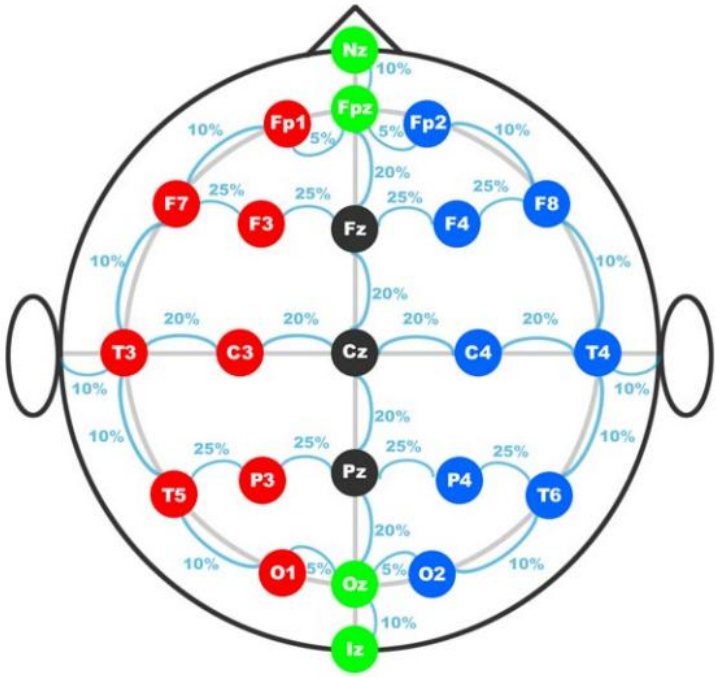

Figure 7. Recording scalp EEG: 10/20 system electrode position and distances (Taken from 10/20 position manual:

http://www.transcranial.com/local/manuals/10_20_pos_man_v1_0_pdf.pdf).

Brain rhythms

Brain activity is recorded over time; we know that brain function arises from neurons firing at different frequencies and with different timing, resulting in oscillating local field potentials. If we want to resolve this rich behaviour in frequency, the signal defined in the time domain can be

transformed into one defined in the frequency domain. This is in general done via Wavelet transform or Fast Fourier Transform (FFT). FFT takes the complex EEG signal and decomposes it into a weighted sum of sine and cosine functions with different frequencies and amplitudes. After the signal is decomposed, one can construct a representation of the relative dominance of various frequencies called a *power spectrum*. Even though this representation does not account for the temporal variation of the EEG signal, it provides a quantitative answer regarding the power relationship between the frequencies that can be very informative (Michel 2009; Tong & Thakor 2009).

Hans Berger, a German psychiatrist and inventor of the EEG, was the first to suggest that brain activity changes in a consistent and recognizable way when the general status of the subject changes (e.g., sleep, wakefulness, etc.) (Tudor et al. 2005). The power spectrum is defined between 0 Hz and half of the sampling frequency. Different pathophysiological and cognitive states result in modulation of the power in different frequency bands. The International Federation of Societies for Electroencephalography and Clinical Neurophysiology in 1974 was the first to make a functionally meaningful taxonomy of brain rhythms, categorising them in five basic groups labelled with Greek letters, as seen below (Buzsaki 2006) (see also Figure 8).

Delta band (0.5-4 Hz)

Delta waves are high amplitude waves usually associated with sleep, also known as slow-wave sleep (SWS).

Theta band (4-8 Hz)

The theta waves are mainly associated with drowsiness and certain sleep stages.

Alpha band (8-12 Hz)

Alpha waves were the first brain waves ever detected by Hans Berger back in 20's (Tudor et al. 2005). They are prominently present in a wakeful relaxation state when eyes are kept closed.

Beta band (12-30 Hz)

Beta waves are associated with conscious alertness, or agitation. This is generally the mental state that most of us have during our waking life.

Gamma band (>30 Hz)

Gamma waves are the fastest brain waves associated with high levels of cognitive functioning.

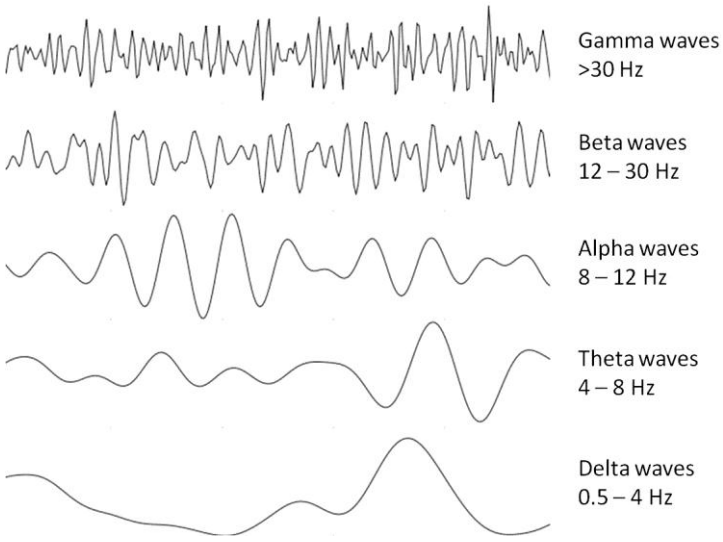

Figure 8. EEG rhythms: example of delta, theta, alpha, beta and gamma activity.

Event related potentials

One of the most popular protocols in EEG research involves event related potentials (ERPs). ERPs are significant voltage fluctuations resulting from evoked neural activity which is initiated by an external or internal stimulus (Michel 2009). They have been widely used to investigate the brain organization of cognitive processes such as perception, memory and language (Hagoort et al. 2004). But how do we actually analyse event related EEG signals? Computationally, the ERP is computed by extracting EEG epochs time-locked to the stimulus presentation, and by calculating the average over the EEG epochs. ERPs in response to specific events (sensory or cognitive) usually consist of a number of peaks and deflections that can be characterised by their morphology, topography and latency (termed ERP components). Despite the fact that ERPs have limited spatial resolution, they have high temporal resolution, providing a continuous measure of the time course of the response.

Pitfalls and obstacles when recording scalp EEG data

Recorded EEG signals are susceptible to artifacts that can be exogenous and/or endogenous. Exogenous artifacts can for example be due to the stimulus presentation (e.g., electrical pain stimulation spikes, electrode/equipment related artifacts) whereas endogenous artifacts can be related to eye movement, sweat potentials, cardiogenic and muscle artifacts (Tong & Thakor 2009). In addition, the difference in conductivity between the tissues attenuates and causes spatial blurring at the scalp. This would not be a problem of course if electrodes could have been placed directly above sources of interest within the brain or in close proximity thereof.

Artifacts in brain signals can be individuated and eliminated using visual inspection or automated or semi-automated methods (Urigüen & Garcia-Zapirain 2015). A powerful approach to address this issue is Independent Component Analysis, according to which the several sources combined into any individual recorded signal can be separated and recognized as either artifact or meaningful brain activity (Bell & Sejnowski 1997; Chaumon et al. 2015).

Invasive EEG recordings

When not responding to drugs, patients with epilepsy undergo an operation in which electrodes are implanted deep into their brain or onto its surface. These are called *intracranial EEG* (iEEG) recordings and they are part of the presurgical evaluation for patients with intractable epilepsy where seizures fail to be controlled by treatment. Provided that the seizure origin in the brain can be localized to one region, the patient can potentially undergo a surgery for its removal.

The electrodes used in iEEG recordings can vary in the shape and in the way are implanted. As we already mentioned, it is possible to implant electrodes into deep structures such as the amygdala and hippocampus. These are typically called depth electrodes.

Alternatively or as a supplement, when a broader coverage of cortical regions is required, Electrocorticographic (ECoG) grids are placed below the dura mater, directly on the cortex. These may include strips containing a single row of electrodes, multiple electrode strips or grids covering the cortical region of interest.

As with scalp EEG recordings, iEEG can be analysed from a variety of perspectives both by analysing their waveforms in

the time domain but also by looking more closely into their spectral properties after applying FFT. The main difference from the scalp data is of course their higher signal-to-noise ratio (SNR).

Animal protocols can be used for fundamental research even without the main clinical application, after approval by an ethics committee.

Montage

In short, EEG measures the difference in voltage displayed over time between two or more electrodes placed on the scalp, and the representation of this difference between EEG channels is referred to as a montage. One can think of the montage as a way of reformatting the same EEG epoch of interest. One can find different representations of the recorded EEG signals with the most popular being the monopolar, average referential and bipolar montages.

In *monopolar montage,* signals are collected at the active site and compared with a common reference electrode. The common electrode should be in a location where cerebral activity should not be prominently measurable, e.g. earlobes or mastoids.

In the *average referential montage*, the outputs of all recorded signals are summed and averaged, and this averaged signal is then derived from each channel.

Bipolar montage is called the overlapping bipolar derivation of adjacent electrodes in straight lines either longitudinally (anterior to posterior) or transversely (left to right) across the scalp. Bipolar montage acts a spatial filter on the recorded EEG channels by removing potentials with similar amplitudes and phases.

Source reconstruction

In the previous section we saw the superiority of iEEG recordings in comparison to scalp recordings in terms of SNR and activity localization. In the former case we do record in a good proximity from the sources of interest without having, for example, skull bone and cerebrospinal fluid interfere with the signal. However, apart from the high cost of the implantation procedure, iEEG recordings are not suitable for common practice.

The closest we can get to computing the activity values of a source that generated a measured electric potential captured by an EEG electrode recorded on scalp is through EEG source modelling. EEG source modelling involves two specular procedures, called the forward and the inverse problem. The forward problem estimates the scalp potentials given an electrical source distribution, while the inverse problem estimates the source parameters out of the recorded scalp potentials based on the solution of the forward problem.

A network perspective

Networks are occupying our everyday life in different forms and flavours. Some exemplars include a group of friends and colleagues comprising our social network, a group of computers in our lab connected to each other, and a country's road network, with the local roads connecting the little towns and villages and the motorways connecting bigger cities and the neighbouring countries to each other.

Over the past decades there has been an increasing interest across different scientific fields, ranging from biology and physics to social sciences, in studying complex networks

(Sporns 2011). In order to better understand these networks one ought not only investigate the basic components that comprise each one of them but also investigate how these components interact and what are the consequences of these interactions. In fact these interactions result in specific patterns, which are the outcome of structured coupling between the elements of a network. This structured coupling is what we describe as connectivity of a network that (depending on the framework) can reflect synaptic connections, metabolic pathways, social networks, and so forth.

In this thesis we will focus on the human brain, a great example of a complex network where its tiniest components, the neurons, are talking to each other through synapses. An increasing number of studies adopt a network perspective to study different functions of the human brain and interactions between neighbouring or remote regions. This is because nowadays there is a clear understanding that the brain's functioning depends on its network structure and the fact that there is a large amount of data available and powerful computers to analyze them.

The human brain is structured into a large number of functionally specialized but widely distributed regions. As a result of the extensive anatomical studies of the brain's cellular circuits, cytoarchitecture and neural fibers, the brain's structural organization is quite well defined (Sporns 2013). These structural organizations form in turn large scale dynamics of the interacting neurons which can be captured as patterns of functional or effective connectivity based measures (Friston 2011; Sporns 2013).

The investigation of such complex systems from a network perspective, and the quantitative analysis of network's

connectivity, has its roots in the mathematical field of graph theory, and it can be adopted to look both at a macroscopic of connectivity between brain regions, as well as at the microscopic level of connectivity between neurons. By exploiting network approaches and tools to study brain dynamics we can better understand how several components become organised and obey functional and metabolic reasons (Sporns 2011). Furthermore, in order to understand thoroughly how the brain works, we need to investigate its functional and structural connections across all scales, ranging from how cells bind to form a neural ensemble and how these neural ensembles are integrated in functional brain regions to how these regions in turn form systems which link brain and body into a complete organism. Additionally, the architectural features of a network reflect the processes by which it was constructed or developed.

The connections across the different neurons, brain regions or more general interconnected elements of the brain system can be visualized through a mathematical representation called a graph which simply comprises a set of nodes and a set of edges in its simpler form.

A *node* in the brain network can represent a single neuron or a cortical region, and the *edges* can represent anatomical connections or dynamic interactions between the activity recorded at the nodes. Anatomical connections refer to different brain regions that are connected to each other via neural fibers, whereas functional connections refer to temporal correlations between regions that are not necessarily anatomically connected. The nodes in a network that are connected with an edge are called neighbours. Networks can be either *undirected*, where all the edges between the nodes are bidirectional, or *directed,* where edges are directed in one orientation (Figure 9). In addition,

edges and nodes can be binary or associated to a weight. Binary connections can only reveal the existence or nonexistence of a connection, while weighted connections can also reveal the strength of a connection.

The criteria according to which we build the brain network we want to analyze, choosing the appropriate nodes and edges that of the network, are usually influenced by the problem that we want to address, and constrained by anatomical parcellation schemes (i.e. frontal, parietal, temporal and occipital lobes) and measures for determining connectivity. Weights can be described in different ways depending on whether they are used in a structural, functional or effective connectivity context (Kaiser 2011). In structural connectivity, weights can be used to describe the bundle of axons (fibers between brain regions), the degree of myelination or the amount of dye travelling to different regions in tract-tracing studies. In dynamic connectivity, weights usually indicate the degree of statistical dependence between the time series. By setting a threshold, where connections exist only if exceed a certain threshold, weighted networks can be converted to binary ones. Binarized networks are usually easier to interpret as the connections between the nodes taken into consideration are eliminated, however thresholds should be chosen with cautious to ensure that the phenomenon under investigation can be still captured.

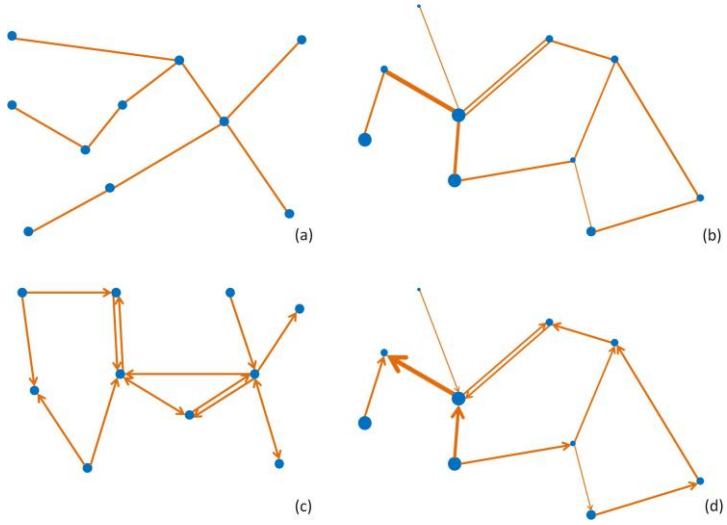

Figure 9. (a) An undirected network where all nodes and edges have the same weight; (b) An un directed network where the edges and nodes have different weights, as indicated by their sizes; (c) same as (a) but now the network is directed; (d) same as (b) but now the network is directed.

When we want to investigate some brain network instead of drawing nodes and edges, we define its topology by the so-called adjacency or connection matrix. The entries of the adjacency matrix depend on whether the edges represent binary or weighted connections. In the former case the adjacency matrix is as (0,1) matrix with 1's reflecting the presence of an edge (connection) between two nodes and 0's the absence of connection. In case of undirected graphs the adjacency matrix is symmetric as the edges of the network are bidirectional where the symmetry is not preserved in the case of directed graphs. An illustration of how a connection matrix can be inferred from a graph in undirected and directed cases can be seen in (Figure 10).

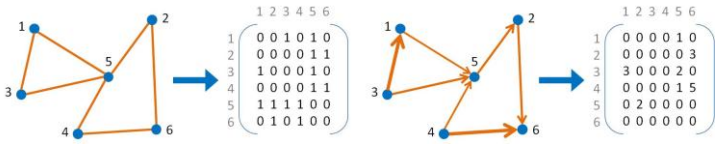

Figure 10. Examples of (a) an undirected network and its mapping on the adjacency matrix; (b) a directed weighted network and its respective mapping on a weight matrix.

One very useful measure that can be derived from the adjacency matrix is the *degree*. For undirected graphs the degree of a node is the number of edges connected to the node.

In directed graphs we distinguish between in-degree and out-degree corresponding to the edges reaching and leaving the node respectively. A node that is receiving more information than sending (more edges arriving than leaving the node) is called *integrator* where one that sends out more information than receiving is called *distributor*. An integrator is influenced by many other nodes while on the contrary the distributor is the one influencing its targeting nodes.

One can also define how 'central' a node is in the network by one more local measure called *betweenness centrality*. It reflects how frequently a node is part of shortest paths where the shortest path between two nodes is defined as the length of the path with the lowest possible number of connections (Figure 11).

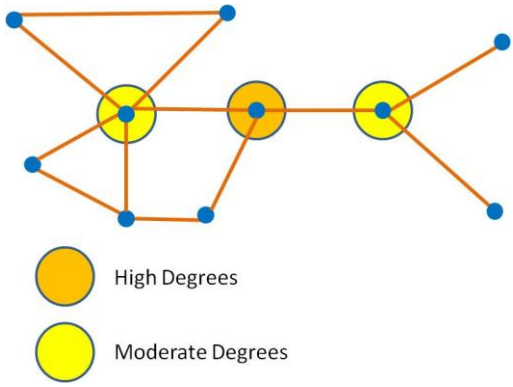

Figure 11. Betweenness centrality: In this example, the node indicated as 'High degrees' has the highest betweenness because it is between entities that are between other entities. These other entities (nodes) have a slightly lower betweenness because they are essentially only between their own cliques. Therefore, even though other neighbouring nodes seem to have a higher degree of centrality, the orange node has more importance within the network.

We now zoom out from the local scale properties and we look at and the global properties of a network. Global properties are important when comparing networks of different brains regions, different layers or cortical columns or even when comparing networks of different species (humans, monkeys). One crucial measure of the global scale is the so called *edge density* also found in the literature as connectivity, which is simple the proportion of the actual (existing) connections (edges) in the network, relative to the maximum possible number of connections between the nodes. From each node of a N-node network, they can be N-1 edges leaving from it so N(N-1) possible edges leaving from all nodes. If the number of existing edges in the network is E then the edge density (ED) will be ED=E/N(N-1) in case of a direct network and ED=E/2N(N-1) in the case of an undirected one. ED is thus a crucial measure to understand how well a network is connected.

In some case there are sets of nodes within a network with larger ED among them than with the rest of nodes within the network. These sets of nodes are called clusters or modules and nowadays there are numerous algorithms developed in different fields able to identify them within a network e.g (Friedman et al. 2015; Khan et al. 2014; Comellas & Miralles 2010; Otte et al. 2015; Palla et al. 2005). These clusters are comprised by tens or hundreds of nodes and are usually linked to a specific function. These densely interconnected regions are responsible for some specialized processing also known as functional segregation. Measures of functional segregation aim to identify these subgroups (clusters) linked to specific brain functions. One of these measures, *clustering coefficient* is defined as the probability that two neighbours of a given node are also neighbours of each other (Figure 12).

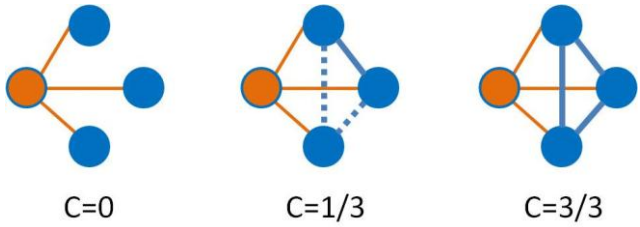

Figure 12. Examples of clustering coefficient for a network of 4 nodes. Solid lines mark a connection between 2 nodes. Dashed lines mark removed links.

Within a network some the clusters might occur in a recurrent fashion and significantly more often than one would expect for a random organization. These are called *network motifs* and can be really useful as they may underlie some particular functional properties of the network.

So far we have introduced some fundamental network measures, but apart from being interested how these measures might differ within or between networks, we are

also interested in defining the different types of networks that might occur and how we classify them. Networks differ from each other having distinct topological and spatial organization.

One of the main classes of networks, termed *random networks*, is constructed by connecting randomly pairs of initially disconnected nodes with a uniform probability (Jeong et al. 2000). In another class, called *regular lattice graphs*, the connections between the nodes are not random but rather follow an ordered pattern. However, both classed follow in a way a homogeneous pattern of connectivity between the nodes, which is not really the case in real world complex networks such as those of the human brain. In the latter case, the influence of each node in the network and its edge density greatly varies. Small worldness is an important phenomenon, rooted in social sciences back in the 50's, which can be seen in such network. The main idea which has been revised by Watts and Strogatz supports that even nodes with each other, the can be reached with a relative short number of steps (Watts & Strogatz 1998).

Segregation and integration place opposite demands on networks:

- Optimal clustering and modularity are inconsistent with high integration (little cross-talk among highly segregated communities)
- Optimal efficiency or integration is only achieved in a fully connected network that lacks any differentiation in its local processing

The bridge between these two opposite requirements is made by heterogeneous contributions by individual nodes

and edges. The small-world configuration optimizes at the same time communication cost and efficiency.

Table 1.

Network modality	Edge representation	Empirical techniques	Network characteristics
Structural connectivity	Physical links (synapses, pathways), biophysical efficacy, time delay	Microscopy: tissue volume reconstruction Neuroanatomy: tract tracing Neuroimaging: diffusion imaging/tractography	Weighted or unweighted, sparse and directed (synapses, projections), sparse and undirected (diffusion MRI)
Functional connectivity	Statistical relationships between neural time courses (e.g. spikes, EEG, BOLD)	Neurophysiology: spike or LFP correlations EEG/MEG: correlation, sync, coherence, phase locking fMRI: BOLD cross-correlations, partial correlations	Full and weighted, or sparse and weighted (or unweighted) after thresholding; undirected
Effective connectivity	Causality inference based on temporal precedence or on generative model	Spikes, EEG/MEG, fMRI: time series analysis (Granger causality, Transfer entropy) or model inference (dynamic causal modeling)	Full or sparse; weighted or unweighted; directed

Taking into consideration all the above we can understand that each node of a network might play a different role with some nodes being more influential on the network's functionality. These nodes are usually more densely connected to the rest of a network and they can often be referred in the literature as 'hubs'. The same way some edges can be more important than others, carrying a heavier load of information and in case other network's edges damage, they can have a more compensatory role on the distributions of information across the network.

Methods to infer and model dynamic connectivity

From what we discussed in the previous section and from Table 1 one can think of functional segregation and functional integration as analytic approaches to functional

brain architecture;. Functional segregation refers to the anatomical segregation of functionally specialized brain regions, while functional integration refers to the functional interaction between these functionally segregated brain regions (Zeki & Shipp 1988). The functional integration can be studied by functional and effective connectivity. Functional connectivity is defined as the study of temporal correlations between spatially distinct neuro-physiological events (K J Friston et al. 1993). It investigates the statistical dependency between two or more time series by investigating whether the null hypothesis of independence can be rejected. Effective connectivity is defined as the influence one neural system exerts over another (Friston et al. 1993) and is based on different hidden neuronal states generating the measurements (Friston et al. 2013).

Functional connectivity measures

Functional connectivity measures are usually distinguished based roughly on three main characteristics. The first is if they reveal directionality of connections (e.g. a node A sends information to node B but not vice versa) or they just reveal the presence of connections (nodes A and B are connected). The second depends on whether the underlying connections are linear or non-linear and the third one on whether these connections are described in the time or frequency domain.

However, it is beyond the scope of this introduction to give an extensive list of the methods falling in each category but rather to present the most widely established mathematical methods for calculating connectivity that are commonly applied to functional high resolution multichannel neurophysiological signals and more specifically electroencephalographic (EEG).

Correlation coefficient

How can we possibly measure the degree of similarity between two signals?

A traditional linear tool widely used to assess the interdependence between two neurophysiological time series in the time domain is correlation also known as Pearson correlation and is defined as follows:

$$\rho_{xy} = \frac{E[(x_n - \mu_x)(y_n - \mu_y)]}{\sigma_x \sigma_y} = \frac{1}{N} \sum_{n=1}^{N} \frac{(x(n) - \mu_x)(y(n) - \mu_y)}{\sigma_x \sigma_y} \quad (1)$$

where x and y will be in our case two EEG signals, N is the number of samples, $E(x)$ and $E(y)$ the expected values of signals x and y respectively, μ_x and μ_y their mean values and σ_x , σ_y their standard deviations. Correlation coefficients values lie in the interval [-1 1] and the sign of the values indicates the direction of the correlation. In case of a perfect increasing linear correlation the Pearson correlation is value is +1, where in case of a perfect decreasing linear relationship the it is equal to -1 (also known as anticorrelation). All the rest values in the interval (−1 1) indicate the degree of linear dependence between the variables with values with valued being closer to the absolute value of 1 indicating higher degree of correlation.

If now our signals are shifted in time with respect to each other the correlation between them is defined as a function of their time lag τ . This variant measure of correlation is known as *cross-correlation*, is defined as follows:

$$\rho_{xy}(\tau) = \frac{E[(x_n - \mu_x)(y_{n+\tau} - \mu_y)]}{\sigma_x \sigma_y} = \frac{1}{N - \tau} \sum_{n=1}^{N} \frac{(x(n) - \mu_x)(y(n+\tau) - \mu_y)}{\sigma_x \sigma_y} \quad (2)$$

This time lag can be of a great interest to us as it may reflect a causal relationship between the signals (Pereda et al. 2005).

Apart from investigating how two signals of interest are correlated in time, we might want to their linear association in the frequency domain. This transformation of our signals from the time to the frequency domain is possible through the fast Fourier transformation (FFT), which resolves a time waveform into its sinusoidal components. In other words, FFT takes a block of time-domain data and returns the frequency spectrum of the data. The counterpart of cross correlation in the frequency domain is called spectral *coherence* and it is obtained by the FFT of equation (2) resulting in the following equation:

$$C_{xy}(f) = \frac{\left|S_{xy}(f)\right|^2}{S_{xx}(f)S_{yy}(f)} \qquad (3)$$

where S_{xy} is the FFT of the cross-correlation of the two signals, called *cross-spectral density* and S_{xx}, S_{yy} are the FFT of the autocorrelation of signals x and y respectively (simply the cross correlation of the signal with itself) called autospectral or *power density*. The estimated coherence C_{xy} values range between 0 and 1. For a given frequency f_0, $C_{xy}(f_0)=0$ indicates that the activities of the signals in this frequency are linearly independent, whereas a value of $C_{xy}(f_0)=1$ gives the maximum linear correlation for this frequency. While correlation and coherence are measures that mainly focus on the mutual synchrony of the activity of two signals, they are not suited to indicate directed influences between the signals.

Effective connectivity measures

When analysing neurophysiological data, one crucial question arising is whether a drive-response relationship exists between to brain regions. To this end, different measures able distinguish between indirect and direct interrelations between signals have been developed both in the time and in the frequency domain. One can find in the literature many comprehensive reviews summarising a fair number of these methods (Sakkalis 2011; van Mierlo et al. 2014; Pereda et al. 2005).

In this thesis we have been particularly interested to study direct interactions between neuronal signals and we have thoroughly investigated how neuronal systems exert over others. To achieve this, we have used measures that can be divided in two main categories - the data driven and the model based ones.

Data driven measures

The concept of "causality" as directed dynamic influences was first introduced by Wiener (1956) and an early implementation on how causality is inferred from two time series was published by Granger (1969) in the field of econometrics.

Granger stated that if we have two time series **X** and **Y** and the past values of **X** are useful in predicting the current values of **Y** in a sense that it significantly reduces its prediction error, then **X** Granger causes (G-causes) **Y**. In other words, if a signal x G-causes a signal y, then the past values of x should contain information that helps to predict y above and beyond the information contained in past values of y alone. From the above we understand that Granger causality is an asymmetric measure meaning that the G-

causality from x to y is distinct from the one from x to y. This allows us to investigate directed dynamic influences between signals.

Granger causality is defined in an autoregressive (AR) based framework. The reader can find more information on different implementations in chapter 2.

DTF (Kaminski & Blinowska 1991) and partial directed coherence (PDC) (Baccalá & Sameshima 2001) are alternatives to GC causality in the frequency domain whose models have been derived by applying a Fourier transformation to the coefficients of the AR model. Again, one can find more information on how both methods have been derived in chapter 2.

DTF and PDC are similar measures of directed dynamic interaction but they differ in the way they are normalised. DTF is normalised with respect to total outflow of information, PDC with respect to the total inflow. These different normalisations helped us to identify the nodes in our networks that acted as integrators of information and those who acted as distributors.

It is worth noting that all these measures were originally defined for pairwise influences, but they can be easily extended to multivariate systems, in which conditioning to the presence of other variables is in order.

Models of brain activity

So far we have discussed measures that were based on data rather than on models, also known us model free measures. Undoubtedly, neurophysiological data are rich in information in a sense that they can give us -when analysed with any of the methods described- a great insight on how a network of

our interest is organised and how this organisation may change due to different factors.

However, it is important to always keep in mind that human cortex is characterised by complex dynamics at different levels. Thus, the development and use of computational models which account for these dynamics can be very insightful as many times our questions relate to neuronal mechanisms and processes that are not directly observable (Deco et al. 2008). Several models have been developed over the past years modelling at the single neuron level, populations of neurons or even large cortical regions (Deco et al. 2008). Diverse information can emerge when using each one of them: modelling single neurons gives insight on how the basic components of the brain -the neurons- receive and send information; modelling populations of neurons, gives us insight on their interaction at a level of microcolumns and cortical columns, macroscopic models inform us on the whole brain dynamics and interactions between large-scale neural systems.

It is beyond the scope of this thesis to extensively describe the computational models which have been built over the years to model brain dynamics at different levels, but we would rather describe the rationale behind them and introduce the ones which have been used later one in this thesis, the neural mass models. Many of them are nicely reviewed in (Deco et al. 2008).

We discussed before that the functional specialisation of the brain is a consequence of a collective network dynamics. The computational elements of these circuits are neurons (Deco et al. 2008). These spiking neurons receive inputs from other neurons, where this input is then transformed into an output spike train, which comprises the output signal of the neuron.

So it is clear that the output spike patterns that are generated by these neural circuits convey information among neurons. This is the main idea behind the family of models that have been built to reflect dynamics on a microscopic level e.g. leaky integrate-and-fire model (LIF) models.

Another family, the *ensemble density models*, aim to model the dynamics of large populations of neurons rather than a single neuron. Each neuron of these populations is usually accompanied by a set of attributes such as post-synaptic membrane depolarisation (V), capacitive current (I), the time since the last action potential. Each of these attributes introduces a dimension in the phase space of each neuron, which in this case will be 3-dimensional. Each neuron then is uniquely defined by a point in the phase space v={V,I,T} $\in R^3$.The basis of these models rests on the probability density over ensembles of neurons described as $p(v,t)$ (also known as ensemble density) and returning the probability density at each point in the phase space.

A special case of ensemble density models are the *neural mass models,* which we will encounter quite a lot in this thesis. The term neural mass models was first used by Freeman (Freeman 1975) to describe the dynamic behaviour of neural masses at the mesoscopic level (Ramirez 2013). The term neural mass refers to a neural system of about 10^4 neurons and about 10^8 synapses. In neural mass models the ensemble density described before is summarised to a single number. In other words, the full ensemble density is replaced by a mass at a particular point and for this particular point the density dynamics are summarised by the location of this mass (Deco et al. 2008).

Dynamic causal modelling: an overview

Dynamic causal modelling was first introduced for the analysis of fMRI data aiming to infer the causal architecture of coupled or distributed dynamical systems (Friston et al. 2003). It was then extended to accommodate the analysis of M/EEG data using very detailed and realistic models describing the interactions between neural masses. For the scope of this thesis only DCM for EEG will be discussed.

So what does dynamic causal modelling refer to? The five key characteristics of DCM as stated in (Stephan et al. 2010) are the following:

i. DCMs are dynamic in the sense that they use linear or non-linear differential equations to describe hidden neuronal dynamics

ii. DCMs are causal in a sense that they describe how dynamics in one neuronal population affect/cause dynamics in another population and how these interactions are being modulated by either endogenous brain activity or external manipulations

iii. DCMs strive for neurophysiological interpretability

iv. DCMs use a biophysiologically inspired and parametrised forward model able to link the modelled neuronal dynamics to specific features of measured data

v. DCMs are Bayesian in all aspects

DCM for EEG designed to investigate the architecture of underlying neuronal dynamics and to make inferences about key neuronal parameters. One can think of a dynamic input/output system where EEG data are modelled as the response of the system to experimental perturbations (David

et al. 2006; Kiebel et al. 2009). Each input of the system is assumed to be processed by a network of interacting neuronal sources where the dynamics of these neuronal sources are modelled in the DCM framework using a neural convolution and conductance-based models. These sources and their interactions are fully described by a set of first-order differential equations.

This distinction simply refers to the consideration of cortical mesocolumns for the convolution models (Freeman 1975) and the consideration of a single cell's electrophysiological properties for the conductance models (Hodgkin & Huxley 1952). Different flavours of these models have been implemented in DCM, e.g., LFP, ERP (event related potential), MFM (mean-field model), CMC (canonical microcircuit model). The choice of the appropriate neuronal model depends of course on the research questions one wants to ask and on the nature of the data. A detailed review on the neural models implemented within DCM framework, can be found in (Moran et al. 2013).

The neural mass model

The neural mass model used in this thesis belongs to the family of convolution-based models, namely the canonical microcircuit model (CMC). The CMC model is a refinement of the macro- column model introduced by (Jansen & Rit 1995). Each source of the CMC is described in terms of the average post-membrane potentials and mean firing rates of four neuronal subpopulations, deployed in a three-layer structure (granular, infragranular, and supragranular layer). Interestingly, in comparison to Jansen & Rit model which comprises three neuronal subpopulations; spiny stellates in the granular layers, inhibitory interneurons and pyramidal cells in infragranular and supragranular layers, the pyramidal

cell population in the CMC model split into two subpopulations the superficial and the deep pyramidal cells occupying the supragranular and the infragranular layers respectively (Figure 13). These distinct subpopulations of pyramidal cells allow a separation of the neuronal populations that elaborate forward and backward connections in cortical hierarchies and crucially, they may exhibit different spectral outputs. The CMC model is based on the work of (Douglas & Martin 1991) who recorded intracellular potentials from cells in a cat's primary visual cortex during electrical stimulation of its thalamic afferents it so accommodates the neuronal sources of forward and backward connections in cortical hierarchies (Bastos et al. 2012; Moran et al. 2013). Each subpopulation has its own intrinsic dynamics but it also has intrinsic (i.e., within-source) connections with the other subpopulations. In addition each source receives extrinsic inputs that can be either some direct sensory input or input from other sources.

To summarise, in the CMC utilises different types of subpopulations to distinguish between forward and backward connections. For the forward connections superficial pyramidal cells excite stellate cells and deep pyramidal neurons, while the backward connections inhibit superficial pyramidal cells and inhibitory interneurons.

It is the depolarization of pyramidal cell populations we assume it gives rise to observed M/EEG data where these depolarizations are expressed in the sensors through a conventional lead-field where each source corresponds to an equivalent current dipole (ECD) (Kiebel et al. 2009; Kiebel et al. 2008).

The model we just described consists of a temporal and spatial part with the temporal part expressed by the

connectivity between two sources and the spatial part by the spatial parameters such as the lead-field parameters. The complete spatiotemporal model takes then the form of a nonlinear state-space model with hidden (unobserved) neuronal states.

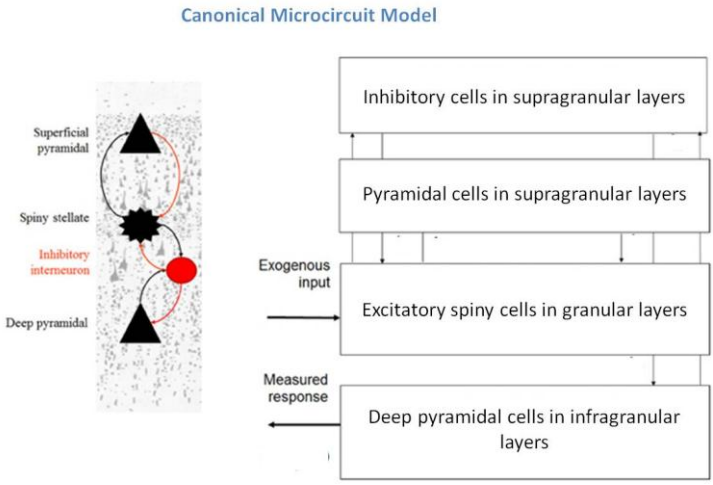

Figure 13. CMC neural mass model of a single source. This model contains four populations occupying different cortical layers: the pyramidal cell population of the Jansen and Rit model is effectively split into two subpopulations allowing a separation of the neuronal populations that elaborate forward and backward connections in cortical hierarchies (Figure adapted from Moran et al., 2013).

If we now invert this model we will be able to estimate conditional densities on the model parameters, which allows us to answer fundamental questions about the underlying system. These parameters can be the biophysical parameters of the neural mass model, synaptic gain parameters etc. As the model inversion is implemented using a Bayesian framework, it provides an approximation to the log model evidence, which is then used to compare alternative DCMs of the same data and compute Bayesian model evidences.

This procedure is called Bayesian model selection (BMS) and allows us to disambiguate between competing models.

DCM applications

One can find in the literature many different applications of DCM such as DCM for mismatch responses, which involves the analysis of multi-channel EEG data acquired under a mismatch negativity paradigm (Garrido et al. 2007; Garrido et al. 2008), DCM for induced responses (Chen et al. 2008), DCM for steady state responses where under stationary assumptions one can analyse the frequency profile e.g. cross-spectral density of data measured over hundreds of milliseconds to minutes (Moran et al. 2009).

In this thesis we will use an extension of DCM for steady state responses, the DCM for cross spectral densities (CSD), which is a generalisation of the former in the complex domain. The CSD is the Fourier transform of the cross-correlation function summarising the activity and statistical dependencies among channels in frequency domain, presenting this way the important information of long time series compactly.

Modulation of brain activity and connectivity

Brain function implies that both activity and connectivity in the brain constantly evolve, reorganize themselves and fluctuate to respond to internal needs or to external stimuli, or as a consequence of an intervention. Intrinsic modulations are due, for example, to mind-wandering, changes of metabolic needs, fluctuations in physiological parameters and aging. They happen over a wide range of temporal and spatial scales. Cognitive modulations involve response to a stimulus, or learning. Pathological modulations are due to dynamic or neurodegenerative diseases, such as epilepsy,

schizophrenia or Alzheimer's disease. Modulations to brain activity and connectivity can also be induced by lesions or reversible interventions, such as Transcranial Magnetic or Direct Current Stimulation.

Epilepsy as a convenient benchmark

Epilepsy is one of the most common neurological disorders, affecting roughly 1% of the population worldwide. It is characterized by recurrent, unprovoked seizures (Fisher et al. 2005) defined as the manifestations of epileptic hypersynchronous activity of neurons in the brain (Blume et al. 2001). During a seizure, a sudden burst of uncontrolled electrical activity occurs within a group of neurons in the cerebral cortex (Valentinuzzi 2007).

We have extensively used data recorded from patients with epilepsy and animals with induced seizures, due in large part to the interesting dynamics occurring at the network level. These dynamics span across multiple spatiotemporal scales; understanding the mechanisms underlying them requires identification of the relations between seizure components within and across these scales, together with the analysis of their dynamic repertoire (Naze et al. 2015).

From our previous discussion of network properties, it is clear that in such an interconnected network as the human brain any dysfunction can easily spread across the linked elements (Fornito et al. 2015). Axonal and synaptic contacts act as conduits leading to pathological cascades that can rapidly affect a large part or even the whole system. A great example is how focal seizures evolve to generalised ones, affecting the whole brain network.

But how exactly does the brain network react to the maladaptive behaviour of some of its elements (e.g.,

subnetworks), and how easily can this behaviour spread, potentially extending to the whole network? In addition one could ask if such a complex and densely interconnected network is able to compensate when one of its subsystems fails to function, and if so how might other subsystems accomplish this? Fornito et al. (2015) nicely summarise the two main classes of neural responses (maladaptive and adaptive) in a diseased network.

By investigating maladaptive responses one can not only localise the pathology but also investigate how it spreads and potentially predict which are the putative areas to be affected next. The main subclasses of maladaptive neural responses are diaschisis, transneuronal degeneration and dedifferentiation, outlined below (see also Figure 14).

Diaschisis occurs when a focal lesion suppresses the function of other remote regions.

Transneuronal degeneration occurs when over time one observes structural deterioration of areas connected to the affected site. As an example, in chapter four of this thesis we have analysed depth recordings of seizures induced in rats. The rats were injected with kainic acid in the right hippocampus, which was lesioned almost immediately after the injection. Although the left hippocampus was initially intact, within a range of days to weeks it was also lesioned.

Dedifferentiation refers to the interaction of the affected regions with the unaffected ones. What is usually observed is a reduced response/function of the neural system comprising the affected region and a diffuse increase of activity to the other unaffected systems connected with the affected one.

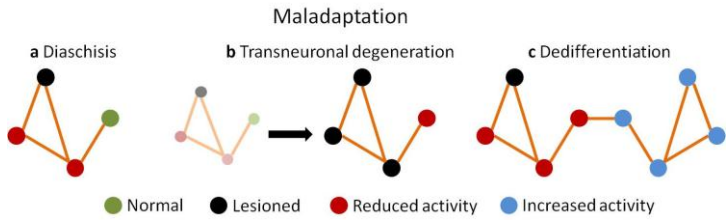

Figure 14. 3 main subclasses of maladaptive neural response. (a) Diaschisis: the lesion node (black) suppresses the function of its connected sites (red nodes); (b) Transneuronal degeneration: Over time the lesioned black node degenerates its connected sites which also become lesioned (black); (c) Dedifferentiation: reduced function of the neural system comprising the affected region and a diffuse increase of activity to the other unaffected systems connected with the affected one (Figure adapted from Fornito et al., 2015).

However, it is also possible that the human brain responds to a neural insult in a more adaptive, compensatory way, trying to preserve its equilibrium state and its performance wherever possible. The three main subclasses of adaptive neural response are compensation, neural reserve and degeneracy (see Figure 15).

Compensation occurs when either the undamaged nodes of the affected network or nodes of other systems increase their activity to compensate for the reduced and maladaptive response of the affected region.

Neural reserve occurs when both the activity and the behavioural performance of the unaffected nodes within the affected system remains the same.

Degeneracy occurs when a second system can take over when the affected one fails to support the function that it was responsible for, without the former having to make any substantial change in its activity. This term reflects neural plasticity.

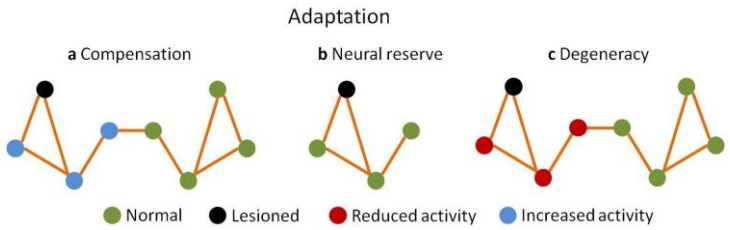

Figure 15. 3 main subclasses of maladaptive neural response (Figure adapted from Fornito et al.2015).

The second chapter of this thesis will put in practice how graph theory and signal processing techniques can be applied to a benchmark example of a dynamical network: the epileptic brain.

References

Baccalá, L.A. & Sameshima, K., 2001. Partial directed coherence: a new concept in neural structure determination. *Biological cybernetics*, 84(6), pp.463–74.

Bastos, A.M. et al., 2012. Canonical Microcircuits for Predictive Coding. *Neuron*, 76(4), pp.695–711.

Bell, A.J. & Sejnowski, T.J., 1997. The "independent components" of natural scenes are edge filters. *Vision research*, 37(23), pp.3327–38.

Berne, R.M., Koeppen, B.M. & Stanton, B.A., 2008. *Berne & Levy Physiology, Page 578*,

Blume, W.T. et al., 2001. Glossary of descriptive terminology for ictal semiology: report of the ILAE task force on classification and terminology. *Epilepsia*, 42(9), pp.1212–8.

Brown, H.R. & Friston, K.J., 2012. Dynamic causal modelling of precision and synaptic gain in visual perception - an EEG study. *NeuroImage*, 63(1), pp.223–31.

Büchel, C. & Friston, K.J., 1997. Modulation of connectivity in visual pathways by attention: cortical interactions evaluated with structural equation modelling and fMRI. *Cerebral cortex (New York, N.Y. : 1991)*, 7(8), pp.768–78.

Buzsaki, G., 2006. *Rhythms of the Brain*,

Chaumon, M., Bishop, D.V.M. & Busch, N.A., 2015. A practical guide to the selection of independent components of the electroencephalogram for artifact correction. *Journal of neuroscience methods*.

Chen, C.C., Kiebel, S.J. & Friston, K.J., 2008. Dynamic causal modelling of induced responses. *NeuroImage*, 41(4), pp.1293–1312.

Comellas, F. & Miralles, A., 2010. A fast and efficient algorithm to identify clusters in networks. *Applied Mathematics and Computation*, 217(5), pp.2007–2014.

David, O. et al., 2006. Dynamic causal modeling of evoked responses in EEG and MEG. *NeuroImage*, 30(4), pp.1255–72.

Deco, G. et al., 2008. The dynamic brain: from spiking neurons to neural masses and cortical fields. *PLoS computational biology*, 4(8), p.e1000092.

Douglas, R.J. & Martin, K.A., 1991. A functional microcircuit for cat visual cortex. *The Journal of physiology*, 440, pp.735–69.

Douglas, R.J., Martin, K.A.C. & Whitteridge, D., 1989. A Canonical Microcircuit for Neocortex. *Neural Computation*, 1(4), pp.480–488.

Felleman, D.J. & Van Essen, D.C., 1991. Distributed hierarchical processing in the primate cerebral cortex. *Cerebral cortex (New York, N.Y. : 1991)*, 1(1), pp.1–47.

Fisher, R.S. et al., 2005. Epileptic seizures and epilepsy: definitions proposed by the International League Against Epilepsy (ILAE) and the International Bureau for Epilepsy (IBE). *Epilepsia*, 46(4), pp.470–2.

Fornito, A., Zalesky, A. & Breakspear, M., 2015. The connectomics of brain disorders. *Nature Reviews Neuroscience*, 16(3), pp.159–172.

Freeman, W.J., 1975. *Mass Action in the Nervous System*, Elsevier.

Friedman, A. et al., 2015. A multistage mathematical approach to automated clustering of high-dimensional noisy data. *Proceedings of the National Academy of Sciences*, 112(14), p.201503940.

Friston, K., 2011. Functional and Effective Connectivity: A Review. *Brain Connectivity*, 1(1), pp.13–36.

Friston, K., 2002. Functional integration and inference in the brain. *Progress in neurobiology*, 68(2), pp.113–43.

Friston, K., Moran, R. & Seth, A.K., 2013. Analysing connectivity with Granger causality and dynamic causal modelling. *Current opinion in neurobiology*, 23(2), pp.172–8.

Friston, K.J. et al., 1993. Functional connectivity: the principal-component analysis of large (PET) data sets. *Journal of cerebral blood flow and metabolism : official journal of the International Society of Cerebral Blood Flow and Metabolism*, 13(1), pp.5–14.

Friston, K.J., Frith, C.D. & Frackowiak, R.S.J., 1993. Time-dependent changes in effective connectivity measured with PET. *Human Brain Mapping*, 1(1), pp.69–79.

Friston, K.J., Harrison, L. & Penny, W., 2003. Dynamic causal modelling. *NeuroImage*, 19(4), pp.1273–302.

Garrido, M.I. et al., 2007. Dynamic causal modelling of evoked potentials: a reproducibility study. *NeuroImage*, 36(3), pp.571–80.

Garrido, M.I. et al., 2008. The functional anatomy of the MMN: a DCM study of the roving paradigm. *NeuroImage*, 42(2), pp.936–44.

Hagoort, P. et al., 2004. Integration of word meaning and world knowledge in language comprehension. *Science (New York, N.Y.)*, 304(5669), pp.438–41.

Hodgkin, A.L. & Huxley, A.F., 1952. A quantitative description of membrane current and its application to conduction and excitation in nerve. *The Journal of physiology*, 117(4), pp.500–44.

Hubel, D.H. & Wiesel, T.N., 1962. Receptive fields, binocular interaction and functional architecture in the cat's visual cortex. *The Journal of physiology*, 160, pp.106–54.

Jansen, B.H. & Rit, V.G., 1995. Electroencephalogram and visual evoked potential generation in a mathematical model of coupled cortical columns. *Biological cybernetics*, 73(4), pp.357–66.

Jeong, H. et al., 2000. The large-scale organization of metabolic networks. *Nature*, 407(6804), pp.651–4.

Kaiser, M., 2011. A tutorial in connectome analysis: topological and spatial features of brain networks. *NeuroImage*, 57(3), pp.892–907.

Kaminski, M.J. & Blinowska, K.J., 1991. A new method of the description of the information flow in the brain structures. *Biological Cybernetics*, 65(3), pp.203–210.

Khan, Y.D. et al., 2014. Iris recognition using image moments and k-means algorithm. *TheScientificWorldJournal*, 2014, p.723595.

Kiebel, S.J. et al., 2009. Dynamic causal modeling for EEG and MEG. *Human brain mapping*, 30(6), pp.1866–76.

Kiebel, S.J. et al., 2008. Dynamic causal modelling for EEG and MEG. *Cognitive neurodynamics*, 2(2), pp.121–36.

Michel, C.M., 2009. *Electrical Neuroimaging*, Cambridge University Press.

Van Mierlo, P. et al., 2014. Functional brain connectivity from EEG in epilepsy: seizure prediction and epileptogenic focus localization. *Progress in neurobiology*, 121, pp.19–35.

Moran, R., Pinotsis, D.A. & Friston, K., 2013. Neural masses and fields in dynamic causal modeling. *Frontiers in computational neuroscience*, 7, p.57.

Moran, R.J. et al., 2009. Dynamic causal models of steady-state responses. *NeuroImage*, 44(3), pp.796–811.

Naze, S., Bernard, C. & Jirsa, V., 2015. Computational modeling of seizure dynamics using coupled neuronal networks: factors shaping epileptiform activity. *PLoS computational biology*, 11(5), p.e1004209.

Otte, W.M. et al., 2015. Aging alterations in whole-brain networks during adulthood mapped with the minimum spanning tree indices: The interplay of density, connectivity cost and life-time trajectory. *NeuroImage*, 109, pp.171–89.

Palla, G. et al., 2005. Uncovering the overlapping community structure of complex networks in nature and society. *Nature*, 435(7043), pp.814–8.

Pereda, E., Quiroga, R.Q. & Bhattacharya, J., 2005. Nonlinear multivariate analysis of neurophysiological signals. *Progress in neurobiology*, 77(1-2), pp.1–37.

Ramirez, J.G., 2013. *A New Foundation for Representation in Cognitive and Brain Science: Category Theory and the Hippocampus*, Springer Science & Business Media.

Sakkalis, V., 2011. Review of advanced techniques for the estimation of brain connectivity measured with EEG/MEG. *Computers in biology and medicine*, 41(12), pp.1110–7.

Sporns, O., 2011. *Networks of the Brain*,

Sporns, O., 2013. Structure and function of complex brain networks. *Dialogues in clinical neuroscience*, 15(3), pp.247–62.

Stephan, K.E. et al., 2010. Ten simple rules for dynamic causal modeling. *NeuroImage*, 49(4), pp.3099–109.

Tong, S. & Thakor, N.V., 2009. *Quantitative EEG Analysis Methods and Clinical Applications*,

Tudor, M., Tudor, L. & Tudor, K.I., 2005. [Hans Berger (1873-1941)--the history of electroencephalography]. *Acta medica Croatica : časopis Hravatske akademije medicinskih znanosti*, 59(4), pp.307–13.

Urigüen, J.A. & Garcia-Zapirain, B., 2015. EEG artifact removal-state-of-the-art and guidelines. *Journal of neural engineering*, 12(3), p.031001.

Valentinuzzi, M.E., 2007. Bioelectrical signal processing in cardiac and neurological applications and electromyography: physiology, engineering, and noninvasive applications. *BioMedical Engineering OnLine*, 6(1), p.27.

Watts, D.J. & Strogatz, S.H., 1998. Collective dynamics of “small-world” networks. *Nature*, 393(6684), pp.440–2.

White, E., 1989. Cortical Circuits - Synaptic Organization of the Cerebral Cortex Structure, | Springer. Available at: http://www.springer.com/gp/book/9781468487237 [Accessed May 7, 2015].

Zeki, S. & Shipp, S., 1988. The functional logic of cortical connections. *Nature*, 335(6188), pp.311–7.

Chapter 2

Mapping the epileptic brain with EEG dynamical connectivity: Established methods and novel approaches

Abstract

Several algorithms rooted in statistical physics, mathematics and machine learning are used to analyze neuroimaging data from patients affected by epilepsy, with the main goals of localizing the brain region where seizure originates from and of detecting upcoming seizure activity in order to trigger therapeutic neurostimulation devices. Some of these methods explore the dynamical connections between brain regions, exploiting the high temporal resolution of the electroencephalographic signals recorded at the scalp or directly from the cortical surface or in deeper brain areas. In this paper we describe this specific class of algorithms and their clinical application, by reviewing the state of the art and reporting their application on EEG data from an epileptic patient.

Introduction

Epilepsy is a common brain disorder with various etiologies, affecting roughly 50 million people worldwide. In many cases epileptic seizures can be controlled by antiepileptic drugs, which are nonetheless ineffective in about one third of the patients (Mormann et al. 2007). For these patients more invasive treatments are available: surgical removal of the epileptogenic region or implantation with a neurostimulation device (Jobst et al. 2010). Advanced techniques for data analysis can be of great help to optimize the success rate of both therapies, by improving epileptologists' interpretation of complex electroencephalogram (EEG) signals and by maximizing the correct and timely detection of an upcoming seizure.

Epilepsy involves recurrent seizures which are characterized by an increase in accumulated energy in specific frequency bands and brain regions. The rapid seizure propagation and its unpredictable nature render the localization of the epileptic focus and the study of its propagation a challenging task. In order to gather information about a physiological system one can measure the temporal evolution of one or more signals which are reflecting its activity. Concerning epilepsy, this has historically been accomplished by the analysis of the EEG recorded from the scalp or from implanted intracranial electrodes (iEEG). The need to quantify the interactions between different brain regions at the same time, when for example large areas of cortex are in synchronous activity, has led to an extensive development and use of multivariate time series techniques. These techniques can be used to detect patterns of interactions between different brain areas and to improve the understanding of the neural information transfer.

Epileptic seizures evolve dynamically thereby modulating local and distributed neuronal networks. Thus, theories and algorithms developed, validated and optimized in the framework of the analysis of dynamic connectivity may provide valuable tools to elucidate the mechanisms underlying epileptic seizures. Therefore, a crucial question to answer is how the epileptiform activity is related to the connectivity of a network of brain regions and how this network topology changes in function of different states (inter-ictal, pre-ictal, ictal) that occur in the epileptic brain.

In this manuscript we describe how the existent connectivity measures are being applied to EEG recordings for epileptic focus localization and seizure detection.

After a review of the state of the art, we will analyze a benchmark dataset with functional and effective connectivity techniques, introducing some novelties that can be useful to shed light on the spatiotemporal dynamic pattern of seizure origination, spreading and fade out.

It is worthy to note that recently connectivity in epilepsy is being studied with both functional magnetic resonance imaging (fMRI) alone (Zhang et al. 2011; Negishi et al. 2011; Pittau et al. 2012; Zhang et al. 2012) or coupled to EEG (Murta et al. 2012).

State of the art

It has always been clear to the eyes of physicists and mathematicians that the key to understanding epilepsy could be found in the analysis of complex systems and their interactions, and that the various states in which we can observe and record the epileptic brain can leave signatures in the chaotic nature of the data (Iasemidis et al. 1990; Pijn

et al. 1991; Lopes da Silva et al. 1994; Lehnertz & Elger 1995) or in their phase space (Martinerie et al. 1998).

Given the fact that brain functioning is a result of the interaction of many complex systems at different scales, it also became clear that insights in the spatiotemporal dynamics of a brain disorder could result from the investigation of how brain regions, near or even distant, are dynamically connected, and that the paths of information transfer throughout the brain can shed light on its functionality and on its breakdown in disease. Indeed, to gain better understanding of which neurophysiological processes are linked to which brain mechanisms, structural connectivity in the brain can be complemented by the investigation of statistical dependencies between brain regions (functional connectivity) or of models aimed to elucidate drive-response relationships (effective connectivity) (Friston 2011)]. As opposed to structural connectivity, where the links between brain regions are established by the presence of anatomical fibers, for dynamical (functional and effective) connectivity we consider every site where brain activity is recorded as a node in a graph, connecting the nodes when information is transferred between them.

Even before these definitions and distinctions became so clear (and fashionable), novel methodologies to evaluate directed and symmetric connections were applied to the epileptic brain with two main purposes: localization of the epileptogenic region in order to maximize the probability of success of a surgical intervention, and early and automated seizure detection both for diagnostic purposes and in order to optimize the efficiency of neural stimulation techniques. Approaches for directed connectivity are mostly employed

for focus localization, whereas symmetrical measures are more used for seizure detection and prediction.

Focus localization

From the point of view of information theory, the epileptogenic region is considered to act as a synchronizing source, namely that part of the brain that initiates a transfer of information to other parts of the brain. Considering the recording sites as nodes of a graph, its localization is thus associated to the individuation of those nodes that, in particular around the onset of the seizure, start to behave abnormally as hubs capable to influence the other nodes. The information content is generally confined to specific frequency bands and that is why methods operating in the frequency domain methods are most commonly used.

In order to detect this behavior, directed connectivity is more informative than its undirected counterpart. As we will discuss more in detail later, directed (effective) connectivity is inferred by looking at how the performance of a predictive model changes when information about the different components of a dynamical system is added or removed from it. Concerning model-based approaches, the Directed Transfer Function (DTF), introduced in (Kamiński & Blinowska 1991) as an extension to the frequency domain of Granger causality (Granger 1969), was used to infer the source and the direction of propagation of mesial and lateral temporal lobe seizures (Franaszczuk & Bergey 1998).

This method has been flanked by other algorithms in view of improving its performance: In (Swiderski et al. 2009) the interpretation of DTF results in order to localize the epileptic focus was improved by single class support vector machine, whereas in (Wilke et al. 2010) the optimal frequency to be investigated by DTF was obtained using wavelets. In order to

track the evolution of connectivity over time, adaptive methods have been developed. An extension of DTF, ADTF, and an investigation of different variations of it, is applied in (van Mierlo et al. 2011). Another time-varying adaptive method, short-time direct DTF (Korzeniewska et al. 2008) is used in (Mullen et al. 2011). This last study proposes a very promising approach that consists of evaluating connectivity between partially-dependent component subspaces of an infomax independent component analysis (ICA) (Bell & Sejnowski 1995) model trained on data from different brain states. The cortical regions are selected using a Bayesian algorithm and then projected back to the cortical surface for visualization. The reason to do this is to eliminate volume-conduction effects and to reduce dimensionality. It would be especially interesting to apply this approach also to scalp data.

Another measure to detect directed connections in the frequency domain, Partial Directed Coherence (PDC), was introduced in (Baccalá & Sameshima 2001). It has been used to identify epileptogenic regions in (Takahashi et al. 2007) and (Varotto et al. 2012). In Methods section we will present the two methods and the differences between them.

Apart from the studies that focus on frequency domain, some studies have explored connectivity in the time domain. A method based on the analysis of the residual covariance matrix of a multichannel autoregressive model was proposed in (Franaszczuk & Bergey 1999). In (Cadotte 2010) Granger causality has been used in an animal model to study information transfer between distant regions of interest, in order to assess abnormal brain activity during a spontaneous seizure onset.

A modification of Granger causality, involving canonical correlation analysis, was applied to both scalp and intracranial recordings, filtered in a specific band of interest, in (Wu et al. 2011). In this case an asymmetry in the connectivity structure was reported, which could reveal the existence of an epileptic focus even in the absence of ongoing seizure activity.

In all the previous studies based on an autoregressive model, the model order has to be chosen according to some criteria. The most popular are Akaike Information Criterion (Akaike 1974) and Bayesian Information Criterion (Schwarz 1978). Other possible choices are the Hannan-Quinn Criterion (Quinn 1980), or a strategy based on machine learning, namely cross-validation (Kohavi 1995).

Together with focus localization, the connectivity approach has been used to validate specific hypotheses on the existence of networks that underlie seizures, following the original idea proposed in (Spencer 2002). In (Ponten et al. 2007) specific graph signatures were associated with different brain states, including epilepsy. In (Kramer et al. 2008) the connectivity matrices obtained by coherence underwent graph theoretical analysis to detect the network architecture associated with seizures.

In (Wendling et al. 2010) the authors hypothesized that the region assumed to generate seizures was a network with variable excitability. Then they considered a simple computational model on two populations in order to quantify functional and effective connectivity measures on them. They first stated that rapid discharges and hyper-excitability between the two populations could be obtained by different model structures such as unidirectional or bidirectional coupling. They also agreed that only nodes with

high levels of excitability were worthwhile to be considered as elements of the fast onset activity. So, when one of the two populations presented hyper-excitability then it was believed to be able to generate a fast activity itself. With an example the authors drew the attention to how connectivity (effective in this case) can be interpreted and how the notion of rapid discharges and propagation should be clarified. So an epileptic network can include nodes that are able to generate a rapid discharge and other ones that are driven from the former one to an altered excitability and to the capability of generating discharges themselves.

In (Terry et al. 2012) the generation of an epileptic seizure out of a network structure was investigated. It was hypothesized that whenever an EEG discharge was present, it was driven by a pattern of brain networks. To support this, a brain network of four regions of interest with some established connections of the same strength were generated. The authors then investigated the differences of varying these connections between the regions of the network versus an introduction of a new brain region in the network, which is characterized by an abnormal activity. In the case of introduction of a region with an abnormal activity, and depending on the connections that they set between each of the regions, there was a rise of focal, primary or secondary generalized seizures. When the connectivity was weakened, an increase in the frequency typical of seizure activity was observed.

Seizure prediction and detection

A connectivity based approach has also proven useful in improving the early detection or prediction of seizures, with respect to considering the complexity of a signal at a certain time. The general motivation behind the first studies in this

sense was that the information gathered studying the complexity of an electroencephalographic time series could be augmented by considering how this complexity is modulated by the interactions with other time series.

In (Lehnertz & Elger 1998) nonlinear time series analysis was used for early prediction of an impending seizure. The basic idea was the timely identification of transitions of the system from lower to higher complexity and from asynchronous to synchronous activity on longer time scales. The EEG recordings from the epileptogenic region of the brain indicated significant changes in nonlinear dynamics up to several minutes prior to the clinical seizure onset as compared to other recording sites.

Sometimes the volume conduction effects could lead to misleading results in several connectivity measures, in particular those relying mostly on the amplitude of the signal; for this reason phase coherence, a method quantifying the symmetrical dependencies between oscillating signals, was successfully applied in (Mormann et al. 2000). In this case this bivariate measure was reported to be more efficient compared to univariate measures in predicting an upcoming seizure. This result is also described and expanded in (Litt & Echauz 2002), and thoroughly validated in (Mormann et al. 2003). In this last study a validation of 30 univariate and bivariate prediction algorithms found in the literature was conducted, starting from the idea that many prediction algorithms lacked in statistical validation as they did not test the specificity of seizure precursors. Bivariate measures showed high statistical performance with a constant baseline, highlighting pre-ictal states even 240 seconds before the seizure onset. Univariate methods were statistically significant on a seizure wise basis, with an adaptive baseline, identifying pre-ictal

changes from 5 to 30 seconds before the seizure. The authors concluded that a combination of univariate and bivariate methods comprising both linear and non-linear approaches provides a promising solution for seizure prediction.

Phase coherence, joint with another synchronization measure, lag synchronization, was also discussed in (Winterhalder et al. 2006), where the issue of the variability between patients was raised. Phase synchronization methods remain among the most successfully applied (Osorio & Lai 2011).

A wavelet-based and frequency specific non-linear similarity index (WNSI) has been applied in (Ouyang et al. 2007) on intracranial recordings to predict epileptic seizures. The fact that the EEG data pattern is not modified by the application of a wavelet transform is considered an advantage of this measure. This characteristic allows investigating the nonlinear dynamics of EEG patterns.

In the same direction as (Mormann et al. 2003), in (Andrzejak et al. 2009) the predictive power of prediction algorithms was tested against well established null hypotheses. They concluded that the time surrogates approach outperforms analytic performance estimates under controlled conditions. This is due to the initial construction of seizure prediction surrogates which is not restricted by specificity, sensitivity or performance definitions while analytic performance estimates are constructed as functions of false positive rates.

In (Kerr et al. 2011) we find another example of exploiting network structure to improve the research on early seizure detection. This method combines spectral techniques with matrix theory. From multi-site stereo-eeg (SEEG) recordings

in epileptic patients, time windows of the same length were considered and connectivity matrices were built for every second window, in order to describe the time dependent correlation between channels. For each one of those matrices, the Singular Value Decomposition is computed in order to track the dominant structure of each matrix over time. The main target was to detect changes of those matrices in pre-ictal and ictal cases. The first singular vector, which represents the dominant effect of each matrix, was sought in both pre-ictal and ictal cases. Then the inner product of the calculated mean ictal singular vector and the first singular vector were calculated for each time window. The results showed significant differences with higher inner products of the singular vectors throughout the seizure time and the average ictal vector compared to one calculated throughout the pre-ictal period.

This idea was exploited and optimized in (Santaniello et al. 2011), in which the time course of the maximum singular value of the connectivity matrix obtained by spectral coherence underwent a fast detection procedure which minimized the false positives. This approach introduced one of the key ideas applied in the present study.

It is worthy to note that the measure described in (Mormann et al. 2000), and applied with more detail in (Mormann et al. 2003) described a decrease of the connection strength during the seizure, while for example in (Iasemidis et al. 2004) and (Varotto et al. 2012) epilepsy is described as a more organized state with increased coupling strength. This could indeed be related to the difference between coupling measures based on phase and amplitude. A critical discussion of amplitude versus phase coupling in epilepsy is contained in (Chávez et al. 2003).

Information theory

An issue that we find particularly relevant is that all these measures could be interpreted in terms of information transfer, allowing an improved mathematical tractability and a generalized framework. This choice is further justified by the fact that Granger causality and its equivalents in the frequency domain do not measure coupling strength but predictive information transfer.

Palus et al. (Palus et al. 2001) interpreted synchronization as an adjustment in information rate, associating different amounts of exchanged information to the ictal and interictal phase.

The discussion about formulation of DTF in terms of information transfer has been started by Eichler (Eichler 2006), and extended and generalized to PDC in (Takahashi et al. 2010). Barnett et al. (Barnett et al. 2009) have shown that under the assumption of Gaussian distribution of the variables Granger causality is equivalent to Transfer Entropy (TE), a model-free measure of directed connectivity (Schreiber 2000). This result has been used to optimize Granger causality analysis to infer connectivity in high dimensional datasets, as those encountered in epilepsy analysis, in (Marinazzo et al. 2012). Connectivity patterns in the epileptic brain obtained by TE are reported in (Sabesan et al. 2009; Stamoulis & Chang 2011; Stamoulis et al. 2012). It is important at this point to note that there is ample evidence that neural data are not Gaussian distributed (see for example the discussion of this topic in (Lindner et al. 2011)). Even if for neural data the equivalence does not exactly hold (preventing for example to measure GC or PDC in bits), we believe that this unified framework can be beneficial both for the computational/methodological part,

and for the interpretation of the results, keeping in mind that model free methods such as the entropy based ones ensure indeed more general validity.

An illustrative example

In this section we apply coherence, DTF and PDC to a benchmark dataset, starting from the approach employed in (Santaniello et al. 2011) for seizure detection, but also trying to incorporate information on the focus localization, tracking the maximum singular value also on individual rows and columns of the directed connectivity matrices.

We recapitulate the main methods and then present some results.

Methods

Coherence

Coherence is a measure indicating the degree of linear association between two time series in the frequency domain. Given two time series X and Y, coherence is given by:

$$C_f = \frac{(cross\ power\ spectrum(X,Y))^2}{power\ spectrum(X)\ power\ spectrum(Y)} = \frac{|S_{xy}(f)|^2}{S_{xx}(f)S_{yy}(f)} \quad (1)$$

Coherence has been extensively used to detect and quantify the interaction of two time series in the frequency band. However, coherence does not allow inferring directionality of the information transfer and is largely influenced by amplitude effects.

Granger causality

The introduction of directed connectivity measures such as Granger Causality (GC) (Granger 1969) in the time domain and its analogues in the frequency domain, Directed Transfer Function (DTF) (Kamiński & Blinowska 1991) and Partial Directed Coherence (PDC) (Baccalá & Sameshima 2001) represented a great improvement in defining the direction of the influences among time series, and are increasingly being applied to neuroscience.

GC was initially introduced in the field of econometrics. Its key idea lies in the improvement of the performance of a predictive model of a time series given some of its past values when information from the past of another time series is incorporated in it. The original model was a bivariate autoregressive model given by:

$$X = \sum_{j=1}^{p} A_{11}(j)X(t-j) + \sum_{j=1}^{p} A_{12}(j)Y(t-j) + e_1(t) \qquad (2)$$

$$Y = \sum_{j=1}^{p} A_{21}(j)X(t-j) + \sum_{j=1}^{p} A_{22}(j)Y(t-j) + e_2(t) \qquad (3)$$

with A_{ik} being the model parameters and e_i the white noise where $i,k = 1,2$.

Granger causality quickly became a standard tool for inferring directed relationships between time series. However, in its original formulation as a bivariate measure it can lead to erroneous results and false positives especially when the channels are fed from common signal sources. The first approach in the literature for applying Granger causality in a multivariate case was, proposed by Geweke (Geweke 1982).

Moreover, the increasing need in analysis of biomedical series, which display evident signatures in rhythms at a given frequency, together with the fact that the use of GC on filtered signals is questionable (Florin et al. 2010; Barnett & Seth 2011) renders the use of equivalent measures in the frequency domain indispensable.

Directed transfer function

The Directed transfer function was formulated in the framework of an autoregressive model (AR) in the frequency domain. It is developed as a measure able to study the interrelation between two signals in relation to all other signals. The AR model is characterized by:

$$\sum_{j=0}^{p} \hat{A}_j x_{t-j} = e_t \qquad (4)$$

where $x_t = (x_{1,t}, x_{2,t}, \ldots x_{k,t})$ is a vector of a k channel process, $e_t = (e_{1,t}, e_{2,t}, \ldots, e_{k,t})$ is a vector of multivariate uncorrelated white noise process, and $\hat{A}_1$, $\hat{A}_2$, … , $\hat{A}_p$ are the *k x k* matrices of model coefficients. Multiplying both sides of (4) by x_{t-s}^T and taking expectation values, gives the coefficients $\hat{A}_1$. This leads to the following equation:

$$\hat{R}(-s) + \hat{A}_1 \hat{R}(1-s) + \ldots + \hat{A}_p \hat{R}(p-s) = 0 \qquad (5)$$

where $\hat{R}(s) = E\left[x_t, x_{t+s}^T \right]$ is the covariance matrix for a lag s.

In order to investigate the spectral properties between the signals, Fourier transformation is applied to equation (4) where the transform functions are of the form:

$$\hat{X}(z) = \hat{H}(z)\hat{E}(z) \tag{6}$$

with

$$\hat{H}(z) = \left(\sum_{j=0}^{p} \hat{A}_j e^{-i2\pi f \Delta t} \right)^{-1} \tag{7}$$

DTF is usually normalized with respect to incoming influence so after normalization it takes the form:

$$\gamma_{ij}^2 = \frac{|H_{ij}(f)|^2}{\sum_{m=1}^{k} |H_{im}(f)|^2} \tag{8}$$

Consequently, the element $H_{ij}(f)$ of the matrix $H(f)$ describes the connection between the j-th input and the i-th output of the system (transmission from channel $j \rightarrow i$). When normalization is applied DTF takes values in the interval [0, 1] where a high value indicates a consistent information transfer in the direction $j \rightarrow i$ and a low value indicates little or no transfer. In the literature different strategies for normalization of DTF (or no normalization at all) are proposed depending on whether the main interest is in the direction rather than in the ratio of influences (Korzeniewska et al. 2003; Kamiński 2005; Eichler 2006).

Even though DTF was initially introduced in (Kamiński & Blinowska 1991) as a bivariate measure, there are studies applying it to multivariate systems. In the latter cases the use of DTF can reveal cascade transfers e.g for channels *a, b, c* if $a \rightarrow b \rightarrow c$ and in this case DTF also detects propagation from $a \rightarrow c$. (Korzeniewska et al. 2003) and (Faes & Nollo 2011) propose a modified version of DTF, the directed DTF (dDTF) which was able to detect whether a connection between two nodes is mediated by a third one. The dDTF is a

combination of the partial coherence function and of the original definition of DTF, emphasizing only direct connections.

Partial directed coherence

When we have K simultaneously recorded signals, the information transfer can also be computed directly by the Fourier transform of model coefficients of (4). This leads to the Partial directed coherence (PDC) which is defined within the framework of Granger causality in the frequency domain and is a measure of the interaction of two time series when the effect of the remaining K - 2 time series is removed. It is designed to describe the relationship of multivariate time series based on the decomposition of multivariate coherences computed from multivariate AR models.

PDC from channel *j* to channel *i* is given by:

$$\pi_{ij}(f)^{\Delta} = \frac{\hat{A}_{ij}(f)}{\sqrt{\hat{a}_j^H(f)a_j(f)}} \tag{9}$$

where the superscript H stands for Hermitian transpose and $\hat{A}_{ij}$ is calculated as:

$$\hat{A}_{ij}(f) = \begin{cases} 1 - \sum_{r=1}^{p} \hat{a}_{ij}(r)e^{-i2\pi fr}, i = j \\ -\sum_{r=1}^{p} \hat{a}_{ij}(r)e^{-i2\pi fr}, i \neq j \end{cases} \tag{10}$$

The PDC is normalized with respect to the outgoing influences resulting in:

$$\begin{aligned} &0 \leq |\pi_{ij}(f)|^2 \leq 1 \\ &\sum_{i=1}^{N} |\pi_{ij}(f)|^2 = 1 \end{aligned} \tag{11}$$

The PDC is able to rank the strength of the direct interactions of a channel j to the other channels which are receiving information from j, a fact that renders it a useful tool for the detection of putative information sinks (Blinowska 2011).

Reporting what is clearly explained in (Faes & Nollo 2011), an important difference between DTF and PDC lies in the normalization: DTF is normalized with respect to the structure that receives the signal, while PDC is normalized with respect to the structure that sends out the signal. Summarizing, we can state that DTF measures influence as the amount of information being transferred between two time series through all (direct and indirect) transfer pathways, relative to the total influence on the target; the PDC measures directed predictive information transfer from source to target through the direct transfer pathway only, relative to the total information leaving the source. We note that this dual interpretation highlights advantages and disadvantages of both measures. DTF has a meaningful physical interpretation as it measures predictive information transfer as the amount of signal power transferred from one process to another, but cannot distinguish between direct and indirect influences measured in the frequency domain. Conversely, PDC clearly reflects the underlying interaction structure as it provides a one-to-one representation of direct causality, but is hardly useful as a quantitative measure because its magnitude quantifies the information flow through the inverse spectral matrix elements (which are not easily interpreted in terms of power spectral density).

Connectivity matrix and Singular value decomposition

A connectivity matrix was built from each data segment and for all different measures. From these connectivity matrices the incoming, outgoing and total information from each

node was then extracted. Of course the distinction between incoming and outgoing information is applicable only to directed measures, thus not to coherence.

The computation of inflow and outflow of information from each channel can provide information on which channels can be potential sinks (receiving information from other channels) or sources (sending out information to the other channels) of information.

The rank of the connectivity matrix indicates the number of the linearly independent rows or columns. So, in cases that connections between the channels are strengthened the rank of the matrix drops. In contrast, when connections are weak the rank increases. Thus, tracking the rank of the connectivity matrices helps to detect the transition to a more organized state in brain activity and thus, gathering relevant information on the dynamics of the seizure onset.

Singular Value Decomposition (SVD) is used to define an m x n matrix A as follows: $A = USV^*$, where U is a $m \times m$ unitary matrix whose columns are the eigenvectors of the matrix AA^*, S is a $m \times n$ matrix with non-zero r diagonal entries, with r representing the rank of A and V a $n \times n$ unitary matrix whose columns represent the eigenvectors of the matrix A^*A. (*) in all cases stands for the conjugate transpose.

We can characterize the connectivity structure by looking at the maximum of the singular values contained in the matrix *S (MSV)* as described in (Santaniello et al. 2011). Here we apply this analysis to the coherence, but we extend it also to directed measures (DTF and PDC) with the aim of efficiently mapping functional and effective connectivity both in space and time.

Data

We consider a dataset consisting of scalp and intracranial EEG recordings from a patient with refractory epilepsy containing 5 seizures from Ghent University Hospital. The intracranial electroencephalographic seizures onsets were marked by experienced epileptologists. The dataset contained 27 scalp electrodes, 48 cortical subdural electrodes, divided into a 4 x 8 array (TG 1 − 32) and a 2 x 8 array (SG 1 − 16), and a depth electrode with 12 contacts (RD 1 − 12). Based on the invasive video EEG monitoring the epileptogenic zone was localized within a dyplastic insular lesion on the right side. Following resective surgery the patients is now seizure free for more than 6 months. A scheme with the position of the intracranial electrode is shown in Figure 1. The sampling frequency of the recorded EEG signals is 256Hz. We extracted from the EEG series a segment that starts 120 s before the electroencephalographic seizure onset (pre-ictal) and ends 120 s after the end of the seizure (post-ictal).

Since epileptiform focus activity is concentrated in frequency bands which are patient-specific, we first identified this band in order to concentrate our analysis on it. We did this by applying a general linear model to ictal and interictal data filtered in the different bands to find out where the maximal differences were. For the analyzed dataset the chosen band was the Beta-Gamma band ([12 45]Hz). In order to track the modulation of the connectivity in time we computed the connectivity matrix in time windows of 5 seconds sliding with a step of 1.5 seconds. The connectivity matrices were computed using spectral coherence as well as two directed measures (DTF and PDC, optimized for evaluating outgoing and incoming information respectively). For each matrix we evaluated the maximum singular value. As an innovation

with respect to (Santaniello et al. 2011), we obtained this measure not only for the global matrix, but also for the single rows and columns, representing for each channel the outgoing and incoming information respectively. This allows gather additional information on the spatiotemporal pattern of the seizure.

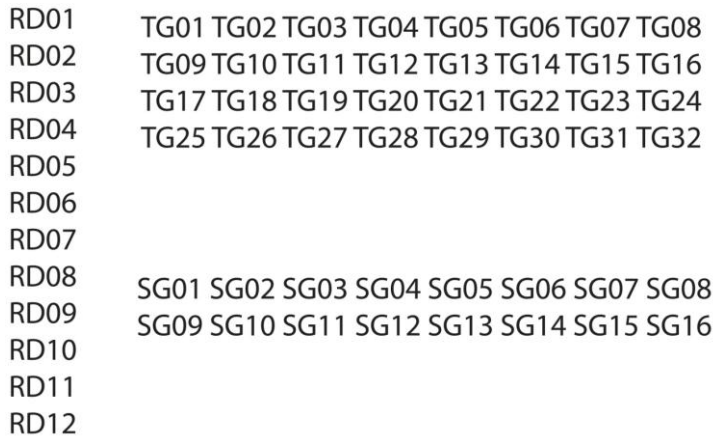

Figure 1. Scheme with the location of the intracranial electrodes. On the left: the depth electrode (RD1 − 12) in the right insular region. On the right upper part: a 32-contact right temporal grid (TG1 – 32), below a 16-contact right frontoparietal grid (SG − 16).

Results

We tracked the maximum singular value described above by observing its evolution over time. In order to evaluate the performance of each one of the measures previously introduced, we computed both the total flow for all the nodes and the inflow and outflow for each one of them.

For the 27 scalp electrodes, coherence captured a drop in the maximum singular value before the time marked as intracranial electroencephalographic onset, followed by a sharp increase. The MSV remained high also after the end of the seizure (Figure 2 top). High values of the maximum

singular value indicate less diversity but stronger components which is in agreement with the concept that during the seizure the brain enters a more organized state. The interpretation of the momentary increase in independence of the nodes resulting in the initial drop in MSV, which could be possibly used for early seizure detection, will require further validation and discussion. For the 60 cortical contacts there is a similar trend compared to the one in the scalp electrodes, with an increased maximum singular value during the electroencephalographic onset. However coherence in case of cortical electrodes proved a bit slower to detect the seizure onset compared to the scalp electrodes, and the MSV returned earlier to baseline values (see Figure 2 bottom for an example).

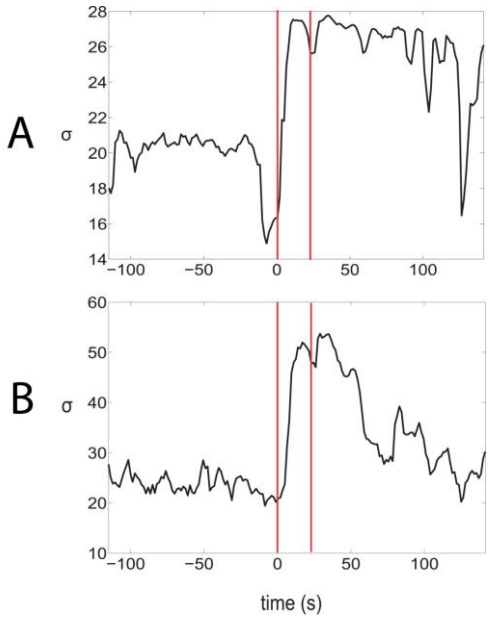

Figure 2. Evolution of the maximum singular value *σ* over time(s). (A): Coherence measured over the 27 scalp electrodes. An increase of *σ* is captured around the intracranial electroencephalographic onset indicating less diversity and more dominant components. (B): Coherence measured over the 60 cortical electrodes. A similar pattern with an earlier increase is observed in the scalp electrodes.

For the outgoing information in the scalp electrodes we observed a decrease in the maximum singular value around the onset and immediate increase after the end of it. The drop in the MSV indicates that the nodes are more independent during the onset while they become more correlated immediately after the end of the seizure.

We observed more variation in the source activity measured by DTF for each cortical node. Indicatively, for some contacts there is a clear drop of the MSV at the electroencephalographic onset (Figure 3, top left), for others a clear drop after the seizure (Figure 3, top right) while for others an increase of the MSV after the end of the seizure (Figure 3, bottom).

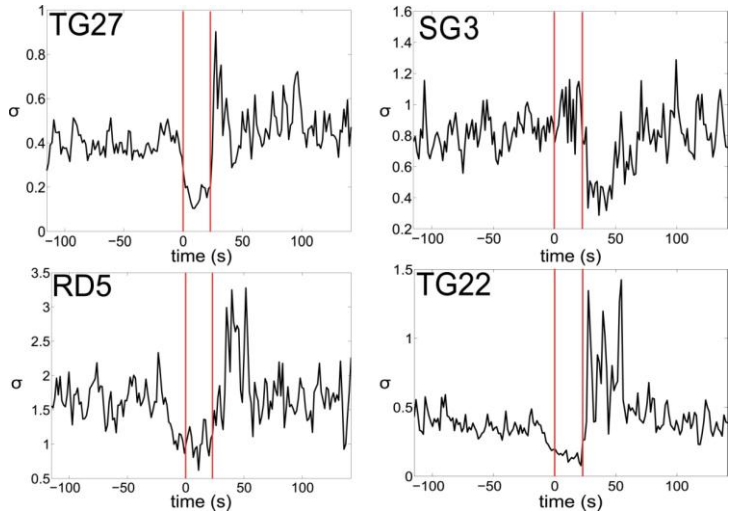

Figure 3. Examples of outgoing information captured by DTF in some cortical contacts for a single seizure (red lines indicate electroencephalographic onset and termination). Some contacts present a clear drop of σ at the electroencephalographic onset, indicating that the components become more random during the seizure (top right), where others present this drop straight after the electroencephalographic onset (top left). In other cases DTF captures a significant rise of σ straight after the end of the electroencephalographic onset (bottom).

As an illustrative example, in Figure 4 we report the scalp map of the percentage variation of MSV for DTF during seizures with respect to baseline.

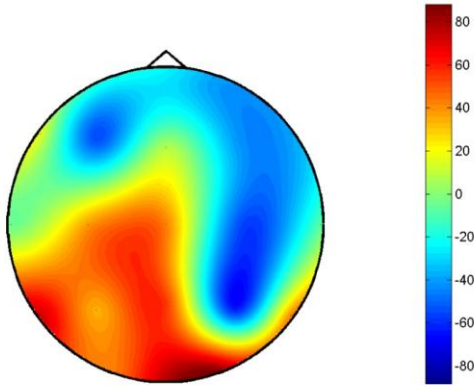

Figure 4. Percentage variation of the MSV for DTF in scalp electrodes, averaged over 5 seizures.

The normalized partial directed coherence is described by the ratio of the outgoing information from a node *j* to a node *i* and the total outgoing information from node *j*. For both scalp and cortical electrodes, PDC calculated sink activity within the interval of the electroencephalographic borders set by the epileptologists. The total incoming information quantified by PDC, shows variability among the 60 cortical contacts. The general trend in the 12 depth contacts is in agreement with results of the total flow, as an increase in the MSV is observed for each one of them (Figure 5, top left). A decrease during the seizure and a raise after it is detected for some of the subdural contacts (Figure 5, top right) while a clear peak and then a drop after the end of the electrographic seizure is indicated in others (Figure 5 bottom).

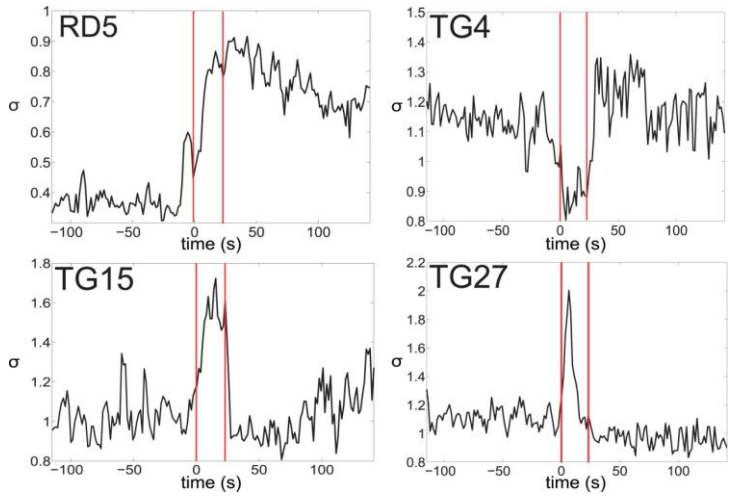

Figure 5. Examples of outgoing information captured by PDC in some cortical contacts for a single seizure (red lines indicate electroencephalographic onset and termination). Some contacts display an increase of *σ* at the electroencephalographic onset indicating more dominant components (top left), where others present lower values during the seizure and a raise immediately after it (top right). For some, high incoming activity is captured at the electroencephalographic onset (bottom).

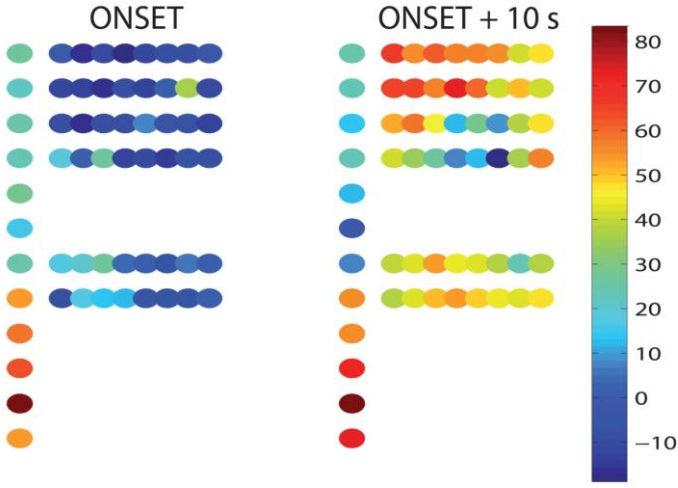

Figure 6. Percentage variation of the MSV for PDC in intracranial electrodes, at the onset of the seizure and 10 seconds after the onset, averaged over 5 seizures. The position of the electrodes reflects the scheme reported in Figure 1.

In Figure 6 we report the map of the percentage variation of MSV for PDC at the onset of the seizure and 10 seconds after with respect to baseline across the intracranial contacts. The maximum percentage variation is reported at one extremity of the depth electrode (RD), confirming the presence of the seizure onset in the deep structures. After 10 seconds we observed an increase also in the cortical electrodes, indicating spreading seizure activity. A similar pattern is observed for the outgoing connections as measured by PDC (Figure 7), but in this case the pattern is more stable during the seizure. We can interpret this difference in view of a recent result (Marinazzo et al. 2012) showing that in a hierarchical network the information going out from each node increases with the number of neighbors while the incoming information stays more or less constant.

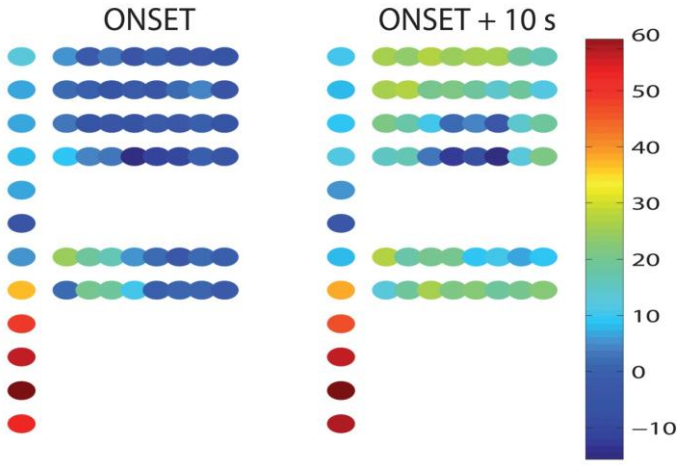

Figure 7. Percentage variation of the MSV for PDC in intracranial electrodes, at the onset of the seizure and 10 seconds after the onset, averaged over 5 seizures. The position of the electrodes reflects the scheme reported in Figure 1.

Moreover, and surprisingly, scalp electrodes are those for which the variation in the connectivity occurs the earliest. Previous studies (Tao et al. 2007) have reported that the

predominance of global synchronization and overall volume conduction induce a great variability of these scalp patterns, but this early modification of the dynamical connectivity could open interesting perspectives for the development of therapeutic measures that may not require invasive recordings and give hints also on the location in space and time of the seizure termination.

Conclusions

We have provided an overview of the methods that explore dynamical connectivity in human EEG recordings to understand the physiological mechanisms underlying epilepsy, and also their application in the detection of the epileptogenic region and prediction of seizure activity. We have shown that, for the analyzed case, some measures that have been previously employed for seizure detection can be also useful for focus localization. Furthermore, the employed algorithms are fast enough to allow for real-time application, thus making them amenable to clinical use. This paper presents preliminary results and its purposes do not reach as far as evaluating their diagnostic value. The point we wish to make is that an integrated spatiotemporal approach, as well as a unified framework such as information theory, may represent an optimal strategy for the future of the analysis of epilepsy from a dynamical network perspective.

References

Akaike, H., 1974. A new look at the statistical model identification. *IEEE Transactions on Automatic Control*, 19(6).

Andrzejak, R.G. et al., 2009. Seizure prediction: any better than chance? *Clinical neurophysiology : official journal of the International Federation of Clinical Neurophysiology*, 120(8), pp.1465–78.

Baccalá, L.A. & Sameshima, K., 2001. Partial directed coherence: a new concept in neural structure determination. *Biological cybernetics*, 84(6), pp.463–74.

Barnett, L., Barrett, A.B. & Seth, A.K., 2009. Granger Causality and Transfer Entropy Are Equivalent for Gaussian Variables. *Physical Review Letters*, 103(23), p.238701.

Barnett, L. & Seth, A.K., 2011. Behaviour of Granger causality under filtering: Theoretical invariance and practical application. *Journal of Neuroscience Methods*, 201(2), pp.404–419.

Bell, A.J. & Sejnowski, T.J., 1995. An information maximization approach to blind separation and blind deconvolution. *Neural Computation*, 7(6), pp.1129–1159.

Blinowska, K., 2011. Review of the methods of determination of directed connectivity from multichannel data. *Med Biol Eng Comput*, 49, pp.521–529.

Cadotte, A. et al., 2010. Granger causality relationships between local field potentials in an animal model of temporal lobe epilepsy. *Journal of Neuroscience Methods*, 189, pp.121–129.

Chávez, M. et al., 2003. Spatio-temporal dynamics prior to neocortical seizures: amplitude versus phase couplings. *IEEE transactions on bio-medical engineering*, 50(5), pp.571–83.

Eichler, M., 2006. On the Evaluation of Information Flow in Multivariate Systems by the Directed Transfer Function. *Biological Cybernetics*, 94(6), pp.469–482.

Faes, L. & Nollo, G., 2011. Assessing directional interactions among multiple physiological time series: the role of instantaneous causality. *Conference proceedings : ... Annual International Conference of the IEEE Engineering in Medicine and Biology Society. IEEE Engineering in Medicine and Biology Society. Conference*, 2011, pp.5919–22.

Florin, E. et al., 2010. The effect of filtering on Granger causality based multivariate causality measures. *NeuroImage*, 50(2), pp.577–588.

Franaszczuk, P.J. & Bergey, G.K., 1999. An autoregressive method for the measurement of synchronization of interictal and ictal EEG signals. *Biological cybernetics*, 81(1), pp.3–9.

Franaszczuk, P.J. & Bergey, G.K., 1998. Application of the directed transfer function method to mesial and lateral onset temporal lobe seizures. *Brain topography*, 11(1), pp.13–21.

Friston, K., 2011. Functional and Effective Connectivity: A Review. *Brain Connectivity*, 1(1), pp.13–36.

Geweke, J., 1982. Measurement of Linear Dependence and Feedback Between Multiple Time Series. *Journal of the American Statistical Association*, 77(378), pp.304–313.

Granger, C.W.J., 1969. Investigating Causal Relations by Econometric Models and Cross-spectral Methods. *Econometrica*, 37(3), p.424.

Iasemidis, L.D. et al., 2004. Dynamical resetting of the human brain at epileptic seizures: application of nonlinear dynamics and global optimization techniques. *IEEE transactions on bio-medical engineering*, 51(3), pp.493–506.

Iasemidis, L.D. et al., 1990. Phase space topography and the Lyapunov exponent of electrocorticograms in partial seizures. *Brain topography*, 2(3), pp.187–201.

Jobst, B.C. et al., 2010. Brain stimulation for the treatment of epilepsy. *Epilepsia*, 51 Suppl 3, pp.88–92.

Kamiński, M., 2005. Determination of transmission patterns in multichannel data. *Philosophical transactions of the Royal Society of London. Series B, Biological sciences*, 360(1457), pp.947–52.

Kamiński, M.J. & Blinowska, K.J., 1991. A new method of the description of the information flow in the brain structures. *Biological cybernetics*, 65(3), pp.203–10.

Kerr, M.S.D. et al., 2011. Multivariate analysis of SEEG signals during seizure. *Conference proceedings : ... Annual International Conference of the IEEE Engineering in Medicine and Biology Society. IEEE Engineering in Medicine and Biology Society. Conference*, 2011, pp.8279–82.

Kohavi, R., 1995. A Study of Cross-Validation and Bootstrap for Accuracy Estimation and Model Selection. In *International Joint Conference on Artificial Intelligence*. pp. 1137–1143.

Korzeniewska, A. et al., 2003. Determination of information flow direction among brain structures by a modified directed transfer function (dDTF) method. *Journal of neuroscience methods*, 125(1-2), pp.195–207.

Korzeniewska, A. et al., 2008. Dynamics of event-related causality in brain electrical activity. *Human Brain Mapping*, 29(10), pp.1170–1192.

Kramer, M. a, Kolaczyk, E.D. & Kirsch, H.E., 2008. Emergent network topology at seizure onset in humans. *Epilepsy research*, 79(2-3), pp.173–86.

Lehnertz, K. & Elger, C., 1998. Can Epileptic Seizures be Predicted? Evidence from Nonlinear Time Series Analysis of Brain Electrical Activity. *Physical Review Letters*, 80(22), pp.5019–5022.

Lehnertz, K. & Elger, C.E., 1995. Spatio-temporal dynamics of the primary epileptogenic area in temporal lobe epilepsy characterized by neuronal complexity loss. *Electroencephalography and clinical neurophysiology*, 95(2), pp.108–17.

Lindner, M. et al., 2011. TRENTOOL: A Matlab open source toolbox to analyse information flow in time series data with transfer entropy. *BMC Neuroscience*, 12(1), p.119.

Litt, B. & Echauz, J., 2002. Prediction of epileptic seizures. *The Lancet Neurology*, 1(1), pp.22–30.

Lopes da Silva, F.H., Pijn, J.P. & Wadman, W.J., 1994. Dynamics of local neuronal networks: control parameters and state bifurcations in epileptogenesis. *Progress in brain research*, 102, pp.359–70.

Marinazzo, D. et al., 2012. Information Flow in Networks and the Law of Diminishing Marginal Returns: Evidence

from Modeling and Human Electroencephalographic Recordings. *PLoS ONE*, 7(9).

Marinazzo, D., Pellicoro, M. & Stramaglia, S., 2012. Causal information approach to partial conditioning in multivariate data sets. *Computational and Mathematical Methods in Medicine*, 2012.

Martinerie, J. et al., 1998. Epileptic seizures can be anticipated by non-linear analysis. *Nature medicine*, 4(10), pp.1173–6.

Van Mierlo, P. et al., 2011. Accurate epileptogenic focus localization through time-variant functional connectivity analysis of intracranial electroencephalographic signals. *NeuroImage*, 56(3), pp.1122–1133.

Mormann, F. et al., 2003. Automated detection of a preseizure state based on a decrease in synchronization in intracranial electroencephalogram recordings from epilepsy patients. *Physical review. E, Statistical, nonlinear, and soft matter physics*, 67(2 Pt 1), p.021912.

Mormann, F. et al., 2000. Mean phase coherence as a measure for phase synchronization and its application to the EEG of epilepsy patients. *Physica D: Nonlinear Phenomena*, 144(3), pp.358–369.

Mormann, F. et al., 2007. Seizure prediction: the long and winding road. *Brain : a journal of neurology*, 130(Pt 2), pp.314–33.

Mullen, T. et al., 2011. Modeling cortical source dynamics and interactions during seizure. *Conference proceedings : ... Annual International Conference of the IEEE Engineering in Medicine and Biology Society. IEEE*

Engineering in Medicine and Biology Society. Conference, 2011, pp.1411–4.

Murta, T. et al., 2012. Dynamic Causal Modelling of epileptic seizure propagation pathways: A combined EEG-fMRI study. *NeuroImage*.

Negishi, M. et al., 2011. Functional MRI connectivity as a predictor of the surgical outcome of epilepsy. *Epilepsia*, 52(9), pp.1733–40.

Osorio, I. & Lai, Y.-C., 2011. A phase-synchronization and random-matrix based approach to multichannel time-series analysis with application to epilepsy. *Chaos (Woodbury, N.Y.)*, 21(3), p.033108.

Ouyang, G. et al., 2007. Application of wavelet-based similarity analysis to epileptic seizures prediction. *Computers in biology and medicine*, 37(4), pp.430–7.

Palus, M. et al., 2001. Synchronization as adjustment of information rates: detection from bivariate time series. *Physical review. E, Statistical, nonlinear, and soft matter physics*, 63(4 Pt 2), p.046211.

Pijn, J.P. et al., 1991. Chaos or noise in EEG signals; dependence on state and brain site. *Electroencephalography and clinical neurophysiology*, 79(5), pp.371–81.

Pittau, F. et al., 2012. Patterns of altered functional connectivity in mesial temporal lobe epilepsy. *Epilepsia*, 53(6), p.no–no.

Ponten, S.C., Bartolomei, F. & Stam, C.J., 2007. Small-world networks and epilepsy: graph theoretical analysis of intracerebrally recorded mesial temporal lobe seizures. *Clinical neurophysiology : official journal of the*

International Federation of Clinical Neurophysiology, 118(4), pp.918–27.

Quinn, B.G., 1980. Order Determination for a Multivariate Autoregression. *Journal of the Royal Statistical Society. Series B (Methodological)*, 42(2), pp.182–185.

Sabesan, S. et al., 2009. Information flow and application to epileptogenic focus localization from intracranial EEG. *IEEE transactions on neural systems and rehabilitation engineering : a publication of the IEEE Engineering in Medicine and Biology Society*, 17(3), pp.244–53.

Santaniello, S. et al., 2011. Quickest detection of drug-resistant seizures: an optimal control approach. *Epilepsy & behavior : E&B*, 22 Suppl 1, pp.S49–60.

Schreiber, T., 2000. Measuring information transfer. *Physical review letters*, 85(2), pp.461–4.

Schwarz, G., 1978. Estimating the Dimension of a Model. *The Annals of Statistics*, 6(2), pp.461–464.

Spencer, S.S., 2002. Neural Networks in Human Epilepsy: Evidence of and Implications for Treatment. *Epilepsia*, 43(3), pp.219–227.

Stamoulis, C. et al., 2012. High-frequency neuronal network modulations encoded in scalp EEG precede the onset of focal seizures. *Epilepsy & behavior : E&B*, 23(4), pp.471–80.

Stamoulis, C. & Chang, B.S., 2011. Multiscale information for network characterization in epilepsy. *Conference proceedings : ... Annual International Conference of the IEEE Engineering in Medicine and Biology Society. IEEE Engineering in Medicine and Biology Society. Conference*, 2011, pp.5908–11.

Swiderski, B. et al., 2009. Single-class SVM and directed transfer function approach to the localization of the region containing epileptic focus. *Neurocomputing*, 72(7-9), pp.1575–1583.

Takahashi, D.Y., Baccal, L.A. & Sameshima, K., 2007. Connectivity Inference between Neural Structures via Partial Directed Coherence. *Journal of Applied Statistics*, 34(10), pp.1259–1273.

Takahashi, D.Y., Baccalá, L.A. & Sameshima, K., 2010. Information theoretic interpretation of frequency domain connectivity measures. *Biological cybernetics*, 103(6), pp.463–9.

Tao, J.X. et al., 2007. The impact of cerebral source area and synchrony on recording scalp electroencephalography ictal patterns. *Epilepsia*, 48(11), pp.2167–2176.

Terry, J.R., Benjamin, O. & Richardson, M.P., 2012. Seizure generation: The role of nodes and networks. *Epilepsia*.

Varotto, G. et al., 2012. Enhanced frontocentral EEG connectivity in photosensitive generalized epilepsies: a partial directed coherence study. *Epilepsia*, 53(2), pp.359–67.

Wendling, F. et al., 2010. From intracerebral EEG signals to brain connectivity: identification of epileptogenic networks in partial epilepsy. *Frontiers in systems neuroscience*, 4, p.154.

Wilke, C. et al., 2010. Neocortical seizure foci localization by means of a directed transfer function method. *Epilepsia*, 51(4), pp.564–72.

Winterhalder, M. et al., 2006. Spatio-temporal patient-individual assessment of synchronization changes for epileptic seizure prediction. *Clinical neurophysiology :*

official journal of the International Federation of Clinical Neurophysiology, 117(11), pp.2399–413.

Wu, G.R. et al., 2011. Multiscale causal connectivity analysis by canonical correlation: theory and application to epileptic brain. *IEEE transactions on bio-medical engineering*, 58(11), pp.3088–96.

Zhang, J. et al., 2012. Pattern Classification of Large-Scale Functional Brain Networks: Identification of Informative Neuroimaging Markers for Epilepsy S. Hayasaka, ed. *PLoS ONE*, 7(5), p.e36733.

Zhang, X. et al., 2011. Social network theory applied to resting-state fMRI connectivity data in the identification of epilepsy networks with iterative feature selection. *Journal of neuroscience methods*, 199(1), pp.129–39.

Chapter 3

Tracking slow modulations in synaptic gain using dynamic causal modelling: Validation in epilepsy

Abstract

In this work we propose a proof of principle that dynamic causal modelling can identify plausible mechanisms at the synaptic level underlying brain state changes over a timescale of seconds. As a benchmark example for validation we used intracranial electroencephalographic signals in a human subject. These data were used to infer the (effective connectivity) architecture of synaptic connections among neural populations assumed to generate seizure activity. Dynamic causal modelling allowed us to quantify empirical changes in spectral activity in terms of a trajectory in parameter space – identifying key synaptic parameters or connections that cause observed signals. Using recordings from three seizures in one patient, we considered a network of two sources (within and just outside the putative ictal zone). Bayesian model selection was used to identify the intrinsic (within-source) and extrinsic (between-source) connectivity. Having established the underlying architecture,

we were able to track the evolution of key connectivity parameters (e.g., inhibitory connections to superficial pyramidal cells) and test specific hypotheses about the synaptic mechanisms involved in ictogenesis. Our key finding was that intrinsic synaptic changes were sufficient to explain seizure onset, where these changes showed dissociable time courses over several seconds. Crucially, these changes spoke to an increase in the sensitivity of principal cells to intrinsic inhibitory afferents and a transient loss of excitatory-inhibitory balance.

Introduction

In this paper we test the hypothesis that systematic changes in observed cross spectral density of electroencephalographic signals can be explained in terms of fluctuations in key model parameters (such as the strength of recurrent inhibitory connections to specific neuronal populations) – and that slow fluctuations in one or more of these parameters can explain changes in brain activity. The methodological advance included here is the use of dynamic causal modelling (DCM) to provide biophysically informed characterisations of electrophysiological responses in terms of slow changes in synaptic efficacy. DCM is a Bayesian framework for comparing different hypotheses or network models of observed (neurophysiological) time series.

Although DCM has been validated in the context of event related responses (Garrido et al., 2009) and steady-state or induced responses (Moran et al., 2011a), it has not been used to track short-term fluctuations in synaptic efficacy. Our focus is therefore on the validity of DCM in recovering slow (pathophysiological) changes in synaptic connectivity from electrophysiological time series. We first establish face validity using physiologically realistic simulations (using the

same model used to characterise our empirical data) and then apply the same procedure to real data, intracranial electroencephalography signals from an epileptic subject. This shows that DCM provides veridical estimates of how the data were generated and establishes the identifiability of the model used for subsequent empirical analyses. The empirical application provides a proof of principle that changes in synaptic efficacy can be measured at single subject level – and shows that pathophysiological changes beyond the seizure onset zone is necessary to explain seizure activity.

We chose epileptic seizure onset as a validation of this framework given the nature of the brain dynamics in this pathological condition. In patients affected by drug-resistant epilepsy and for which surgical treatment is thus sought, intracranial EEG is considered the gold standard for delineating the seizure onset zone (SOZ). Intracranial recordings allow one to characterise seizure activity with a high temporal resolution and track its temporal evolution. It should be noted that the onset of seizure activity may not be limited to the seizure onset zone but may be modulated – or be mediated by – distributed dynamics in brain networks.

The need to accurately track and quantify seizure dynamics has led to the development of multivariate time series analyses of signals recorded simultaneously (Pereda et al., n.d.; Lehnertz, 1999). The fact that brain function involves distributed neuronal activity – and that this functional integration is modulated by cognitive or pathophysiological factors – motivates a focus on dynamical interactions not limited to the seizure onset zone but involving distal regions. Consequently, methods grounded in information theory and dynamical systems represent promising candidates, given their potential to describe the intricate pattern of dependencies in multivariate time series.

Materials and Methods

This report introduces the concepts and procedures that allow one to estimate slow changes in synaptic parameters that may underlie changes of brain states. Its focus is on describing the approach and providing some face validation (showing it does what it says it does). This validation uses data from a single patient to provide plausible model architectures and parameters – that were used to create synthetic data. We then invert models of those data – to ensure we can recover the (known) parameters. In subsequent publications we will apply this analysis to examine its reproducibility and predictive validity in patient cohorts.

We used data recorded from a patient (female, 50 years old) with refractory epilepsy who had a total of three epileptic seizures during video-EEG monitoring. The patient was implanted at Ghent's University Hospital with 52 intracranial contacts monitoring eight regions of interest according to the following configuration: bilateral occipito-hippocampal depth electrodes with 12 contacts each (Left: LH1-LH12, Right: RH1-RH12); four subdural strips with four contacts each, monitoring the anterior temporo-basal and the posterior temporo-basal region (Left: anterior LTA 1-LTA4 and posterior LTM1-LTM4, Right: anterior RTA1-RTA4 and posterior RTM1-RTM4) and two subdural strips of six contacts each, monitoring the temporo-lateral region (Left: LTP1-LTP6, Right: RTP1-RTP6). Based on the invasive video-EEG monitoring the ictal onset zone was localized to the left hippocampus, primarily involving LH2-4. The patient underwent a selective amygdalo-hippocampectomy in 2007 and has been seizure free since that time.

The data were epoched to a segment starting 20 seconds before electroencephalographic seizure onset (pre-ictal). The

segment included the whole duration of seizure activity, which varied over the three seizures from 229 to 262 seconds. The beginning and the end of the seizure were marked by epileptologists. The sampling frequency of the EEG recordings was 256 Hz and a band pass filter was applied to the data (0.5Hz - 48Hz). The intracranial data were re-referenced by applying a bipolar montage corresponding to a series of overlapping bipolar derivations (acting as spatial filter).

Our analysis focused on two sources of activity: a primary source within the subsequently resected area, whose activity was confirmed to be part of the seizure onset zone after postsurgical follow-up (LH4-LH5) and a second source (LH6-LH7) lying just outside the area of resection (Figure 1). 10 seconds of activity before and after seizure onset were modelled, where each segment was partitioned into nine contiguous windows with 50% (1 second) overlap, for a total of 18 time windows.

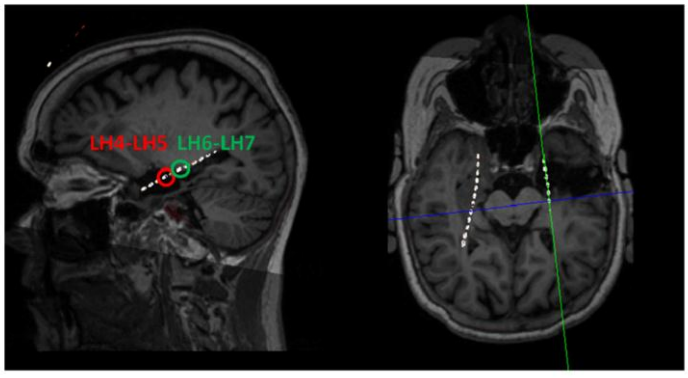

Figure 1. Location of the two intracranial electrodes and sources considered in the dynamic causal modelling. The stereotactic trajectories of the electrodes are superimposed upon the individual structural MRI scan. The leftmost circle (LH4-LH5) corresponds to the first source – considered the onset zone, while the one on the right (LH6-LH7) indicates our second source.

Dynamic causal modelling

Dynamic causal modelling (DCM) is an established procedure in the analysis of functional magnetic resonance imaging in brain mapping (Daunizeau et al., 2011; Friston et al., 2012) and is now being used increasingly for the characterisation of electrophysiological time series. DCM is used to identify the connectivity architectures and connection strengths in distributed networks using (observable) measurements of (hidden) neuronal activity. It is essentially a Bayesian model comparison scheme that allows one to evaluate competing hypotheses (or architectures) in terms of their Bayesian model evidence or marginal likelihood. Having established the best model architecture, Bayesian estimates of the model parameters provide a quantitative characterisation of effective connectivity and other (synaptic) parameters. There is an extensive literature on the validation of DCM ranging from face validation studies (David et al., 2006) to validation in terms of multimodal measurements (David et al., 2008a), pharmacological manipulations (Moran et al., 2011a, 2011b) and psychophysical constructs (Brown and Friston, 2012). Its predictive validity has been established in a number of studies in terms of pathophysiology (Boly et al., 2011).

Quantifying the effective connectivity between coupled neuronal sources corresponds to inferring the causal relationships among them, in relation to a model of those dependencies (Stephan et al. 2007). The nodes of dynamic causal models can reflect different regions in the brain that are connected by (extrinsic) forward and backward connections according to the laminar specificity established by Felleman and Van Essen (Felleman and Van Essen, 1991). Different models can be used within DCM depending on the

question of interest and the most informative data features at hand (Moran et al., 2013).

The analysis described in this section uses standard procedures developed in DCM for cross spectral density (CSD) (Friston et al., 2012), which is a generalisation of DCM for steady state responses. The CSD is the Fourier transform of the cross-correlation function, which summarizes the activity and statistical dependencies among channels in frequency space. It can be thought of as reporting the correlations at each frequency. Usually, DCM for CSD is applied to a single cross spectrum (for a given timeseries). However here, we model successive time windows; effectively summarizing the timeseries with its time-frequency decomposition. The reason that we choose these (cross spectral) data features is that they contain information about the underlying connectivity that can be accessed through estimating the spectral density (second-order statistics) of endogenous activity. This contrasts with modelling of the timeseries *per se*, which would require the time-dependent (first-order statistics) endogenous input (e.g., the input associated with a stimulus in the event related potential studies).

This DCM has been applied in several contexts previously. Technical details can be found in (Moran et al., 2007, 2009) and its applications to in vivo synaptic assays are described in (Moran et al., 2011a, 2011b). In brief, parameter estimation uses standard (variational) Bayesian model inversion, where the forward or generative model predicts cross spectral responses from models of coupled neuronal masses. These models are specified in terms of equations of motion (i.e., state space models in continuous time). The equations are based upon standard neural mass models and define transfer functions linking endogenous activity at each

source to spectral responses measured over channels. This allows one to predict observed cross spectra for any given model architecture and parameters; thereby providing an observation or forward model of spectral responses. Inversion of this model provides the model evidence (for model comparison) and posterior densities over model parameters in the usual way. Usually, one tries to explain differences in spectral responses among conditions, in terms of changes in a small number of synaptic parameters, where these changes define the model.

The novel aspect of the current analysis is the application of a standard DCM to test for slow changes in model parameters (e.g., the strength of inhibitory recurrent connections). We do this by exploiting the differences in timescales between the fast neuronal activities and slow changes in synaptic efficacy. This allows one to make local stationarity assumptions and treat successive epochs of data as different conditions – where these conditions or epochs induce fluctuations in specified parameters. Again, using the usual Bayesian model comparison procedures, we can then identify changes in parameters during seizure onset that best explain the sequence of (cross spectral) responses.

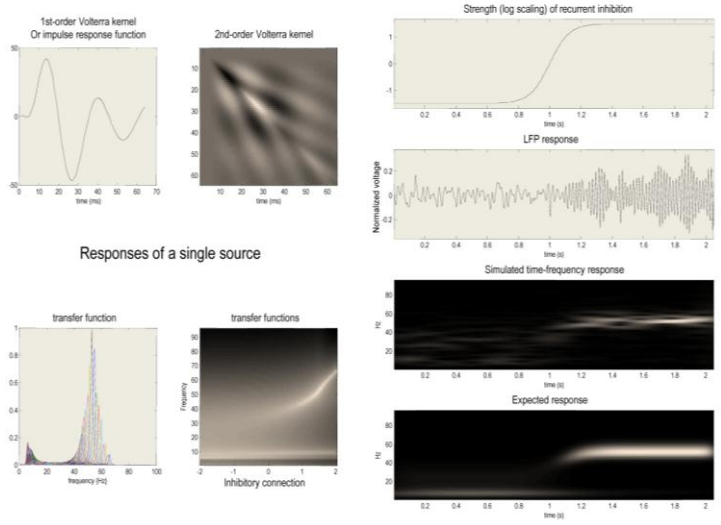

Figure 2. Left panels: Response characteristics of a single source within a dynamic causal model of the sort used in subsequent analyses (a canonical microcircuit neural mass model). The upper panels show the first and second order impulse response functions of time in terms of their impulse responses (Volterra kernels). These reflect the impact of inputs on observed responses and are a function of the model's parameters. The equivalent formulation of the impulse response in frequency space is shown in the lower panels graphically (on the lower left) and in image format for different values of the inhibitory connection (on the lower right). These are called (modulation) transfer functions and represent the frequencies in the inputs that are expressed in the output. In this example, we have shown the responses as a function of (the log scaling of) recurrent inhibitory connectivity to one of four neuronal populations comprising the source (see Figure 3). These response functions can be used to compute the expected cross spectral density for any values of the parameters. Right panels: these illustrate changes in neuronal activity when increasing recurrent inhibition. The top panel shows strength of recurrent inhibition as a function of time in seconds, while the second panel shows a simulated response obtained by integrating the neural mass model with random fluctuating inputs, with the value of inhibitory connection set to 1.5. The simulated time frequency response is shown below in terms of the spectral power over 4 to 96 Hz. The lowest panel shows the predicted power based upon the transfer functions shown on the left.

For this study, we employ a DCM for cross spectral densities (CSD) (Friston et al., 2012), which is a generalisation of DCM for steady state responses (Moran et al., 2007, 2009) to the

complex domain. In brief, this form of DCM is used to explain complex cross spectral responses from multiple channels (here two channels) in terms of coupled sources, each comprising several neuronal populations or neural masses (here four neuronal populations). Given the parameters of a neural mass model, it is easy to compute the transfer functions that map from endogenous neuronal fluctuations within each source to the observed responses in channel space. These transfer functions specify the cross spectral densities one would expect to observe empirically. Effectively, the dynamic causal model is a forward model that includes the neuronal process generating neuronal states and the (electromagnetic) mapping from neuronal states to measured data. Bayesian model inversion is then used to estimate the parameters that best explain empirical spectra and provide the Bayesian model evidence for the particular model used (e.g., with or without changes in particular connections).

In summary, DCM solves the inverse problem of recovering plausible parameters (of both neuronal dynamics and noise) that explain observed cross spectra. It uses standard variational Bayesian procedures (Friston et al., 2007) to fit time-series or cross spectra – under model complexity constraints – to provide maximum *a posteriori* estimates of the underlying model parameters and the evidence for any particular model; see (Friston et al., 2012) for more details in this particular setting. Figure 2 illustrates the basic idea behind the application of dynamic causal modelling to cross spectral responses. The key point made by this figure is that changes in connectivity can have profound effects on spectral behaviour responses to endogenous input. It is these effects that are used to estimate (changes in) the underlying connectivity (Friston, 2014). If we take the modifications in the amplitude and frequencies produced by

changes in model parameters as a simple model of seizure onset, one can use the predicted spectral responses as a likelihood model of empirical responses and thereby estimate the time-dependent changes in parameters. The simulations reported in Figure 2 can be reproduced using the seizure onset demonstration in the neuronal modelling toolbox of the academic SPM freeware (http://www.fil.ion.ucl.ac.uk/spm). These simulation results use standard parameter values (prior expectations: see Table 1).

In the analyses reported below, we modelled frequencies between 8 and 48 Hz, thereby removing fluctuations in the theta range and allowing the model to explain activity at higher frequencies before and after seizure onset. The choice of frequencies to model is partly dictated by the phenomenology of observed seizure activity and the level of modelling supported by the data. Clearly, seizure activity encompasses both low (e.g., theta) and high (gamma) frequencies – so why did we restrict the range? This choice was partly motivated by the level of detail in the models (i.e., complexity) supported by the data. In other words, to maximize model evidence, models should provide an accurate account of spectral responses but in a parsimonious way (see below). This places constraints on the range of frequencies that can be modeled (given a limited number of parameters that entail synaptic time constants that shape spectral responses). The neural mass model used in this paper was chosen to explain frequencies between alpha and (high and low) gamma. In this case, the most prominent seizure related changes were observed largely in the beta band.

The neural mass model

Neural mass models comprise ordinary differential equations that (using a mean field approach) model the dynamical behaviour of neuronal populations. These models have been developed to accommodate interacting cell types and their connectivity (Moran et al., 2013). In this work we use the canonical microcircuit neural mass model (CMC) based on the extrinsic and intrinsic connectivity described in Bastos et al. (Bastos et al., 2012). This particular model has been used previously to characterise phenomena like intrinsic gain control mechanisms in hierarchical visual processing (Brown and Friston, 2012) to impaired top-down connectivity in minimally conscious states (Boly et al., 2011).

Table 1. Model parameters used for subsequent dynamic causal modelling. The left column lists the parameters (corresponding to the equations in Figure 3). The final two columns provide the prior mean and variance for dynamic causal modelling. Note that the variance is not the prior variance of the value *per se* but on its log scaling.

Description of parameter	Prior mean	Prior variance of log scaling
Intrinsic connections d_{ij} (Hz)	$[\frac{4}{5}, \ldots, \frac{1}{5}] \cdot 1000$	$\frac{1}{8}$
Extrinsic connections (Hz)	$\frac{1}{5} \cdot 1000$	$\frac{1}{8}$
Rate constants κ_i (Hz)	$[\frac{1}{2}, \frac{1}{2}, \frac{1}{16}, \frac{1}{28}] \cdot 1000$	$\frac{1}{16}$
Slope of sigmoid γ	$\frac{2}{3}$	$\frac{1}{32}$
Intrinsic delays τ (ms)	1	$\frac{1}{32}$
Extrinsic delays τ (ms)	8	$\frac{1}{32}$
Amplitude of endogenous neuronal input	1	$\frac{1}{128}$
Power law exponent of neuronal input	1	$\frac{1}{128}$
Amplitude of measurement noise	1	$\frac{1}{128}$
Power law exponent of measurement noise	1	$\frac{1}{128}$

The CMC model distinguishes between forward and backward connections that arise from different types of principal cells (e.g., superficial and deep pyramidal cells in the cortex). In addition, this model includes excitatory and inhibitory populations that send intrinsic connections to

other populations (e.g., of excitatory spiny stellate and inhibitory interneurons in the cortex). Figure 3 shows the architecture of the two source CMC model we used, with four populations per source and extrinsic connections between the sources. The boxes detail the equations of motion that constitute the neural mass model of a single source. These are delay differential equations because the sigmoid function of presynaptic input operates on the mean depolarisation of the presynaptic source in the recent past – to accommodate axonal conduction delays. Intrinsic conduction delays are about 1 ms while extrinsic delays are about 8 ms. This figure shows the four populations in relation to their laminar relationships in the cortex. Note that the equations of motion in the figure appear to violate Dale's principle of one transmitter per cell type; for example, they include inhibitory connections from excitatory populations. This reflects the complexity of neural mass models that can be supported by the data at hand. In short, for any given data there will be an optimal model evidence (or marginal likelihood) that can be decomposed into accuracy and complexity. This means that models have to have the optimal level of complexity (i.e., number of parameters) to maximize model evidence. In the context of the neural mass model used in this work, several inhibitory interneurons populations have been absorbed into a negative effective connectivity. For example, recurrent connections among superficial pyramidal cells are assumed to be mediated bi-synaptically by intervening inhibitory interneurons (that are not modeled). This reproduces the same dynamics but avoids using too many model parameters.

One might ask whether using a (cortical) canonical microcircuit model is appropriate for sub cortical structures such as the hippocampus modeled in this paper. Strictly

speaking, this is an issue that would be best addressed using Bayesian model comparison, for example comparing the canonical microcircuit with the bespoke model of hippocampal circuitry described in (Moran et al., 2014). However, for our current purposes having four subpopulations appears to be sufficient. Our previous experience with these models suggests that the canonical microcircuit model is sufficient to model hippocampal responses; perhaps because the basic connectional architecture is conserved over cortex and structures like the hippocampus (i.e., a circuit with excitatory input and output cells and an inhibitory and excitatory pair).

Bayesian Model Comparison

DCM was used to compare alternative hypotheses about which synaptic parameters were responsible for changes in cross spectral density during seizure onset – after establishing the basic architecture of extrinsic connections between the two sources. Our analyses were therefore based upon a two-step Bayesian model comparison procedure. In the first step, we identified the best model architecture – distinguishing between extrinsic forward and backward connections between the primary ictal source (LH4-LH5) to the secondary source (LH6-LH7) and the reverse architecture with backward connections from the primary to secondary source (Figure 4a). To disambiguate these two architectures we inverted all 18 time windows, allowing only a number of connections to change over time (see below). The most likely architecture was identified using Bayesian model comparison by pooling the evidence for the two alternative models over windows from all three seizures. This allowed us to establish whether the extrinsic connections from the first to the second source were of a forward or backward type (and *vice versa*).

The second stage of the analysis focused on the changes in intrinsic and extrinsic connectivity over time windows – and implicitly between pre-ictal and ictal states. Using the most likely model from the first step, we allowed various combinations of intrinsic and extrinsic connections to change over time (using third order polynomial functions of time, for the pre-and post-ictal windows). This allowed us to estimate the trajectory of coupling parameters within and between pre-ictal and ictal time windows – while holding all other parameters at the same values (e.g., conduction delays that should not change over time). The parameters we allowed to vary corresponded to extrinsic connection strengths between the two sources and their intrinsic connectivity. Following Wendling et al. (Wendling et al., 2005) we associated changes in intrinsic connectivity with the influence of inhibitory interneurons on (superficial) principal cells. The possible combinations are described by 16 models, with and without changes in: intrinsic connectivity in the primary source, intrinsic connectivity in the secondary source, forward connectivity and backward connectivity. A schematic of the 16 models tested is provided in Figure 4b. It is changes in these connections that we hoped would explain both variability within the pre-and ictal states and the slow changes that underlie seizure onset.

.

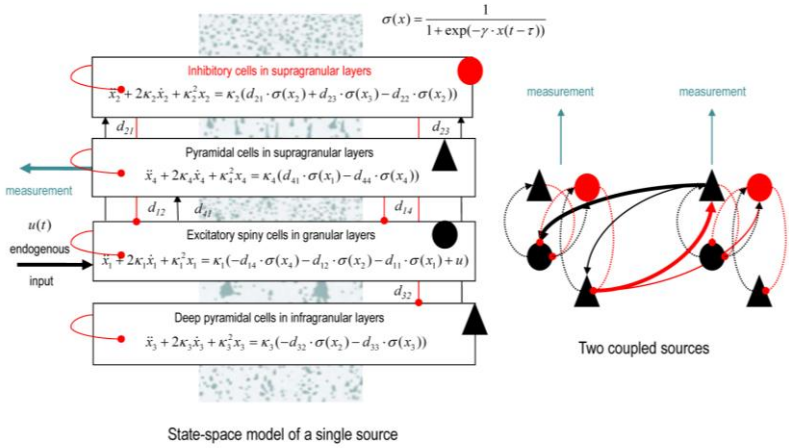

Figure 3. This schematic illustrates the state-space or dynamic causal model that we used for the dynamic causal modelling reported subsequent figures. Left panel: this shows the differential equations governing the evolution of depolarisation in four populations constituting a single electromagnetic source (of EEG, MEG or local field potential measurements). These populations are divided into input cells, inhibitory interneurons and (e.g., superficial and deep) principal cell populations that constitute the output populations. The equations of motion are based upon standard convolution models for synaptic transformations, while coupling among populations is mediated by a sigmoid function of (delayed) mean depolarisation. The slope of the sigmoid function corresponds to the intrinsic gain of each population. Intrinsic (within source) connections couple the different populations, while extrinsic connections couple populations from different sources. See Table 1 for a list of key parameters and a brief description. Right panel: this shows the simple two source architecture used in the current paper. The intrinsic connectivity (dotted lines) and extrinsic connectivity (solid lines) conform to the connectivity of the canonical microcircuit and the known laminar specificity of extrinsic connections (Bastos et al. 2012). Excitatory connections are in red and inhibitory connections are in black. Endogenous fluctuations drive the input cells and measurements are based on the depolarisation of superficial pyramidal cells.

Face validation studies

To establish the face validity of this application of DCM, we analysed both simulated and real data. Crucially, the

parameters used to simulate the (cross spectral) data were based upon biologically plausible estimates from the empirical data. However, because the simulated data were generated under known model parameters (connectivity and time-dependent changes) we knew the ground truth and we could establish that the true values fall within the 90% posterior confidence intervals. For the simulation studies, we generated 18 time windows of cross spectral data using the prior expectations for intrinsic and extrinsic connectivity for the first (nine pre-ictal) windows and mono exponentially decaying connection strengths during the (nine) ictal windows. We used forward connections from the primary to the secondary source and restricted seizure-related changes in connectivity to the forward connectivity and intrinsic inhibitory connections to superficial principal cells in both sources. These changes modelled a transient increase in the excitability of principal cells mediated by both intrinsic and extrinsic connectivity. The time constant of extrinsic decay (back to the prior expectation) was two seconds and the time constant of intrinsic decay was eight seconds. The values of all other parameters were set at the posterior estimates from the empirical analysis of the first seizure described below.

To create realistic simulated data, residuals from the empirical analyses (randomly permuted over windows) were added to the simulated cross spectra to ensure that the sampling noise and its correlation structure had the same amplitude and form that would be encountered empirically. We used a signal to noise ratio of four, over all channels and time windows.

Analysis of real data

We performed model comparison and repeated the above analysis to estimate the trajectory of model parameters for the three successive seizures. These analyses used Bayesian updating, where the posteriors from the first seizure were used as priors for the second seizure and similarly for the second and third seizures. This enabled us to accumulate evidence for different models, while allowing for changes in parameters that could change from seizure to seizure (for example electrode gain). We then pooled the evidence over seizures to identify the best model. Finally, we identified the parameter estimates of the best model to quantify trajectories in the parameter space for each seizure.

Results

Face validation

The results of the face validation (simulation) study are shown in Figure 5a: this shows the time-dependent changes in (log scaling of) the intrinsic and extrinsic connections as a function of window number. The posterior expectations correspond to the coloured lines (blue and cyan correspond to intrinsic connectivity, while green and red lines report the forward and backward connectivity respectively). The true values are shown as broken lines and the posterior estimates as full lines. In this example, we precluded changes in the backward connections from first to the second source. There is a pleasing correspondence between the posterior estimates and the true values. Indeed, for the intrinsic changes (blue and cyan) they are virtually indistinguishable. Note the characteristic overconfidence of these estimators (due to the mean field approximation in the variational scheme). This means that in some cases the true value lies

just outside the 90% confidence intervals (grey areas). This is particularly evident for the forward connectivity (green) shortly after seizure onset. These results suggest that the trajectory of parameters can be recovered even under fairly realistic levels of sampling noise and biologically plausible values for the neuronal dynamics.

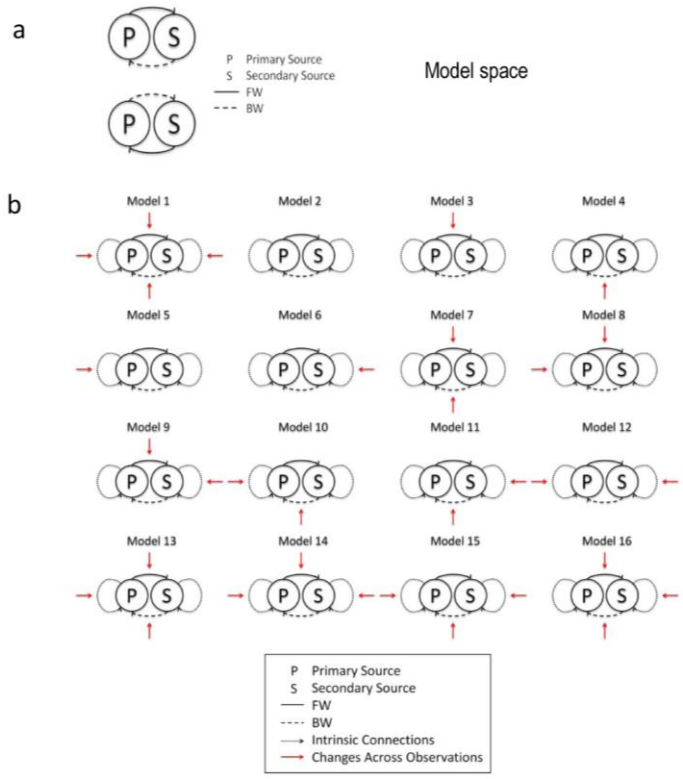

Figure 4. a) Alternative model architectures for the extrinsic coupling between the primary and secondary sources. FW: forward connectivity; BW: backward connectivity. b) Schematic showing the 16 models we tested. These models correspond to alternative hypotheses about changes in synaptic coupling that can explain changes in spectral activity before and after seizure onset. The 16 models correspond to all combinations of changes in intrinsic connectivity (in the primary and secondary sources) and changes in forward and backward extrinsic connections. The changes in intrinsic connectivity were modeled as changes in the inhibitory recurrent or self connections among superficial pyramidal cells.

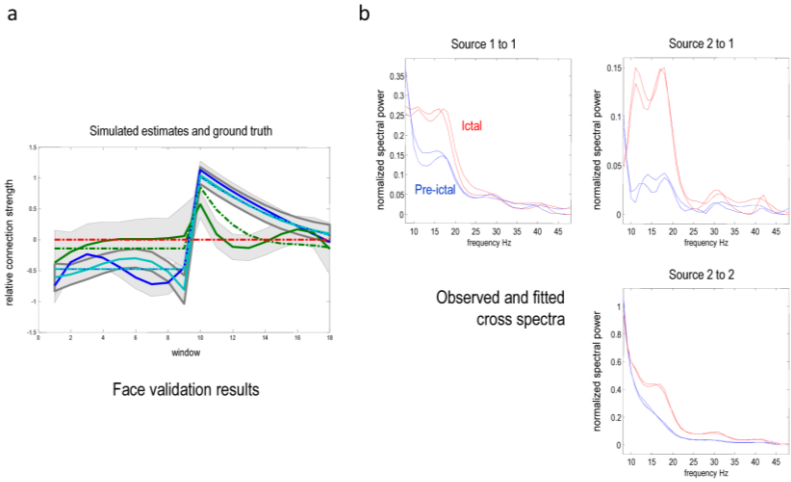

Figure 5. a). This panel shows the time-dependent changes in (log scaling of) the intrinsic and extrinsic connections as a function of window number. The posterior expectations correspond to the coloured lines (blue and cyan correspond to intrinsic connectivity, while green and red lines report the forward and backward connectivity respectively). The true values are shown as broken lines, the posterior estimates as full lines and the 90% confidence intervals as grey areas. b) Predicted (solid lines) and observed (dotted lines) cross spectra for pre-ictal (blue) and ictal (red) periods. This example uses average spectra from the first seizure to illustrate the quality of the model fit and the spectral data features that inform the posterior estimates of the model parameters. The absolute values of the (complex) cross spectra are shown in the upper right panel.

Empirical analyses

A typical model fit to the observed (empirical) cross spectra is provided in Figure 5b – showing the characteristic changes in complex cross spectra from a pre (blue) to post (red) ictal window. This example shows the typical excess of power (and coherence) in the beta band following seizure onset. Bayesian model comparison of competing models with different extrinsic (forward and backward) connections suggested that we can be almost certain that the forward connection originates in the primary source, with a log

evidence difference of over 100 (Penny et al.2004). Differences in log evidence are the same as log Bayes factors, where the Bayes factor is an odds ratio comparing the evidence or marginal likelihood of two models.

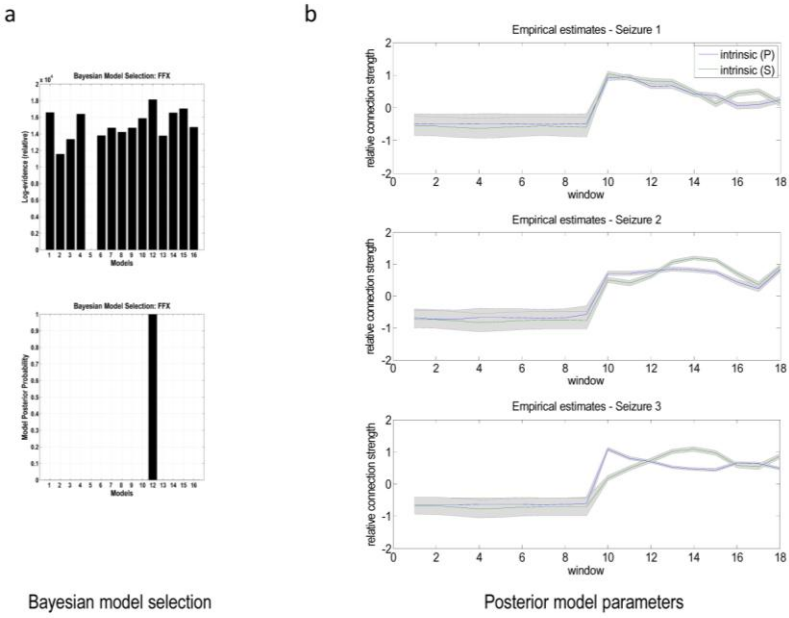

Figure 6. a) Upper panel: these are the variational free energy approximations to log model evidence for the 15 models covering changes in one or more synaptic parameters before and after seizure onset. Lower panel: this shows the corresponding posterior probability over models and identifies a single model with almost 100% posterior confidence. b) Changes (across consecutive windows, for each of the three seizures) in the synaptic parameters that were allowed to change in the winning model. Changes are shown in terms of log scaling to clarify the profile of changes over time. Each window corresponds to one second. The blue and the green lines report the intrinsic inhibition of the primary and secondary sources respectively and the grey areas represent the 90% confidence intervals.

Having established the most probable model architecture, we then compared the 16 models of time-dependent changes in intrinsic and extrinsic connectivity. One model (model 11) failed to converge during model inversion and

was excluded from subsequent analysis. The pooled evidences of the remaining 15 models are shown in Figure 6a.

The winning model (**model 12**) allowed changes in intrinsic connectivity in both the primary and the secondary sources. This model had greater evidence than any competing model. Typically, a difference in log evidence of three is considered strong evidence in favour of one model over another (this corresponds to a log marginal likelihood ratio of about 20 to 1). The difference between the best and next best models was much greater than three. Note that the model with the highest evidence was not the model with the greatest number of parameters (**model 1**). This reflects the complexity penalty inherent in Bayesian model comparison. In other words, changes in forward and backward connectivity did not improve accuracy sufficiently to justify their inclusion.

Finally we examined the posterior estimates (expectations) to quantify fluctuations in the parameters around seizure onset. The results are shown in Figure 6b. Intrinsic connectivity increases markedly in both sources with seizure onset and then decreases within the first 20 seconds of seizure activity (the observed change in log scaling of about two corresponds to an eightfold increase in intrinsic connectivity). The trajectories are qualitatively consistent, given that they were estimated from independent data. The intrinsic connectivity modelled here is a sensitivity of (superficial) principal cells to presynaptic inputs from inhibitory interneurons. This fits comfortably with the conclusions of Wendling et al.(Wendling et al., 2005) who model seizure onset in terms of slow ensemble dynamics involving pyramidal cells and local interneurons, highlighting the increases in excitability that peak at seizure onset.

In summary, these results show that seizure onset appears to be mediated by an inhibition of superficial pyramidal cells in both sources. The key observation here is that the synaptic changes necessary to explain observed seizure activity (in terms of cross spectral density) are distributed, i.e. not restricted to the sole SOZ, and show slow dissociable time courses over several seconds. Furthermore, these changes are restricted to local or intrinsic fluctuations in synaptic parameters that are (presumably) a response to interactions among distal sources. Notice that the (reciprocal) extrinsic connections play a crucial role in the ensemble dynamics, in the sense that they mediate distributed interactions both before and after seizure onset. In short, the changes we have identified speak to a change in the recurrent interactions between excitatory principal cells (that originate forward type connections) and local inhibitory interneurons, reflecting a transient loss excitatory-inhibitory balance or gain control within a distributed epileptogenic network.

The reason that we can make definitive statements about directed connections among specific populations is that the (winning) DCM entails these specific changes. This illustrates the utility of having a biophysically explicit and plausible model of how data are caused – and the importance of Bayesian model comparison in adjudicating among different hypotheses.

Discussion

Neuronal models are being increasingly used to characterize brain activity in different states, and the transition between these states. These transitions are most evident and crucial when the phenomenon to be modelled is the onset of an epileptic seizure.

A neuronal model of activity during different stages preceding and following seizure onset was proposed (Wendling et al., 2005), highlighting that the transition from the pre-ictal to the ictal state may not only be due to an increase of excitation (and a decrease of an inhibition) but rather to slow ensemble dynamics involving pyramidal cells and local interneurons, highlighting their increases in excitability that peak at seizure onset. A recent study (Nevado-Holgado et al., 2012) characterized the evolution of an absence seizure as a path through the parameter space of a neural mass model. In another approach (Hocepied et al., 2013) a similar scheme was proposed for early seizure detection. In both cases, the authors suggest that tracking a set of parameters over time can disclose the nature of ictogenesis. Characterising the trajectory of biophysical neural model parameters during seizure onset may provide insights into the underlying slow metabolic mechanisms.

The common theme in studies modelling seizure generation is a departure from the normal regime of functioning in populations of cells. This departure appears to be based on the interactions among excitatory pyramidal cells (Thomson and Radpour, 1991; Whittington et al., 1997) and their inhibitory interneurons (Miles et al., 1996; Banks et al., 1998; White et al., 2000). Several studies have investigated and reviewed the intracellular and extracellular mechanisms underlying slow changes in synaptic parameters during seizure activity (Jefferys et al., n.d.; McNamara, 1994, 1995; Isomura et al., 2008). McCormick and Contreras (McCormick and Contreras, 2001) reported how periods of excitation, followed by synaptic inhibition and/or activation of intrinsic hyperpolarizing conductances can give rise to inter-ictal spikes, which can then be sustained during seizure activity.

Both David et al. (David et al., 2008b) and Krishnan et al. (Krishnan et al., 2013) addressed the causes of pathological synchronization, pointing out that changes in the extracellular ionic concentrations or modifications to excitation and inhibition can contribute to synchronized epileptiform firing. Increase in extracellular K+ concentration and decrease in Ca2+ are the most likely candidates for mediating these slow changes in excitability (and disinhibition). Other variables related to energy metabolism (levels of extracellular K^+, oxygen, ATP consumption) have been modelled as a slow *permittivity* variable in a dynamical model of seizure generation (Jirsa et al., 2014). This model highlights the separation of temporal scales in the genesis of seizure activity and highlights the role of slow fluctuations in excitability that our results appear to be consistent with.

Dynamic causal modelling was applied to intracranial EEG data recorded during 1 Hz electrical stimulation in patients with drug-resistant focal epilepsy (David et al., 2008b). DCM was used to model short term plasticity – as modulations of synaptic efficacies in either intrinsic or extrinsic connections. The observed fast transition from the pre-ictal to the ictal state may be due to changes in intrinsic connectivity. DCM revealed variations of the postsynaptic efficacies at the ictal zone. Their results suggested that electrically induced seizures in the temporal lobe could depend in part on a pre-ictal increase in sensitivity to hippocampal afferents from the temporal pole. Again, this is consistent with the notion that seizure activity results from distributed ensemble dynamics engaging both intrinsic and extrinsic connections.

It is clear that (slow) drifts in synaptic efficacy or coupling provide a sufficient account for the (fast) neuronal dynamics characteristic of seizure activity – and that these drifts involve involving regions distributed beyond the seizure

onset zone. This perspective has been recently exploited. A bifurcation analysis of a physiological model of large-scale brain activity was used to obtain a parsimonious and unifying explanation of the defining features of seizure onset and spreading in (Breakspear et al. 2006). Goodfellow at al. (Goodfellow et al., 2011) associated the emergency of epileptiform rhythms to two different scales of inhibition in a cortical neural mass model; in the work mentioned above: Jirsa et al. (Jirsa et al., 2014) propose a minimal canonical model of epileptogenesis based upon a careful bifurcation analysis. This model exhibits spontaneous transitions between multi-stable states – resting on both slow and fast state variables. The dynamics emerging from both studies may provide a formal framework to study the neurophysiological mechanisms considered above.

In this paper we adopt a similar if complementary approach. We start from a canonical microcircuit model of neuronal sources and infer the evolution of its synaptic parameters around seizure onset. However, dynamic causal modelling takes its constraints from the known anatomy and physiology of neuronal circuits – as opposed to the formal (phenomenological) constraints offered by bifurcation analyses and dynamical systems theory. This means that the agenda is to parameterise seizure activity in terms of underlying synaptic mechanisms as opposed to their mathematical architecture. Crucially, we do not model a single epileptogenic region, but consider the distributed interactions with another population. This allowed us to use Bayesian model comparison to ask whether seizure activity was sufficiently explained by changes in one (epileptogenic) source – or required distributed changes throughout a simple network. Our results clearly point to a distributed explanation that rests upon coupled dynamics over both space and time. Nonetheless, given that the pathophysiology

of epilepsy may be local (and mediated by non-specific extracellular factors), intrinsic plasticity may play a predominant role in seizure onset. In principle, it should be possible to extend this dynamic causal modelling approach to identify the causal architecture of these changes by explicitly modelling a slow (hidden) permittivity variable (such as extracellular potassium concentration) and testing different models. An important aspect of the current results is the dissociation in the temporal evolution of extrinsic (negligible) and intrinsic (marked) synaptic parameters. The nature of this dissociation may be important for understanding the intracellular and extracellular pathophysiology (what causes what) and clearly motivates further study in this area.

As with all dynamic causal modelling, the qualities of the models (model evidence) are only defined in relation to each other – and there is no supposition that the selected model represents some true or veridical architecture generating the data. In this sense, model comparison – and the interpretation of posterior estimates – is better thought of as testing specific hypotheses. In this instance, we wanted to test the hypothesis that a small number of (intrinsic) coupling strengths were sufficient to explain fluctuations in cross spectral density associated with seizure onset. To test more detailed hypotheses, one would have to specify a greater range of competing models and evaluate their evidence. A key point here is (as noted above) that at some point, the data at hand will not be able to disambiguate between models that are too complex (because their evidence will fall). It is at this point that one might turn to alternative sources of data – such as laminar-specific intracranial recordings.

In this paper we have focused on modelling spectral responses over epochs or windows around seizure onset using dynamic causal modelling for cross spectral density. It is interesting to consider alternative approaches. The first choice that one has to make in this context is whether to model the first-order responses in time or the second-order (spectral) responses in frequency space. In modelling endogenous activity, of the sort presented by seizure activity, modelling the timeseries can be difficult. This is because the time varying neuronal states generating data are unknown and have to be estimated. Although this is possible, it can be inefficient because one has to estimate both hidden neuronal states and unknown (connectivity) parameters. There are generalized (variational) Bayesian filtering techniques – that generalize the Kalman filter – which have been applied to fMRI timeseries (Li et al., 2011); however, they are relatively less common in electrophysiological timeseries analysis, see (Freestone et al., 2011) for an application in the framework of neural field modelling. This is because the number of time bins and hidden neuronal states can be prohibitively large. In short, the more efficient way to model seizure activity is to focus on the time-frequency responses that reflect second-order statistics of neuronal activity. This means that hidden neuronal states do not have to be estimated and the data can be used to estimate unknown parameters (e.g., transfer functions and cross spectral predictions). In principle, it should be possible to model time varying parameters causing time-dependent changes in cross spectral measurements; however, we have chosen the simpler approach of using a piecewise linear approximation to these slow parameter changes. This allows us to use established model procedures for modelling complex cross spectra. We hope to compare this approach to explicit models of time

frequency responses and, possibly, stochastic DCMs that estimate hidden neuronal states in the future.

This study is not meant to be a comprehensive illustration of dynamic causal modelling of seizure activity – rather a demonstration of the issues that are entailed and the nature of the questions that can be asked. The particular Bayesian updating scheme introduced here could be applied to measure synaptic modification on the scale of seconds to minutes. This may be useful for both epilepsy research and also studies of synaptic plasticity in studies of short or long-term potentiation or associative learning.

References

Banks MI, Li TB, Pearce RA (1998) The synaptic basis of GABAA,slow. J Neurosci 18:1305–1317

Bastos AM, Usrey WM, Adams RA, Mangun GR, Fries P, Friston KJ (2012) Canonical microcircuits for predictive coding. Neuron 76:695–711

Boly M, Garrido MI, Gosseries O, Bruno M-A, Boveroux P, Schnakers C, Massimini M, Litvak V, Laureys S, Friston K (2011) Preserved feedforward but impaired top-down processes in the vegetative state. Science 332:858–862

Brown H, Friston KJ (2012) Free-energy and illusions: the cornsweet effect. Front Psychol 3:43

Daunizeau J, David O, Stephan KE (2011) Dynamic causal modelling: a critical review of the biophysical and statistical foundations. Neuroimage 58:312–322

David O, Guillemain I, Saillet S, Reyt S, Deransart C, Segebarth C, Depaulis A (2008a) Identifying neural drivers with functional MRI: an electrophysiological validation. PLoS Biol 6:2683–2697

David O, Kiebel SJ, Harrison LM, Mattout J, Kilner JM, Friston KJ (2006) Dynamic causal modeling of evoked responses in EEG and MEG. Neuroimage 30:1255–1272

David O, Woźniak A, Minotti L, Kahane P (2008b) Preictal short-term plasticity induced by intracerebral 1 Hz stimulation. Neuroimage 39:1633–1646

Felleman DJ, Van Essen DC (n.d.) Distributed hierarchical processing in the primate cerebral cortex. Cereb Cortex 1:1–47

Freestone DR, Aram P, Dewar M, Scerri K, Grayden DB, Kadirkamanathan V (2011) A data-driven framework for neural field modeling. Neuroimage 56:1043–1058

Friston K, Mattout J, Trujillo-Barreto N, Ashburner J, Penny W (2007) Variational free energy and the Laplace approximation. Neuroimage 34:220–234

Friston KJ (2014) On the modelling of seizure dynamics. Brain 137:2110–2113

Friston KJ, Bastos A, Litvak V, Stephan KE, Fries P, Moran RJ (2012) DCM for complex-valued data: cross-spectra, coherence and phase-delays. Neuroimage 59:439–455

Garrido MI, Kilner JM, Kiebel SJ, Friston KJ (2009) Dynamic causal modeling of the response to frequency deviants. J Neurophysiol 101:2620–2631

Goodfellow M, Schindler K, Baier G (2011) Intermittent spike-wave dynamics in a heterogeneous, spatially extended neural mass model. Neuroimage 55:920–932

Hocepied G, Legros B, Van Bogaert P, Grenez F, Nonclercq A (2013) Early detection of epileptic seizures based on parameter identification of neural mass model. Comput Biol Med 43:1773–1782

Isomura Y, Fujiwara-Tsukamoto Y, Takada M (2008) A network mechanism underlying hippocampal seizure-like synchronous oscillations. Neurosci Res 61:227–233

Jefferys JG, Borck C, Mellanby J (n.d.) Chronic focal epilepsy induced by intracerebral tetanus toxin. Ital J Neurol Sci 16:27–32

Jirsa VK, Stacey WC, Quilichini PP, Ivanov AI, Bernard C (2014) On the nature of seizure dynamics. Brain 137:2210-30.

Krishnan GP, Filatov G, Bazhenov M (2013) Dynamics of high-frequency synchronization during seizures. J Neurophysiol 109:2423–2437

Lehnertz K (1999) Non-linear time series analysis of intracranial EEG recordings in patients with epilepsy--an overview. Int J Psychophysiol 34:45–52

Li B, Daunizeau J, Stephan KE, Penny W, Hu D, Friston K (2011) Generalised filtering and stochastic DCM for fMRI. Neuroimage 58:442–457

McCormick DA, Contreras D (2001) On the cellular and network bases of epileptic seizures. Annu Rev Physiol 63:815–846

McNamara JO (1994) Cellular and molecular basis of epilepsy. J Neurosci 14:3413–3425

McNamara JO (1995) Analyses of the molecular basis of kindling development. Psychiatry Clin Neurosci 49:S175–S178

Miles R, Tóth K, Gulyás AI, Hájos N, Freund TF (1996) Differences between somatic and dendritic inhibition in the hippocampus. Neuron 16:815–823

Moran R, Pinotsis DA, Friston K (2013) Neural masses and fields in dynamic causal modeling. Front Comput Neurosci 7:57

Moran RJ, Jones MW, Blockeel AJ, Adams RA, Stephan KE, Friston KJ (2014) Losing Control Under Ketamine: Suppressed Cortico-Hippocampal Drive Following Acute Ketamine in Rats. Neuropsychopharmacology

Moran RJ, Jung F, Kumagai T, Endepols H, Graf R, Dolan RJ, Friston KJ, Stephan KE, Tittgemeyer M (2011a) Dynamic causal models and physiological inference: a validation study using isoflurane anaesthesia in rodents. PLoS One 6:e22790

Moran RJ, Kiebel SJ, Stephan KE, Reilly RB, Daunizeau J, Friston KJ (2007) A neural mass model of spectral responses in electrophysiology. Neuroimage 37:706–720

Moran RJ, Stephan KE, Seidenbecher T, Pape H-C, Dolan RJ, Friston KJ (2009) Dynamic causal models of steady-state responses. Neuroimage 44:796–811

Moran RJ, Symmonds M, Stephan KE, Friston KJ, Dolan RJ (2011b) An in vivo assay of synaptic function mediating human cognition. Curr Biol 21:1320–1325

Nevado-Holgado AJ, Marten F, Richardson MP, Terry JR (2012) Characterising the dynamics of EEG waveforms as the path through parameter space of a neural mass model: application to epilepsy seizure evolution. Neuroimage 59:2374–2392

Pereda E, Quiroga RQ, Bhattacharya J (n.d.) Nonlinear multivariate analysis of neurophysiological signals. Prog Neurobiol 77:1–37

Thomson AM, Radpour S (1991) Excitatory Connections Between CA1 Pyramidal Cells Revealed by Spike Triggered Averaging in Slices of Rat Hippocampus are

Partially NMDA Receptor Mediated. Eur J Neurosci 3:587–601

Wendling F, Hernandez A, Bellanger J-J, Chauvel P, Bartolomei F (2005) Interictal to ictal transition in human temporal lobe epilepsy: insights from a computational model of intracerebral EEG. J Clin Neurophysiol 22:343–356

White JA, Banks MI, Pearce RA, Kopell NJ (2000) Networks of interneurons with fast and slow gamma-aminobutyric acid type A (GABAA) kinetics provide substrate for mixed gamma-theta rhythm. Proc Natl Acad Sci U S A 97:8128–8133

Whittington MA, Traub RD, Faulkner HJ, Stanford IM, Jefferys JG (1997) Recurrent excitatory postsynaptic potentials induced by synchronized fast cortical oscillations. Proc Natl Acad Sci U S A 94:12198–12203

Chapter 4

The pathophysiology of epilepsy: A dynamic causal modelling study of seizure activity in a rat model

Introduction

In the previous chapter we presented a framework of analysis aimed to shed light on the synaptic mechanisms underlying epileptic seizure onset and their modulation.

This chapter will present an extension and an improvement of the aforementioned approach. The object of our study will be an animal model of epilepsy, in which the same experimental protocol was used to trigger spontaneously emerging epileptogenic behaviour, even though the pathological behaviour assumed different characteristics across animals.

A dynamic causal modelling (DCM) of seizure activity and a Bayesian model selection procedure is used to test a number of key hypotheses about the genesis of seizure activity and longitudinal changes in the underlying pathophysiology over the weeks following seizure induction. The data we

examined was obtained from a series of rats who received kainic acid injections in the right hippocampus, in order to artificially create an epileptogenic zone. All the rats were implanted with depth electrodes in the right (lesioned) and left (perilesional) hippocampus.

It is worth to note that the lesion is in a first moment localized in the right hippocampus, but eventually spreads to the left one (hippocampi are tightly connected in rats). After some weeks seizures can originate even from the left hippocampus . This experimental model and its data afford the opportunity to ask a number of important questions about epigenesis; for example, what are the differences between the lesioned and perilesional hippocampi? are there systematic changes in pathophysiology over the weeks following lesion? and is the pathophysiology restricted to the primary lesion site or is it more distributed?

We focus on the last question and characterise the pathophysiology of seizure onset – shortly after the lesion – in terms of physiologically plausible variables such as changes in synaptic efficacy and rate constants. Specifically, we ask whether seizure onset can be explained by fluctuations in intrinsic connectivity and synaptic rate parameters, changes in the endogenous afferent activity from other areas, or both.

To characterise the physiological basis of seizure activity, we used biophysically informed modelling with neural mass models in the setting of dynamic causal modelling . Dynamic causal models allow one to predict observed electrophysiological activity (in our case spectral density) in terms of electromagnetic sources that comprise coupled neuronal populations, driven by endogenous neuronal activity. These models involve parameters encoding intrinsic

connection strengths, synaptic rate constants and endogenous input. Using successive epochs of data, we aimed to effectively track the trajectory of model parameters that best explained epoch by epoch changes in spectral density during seizure onset.

Crucially, we advance the methodology presented in (Papadopoulou et al. 2015). DCM inversion is now implemented by using a Bayesian belief-updating scheme of seizure activity (Cooray 2015, submitted). Conversely with respect to the standard Bayesian inversion techniques used before, according to the proposed scheme the optimal parameters of the model of each window (the posteriors) are used as initial guess for the model of the following one (the priors). Several models are tested, each one allowing different parameters to change over epochs or to stay constant. Bayesian model comparison then indicates which parameters are most likely responsible for the onset of seizure. The collection of parameter trajectories that best explain the peri-ictal activity will indicate whether the parametric changes involved the intrinsic connectivity among the neuronal populations (and their time constants), the spectral form of endogenous (afferent) neuronal input, or both.

This paper comprises three sections. In the first we describe the data available to us and the selection criteria for the three rats studied. This section includes a description of the preprocessing and the computation of spectral density over consecutive epochs of data surrounding seizure onset. The second section provides a brief description of dynamic causal modelling in this context (DCM for cross spectral density), with a special focus on the Bayesian belief updating used to track parameter trajectories. The final section presents the results of Bayesian model comparison and a discussion of

the physiological implications of our results. We discuss how these will be used to constrain subsequent studies of the differences between lesioned and non-lesioned hippocampi and the evolution and differentiation of seizure activity over a period of weeks.

Materials and Methods

Data

Wistar rats of approximately the same age and weight were injected with kainic acid (KA) in the right hippocampus. Before the injection, the same surgical protocol for implantation has been used for all rats; two depth electrodes in the right hippocampus (RH) (**dr**1 &**dr**2) separated by 0.5mm, one depth electrode **dl** in the left hippocampus (LH) and finally an epidural electrode over the right frontal cortex (Figure 1). A detailed description of the data can be found in (Raedt et al. 2009).

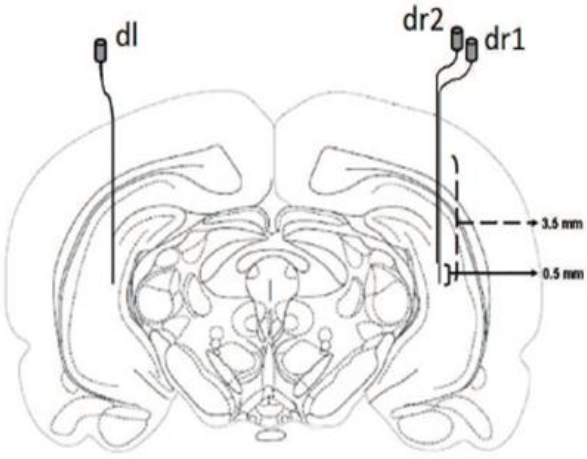

Figure 1. Illustration of the position of the hippocampal depth electrodes. There are two depth electrodes in the RH (dr1 & dr2) and one in the LH (dl).

Starting from a week after the injection with KA, spontaneous seizures have been monitored for 21 weeks. The video-EEG monitoring was performed under environmentally controlled conditions (12 h normal light / dark cycles) in an isolated room.

For this work we have used data recorded from 3 animals (A,B,C). We restrict our analysis to the 10 and 11th week after the injection. The animals can be classified in terms of their seizure frequency; Rat B developed more than one seizures per day and rats A & C had more sparse seizures (less than one per day). The reason for this variation in seizure frequency lies in different aspects of epileptogenesis. Since the intervention aimed to trigger epileptogenesis, was the same for all rats, the added value for the approach presented here would be a mapping between the model parameters and the clinical characteristics of the seizures.

We have modelled the activity of the second depth electrode of the RH (dr2 in Figure 1), and of the one of the LH (dl in Figure 1). For simplicity in what follows we will refer to them as RH and LH electrodes. For each seizure, data consisted of a continuous peri-ictal segment of 30 seconds, starting 10 seconds before seizure onset as noted by the epileptologists.

Data were acquired with a sampling frequency of 200 Hz. The time series for each rat were divided into consecutive windows of 2000 ms with a constant overlap (250ms). This choice corresponded to the maximum length over which the spectrum remained approximately constant, guaranteeing the best possible frequency resolution. A Bayesian multivariate autoregressive model was used to estimate the spectral density of the data for each window. The resulting spectrum was averaged over the available recorded seizures during the weeks of interest (locked to the time of seizure

onset). We modelled fluctuations in spectral power between 3Hz and 70Hz. To improve the fits and the transitions between adjacent windows, the time-frequency representation of the whole peri-ictal period was smoothed with a moving Gaussian kernel.

Before averaging the seizures for each rat, we first looked at the time-frequency (TF) plots to ensure that the seizures were qualitatively similar and that the spectral modulations were correctly aligned around the seizure onset time indicated by the epileptologists. These plots are reported below for each rat.

Rat A

Three seizures were available for this rat during the period of interest. After having ensured that the alignment is the correct one, we concluded that the full 30 seconds segment length (10 seconds pre-ictal, 20 seconds ictal) could be used for this rat.

The TF plots of the seizure for both hippocampi (Figures 2, 3) showed that seizures had similar spectral features which allowed us to proceed with averaging.

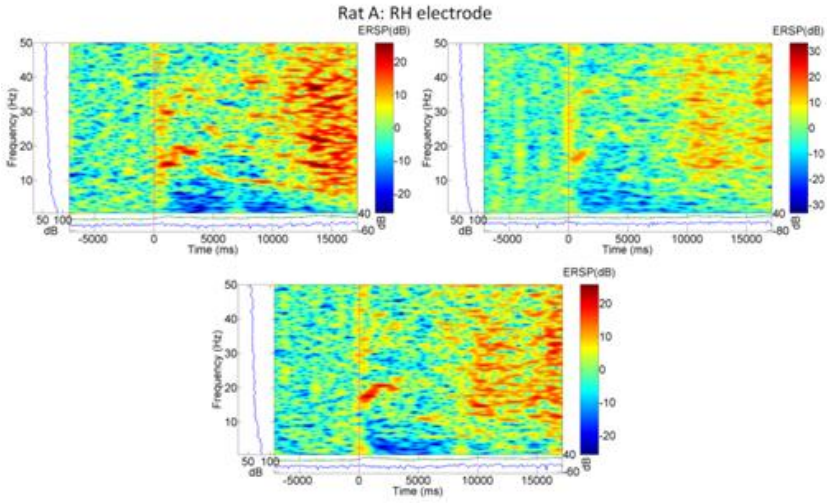

Figure 2. TF plots of the three 30 seconds peri-ictal segments used from data recorded at the RH electrode from Rat A. Time 0 indicates the seizure onset.

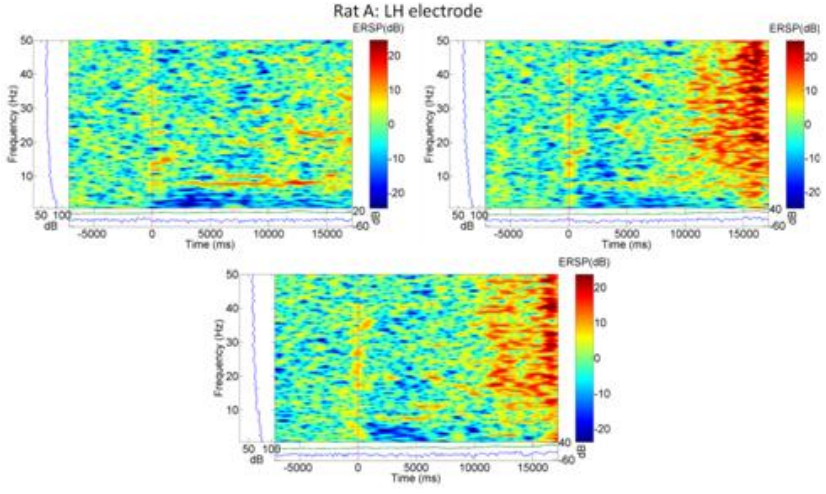

Figure 3. TF plots of the three 30 seconds peri-ictal segments used from data recorded at the LH electrode from Rat A. Time 0 indicates the seizure onset.

Rat B

Seven seizures were recorded for this rat during the period of interest. In this case some realignment of the onset time was necessary, resulting in peri-ictal segments of 27 seconds (13 seconds pre-ictal and 14 seconds ictal).

The TF plots of the seizure for both hippocampi can be seen below (Figures 4,5).

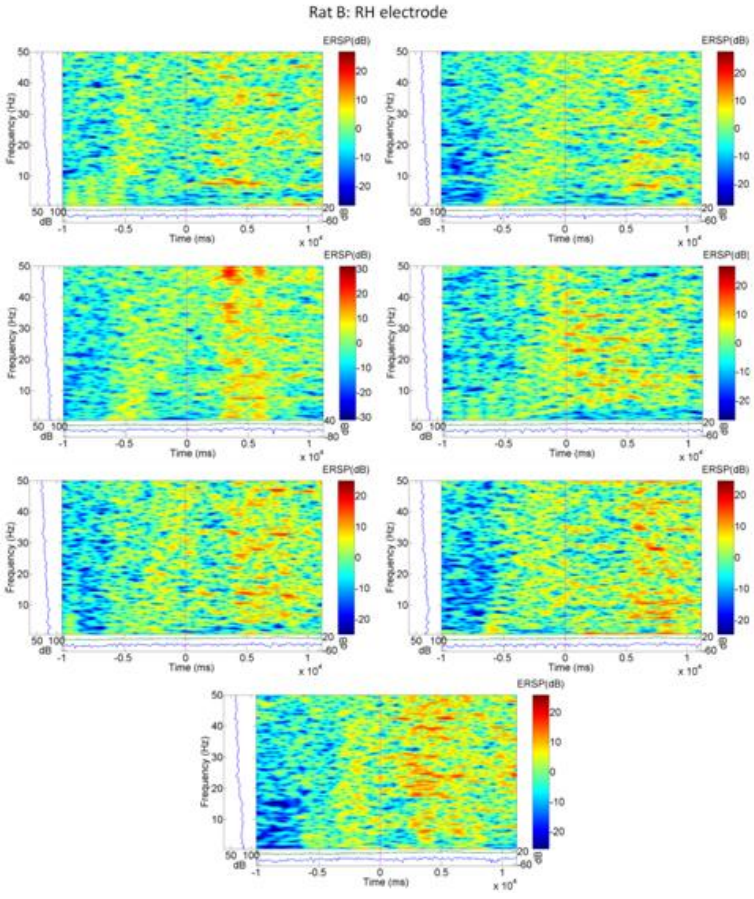

Figure 4. TF plots of the seven 27 seconds peri-ictal segments used from data recorded at the RH electrode from Rat B. Time 0 indicates the seizure onset.

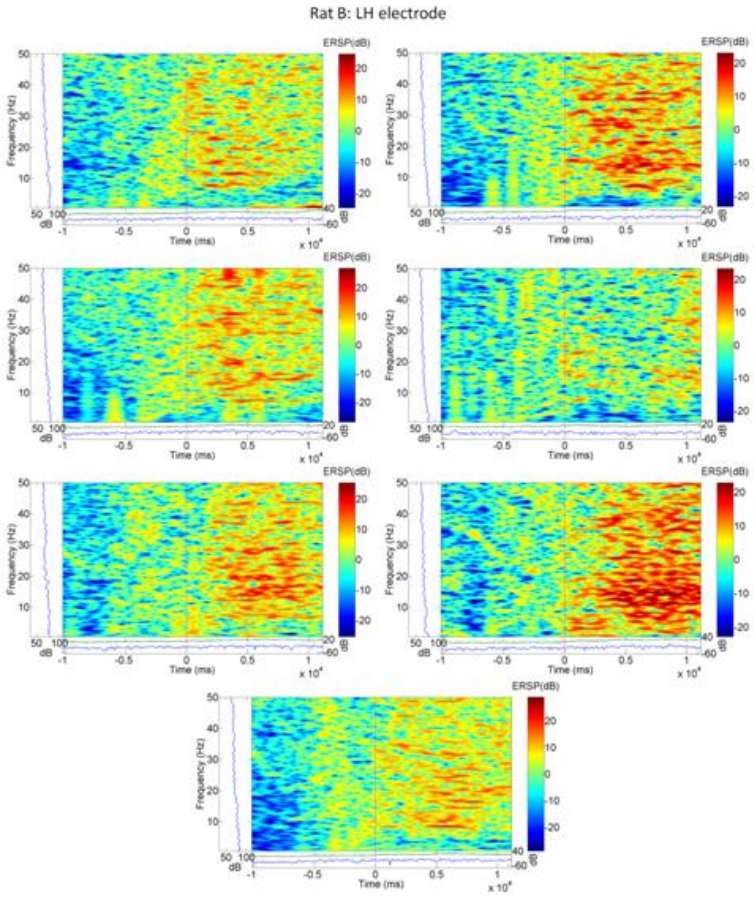

Figure 5. TF plots of the seven 27 seconds peri-ictal segments used from data recorded at the LH electrode from Rat B. Time 0 indicates the seizure onset.

Rat C

Three seizures were recorded for this rat during the period of interest. The realignment procedure resulted in a 22 seconds segment peri-ictal segment (9 seconds pre-ictal and 13 seconds ictal). The TF plots of the seizure for both hippocampi can be seen below (Figures 6,7).

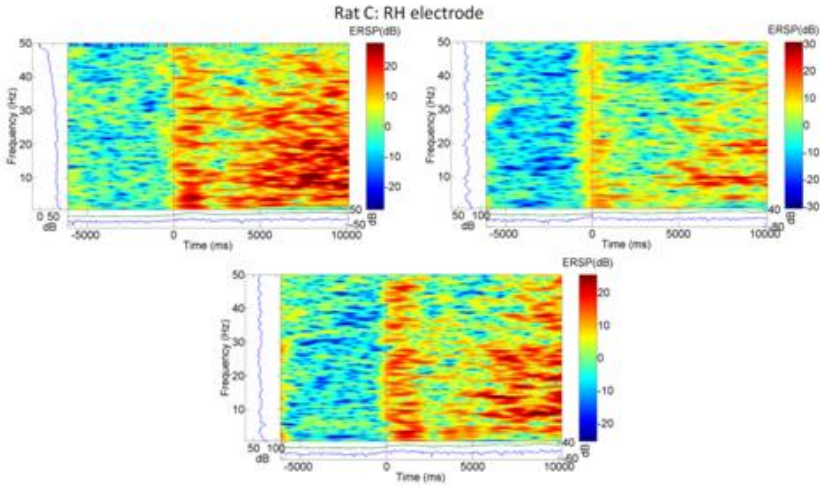

Figure 6. TF plots of the three 22 seconds peri-ictal segments used from data recorded at the RH electrode from Rat C. Time 0 indicates the seizure onset.

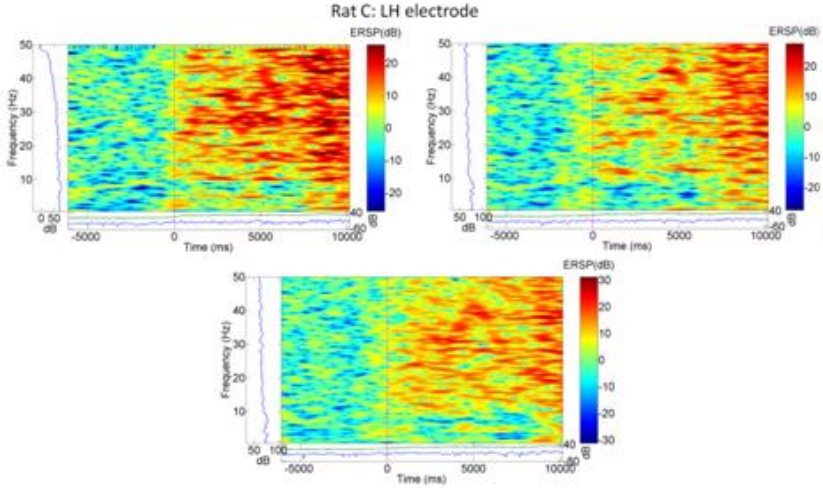

Figure 7. TF plots of the three 22 seconds peri-ictal segments used from data recorded at the LH electrode from Rat C. Time 0 indicates the seizure onset.

Dynamic causal Modelling

The neural mass model

The neural mass model used to predict peri-ictal activity is the canonical microcircuit model (CMC) based on the model by Jansen and Rit (Jansen & Rit 1995). Jansen and Rit's model comprises three cell subpopulations; spiny stellate cells in granular layer IV, pyramidal cells and inhibitory interneurons in extra granular layers (II and III; V and VI). The main difference with respect to the original model is that the CMC considers four subpopulations by splitting the pyramidal cell population into two subpopulations , so it eventually contains distinct superficial and deep pyramidal cell populations occupying the supragranular and the infragranular layers respectively. In addition excitatory spiny stellate cells occupy the granular layers and inhibitory cell the supragranular ones (Figure 3 in Chapter 3).

The EEG measurements were modelled as a weighted average of the postsynaptic potential of the pyramidal cells. A more detailed description of the CMC model can be found in (Moran et al. 2013; Bastos et al. 2012). In this work we use the CMC to explain the evolution of complex cross spectra produced by seizure activity as seen in (Papadopoulou et al. 2015; Cooray et al. 2015).

DCM for cross spectral densities

The analysis described in this section employs a dynamic causal model for cross spectral densities (CSD) , a generalisation of DCM for steady state responses in the complex domain (Friston et al. 2012). In DCM for CSD neuronal activity is summarised in terms of its spectral density when we model a single source or cross spectral density when we model multiple sources. In this work, we

model each single source separately (dr2 in the RH & dl in the LH).

In our previous work (Papadopoulou et al. 2015) a different policy was adopted, where successive time windows were modelled, effectively summarizing the time series with its time–frequency decomposition. This means that we had to invert a model of multiple epochs, which in some cases was computationally very expensive. In order to tackle this problem, in this work we use an alternative scheme, the Bayesian belief updating presented in, where certain parameters were allowed to change between epochs and others are held at the same value.

Bayesian belief updating

Our application of dynamic causal modelling calls upon Bayesian belief updating to track the trajectories of parameters over successive epochs of data that are summarised in terms of their spectral density. This procedure is a simple form of Bayesian filtering – at the between epoch level – based upon a random walk. In brief, Bayesian updating corresponds to using the posterior estimate (expectation) from the preceding epoch as the prior expectation for the current epoch. Similarly, the prior covariance is replaced by the posterior covariance. Because the posterior covariance is always less than the prior covariance, the posterior covariance shrinks over successive epochs and clamps the posterior expectations to a relatively stable value. However, for some connections interest e.g. intrinsic excitatory and inhibitory connections we allow epoch to epoch fluctuations by supplementing the posterior covariance with the initial prior covariance. This allows some parameters to pursue a random walk through parameter space that best accounts for the spectral data. In this

instance, the initial prior covariance corresponds to our beliefs, not about the possible dispersion of parameters but about their epoch to epoch changes. Note that this procedure allows all the parameters to change to a certain extent from epoch to epoch. The key difference between parameters that are and are not expected to change is that the former have a lower bound on their covariance; namely, the initial prior covariance. This procedure provides a time series of posterior parameter expectations.

Bayesian model comparison

DCM was used to compare alternative hypotheses about which sets of parameters were responsible for changes in cross spectral density during seizure onset. Two sets of parameters were allowed to vary between epochs. The first set comprises intrinsic connectivity among the neuronal populations (inhibitory and excitatory) and their time constants; the second set refers to the endogenous afferent activity from other areas (spectral input). We inverted eventually three models for each source in the two hippocampi; the first one allows both set of parameters to vary across time (epochs), the second one allows only the intrinsic connectivity among the neuronal populations and their time constant to vary while the endogenous afferent activity of other regions was kept constant and finally the third one allows the endogenous afferent activity of other regions to vary while intrinsic connectivity among the neuronal populations and their time constant were kept constant. Model comparison was performed among the 3 models for each source in both hippocampi. This procedure was repeated for the three rats.

Results

Model inversion

In the following we will describe the results of the model for both hippocampi in the three rats. We will report the time-frequency representation of observed and predicted data as well as the spectral changes over time of the individual subpopulations. Please note that we are interested in visualizing the relative changes in the period of interest, and not the absolute spectral power nor the perturbations with respect to the baseline level.

RH electrode
(Right Hippocampus, site of the primary lesion)

For the rats A and B the model with the highest evidence was the one allowing for variations of endogenous afferent activity from other areas while the intrinsic inhibitory and excitatory connections were kept constant. For rat C the model with the highest evidence was the one allowing variation of both inhibitory and excitatory connectivity and spectral input. In (Figure 8) we depict the observed and the predicted seizure activity for the RH electrode for the three rats. Even though the winning model for rat C differs from the one of rats A and B, they all involve variation in the endogenous afferent activity from other areas. This suggests that afferent activity from other areas to the seizure onset zone (located in the kainic acid treated RH) is implicated in seizure activity (Cooray et al. 2015; Terry et al. 2012).

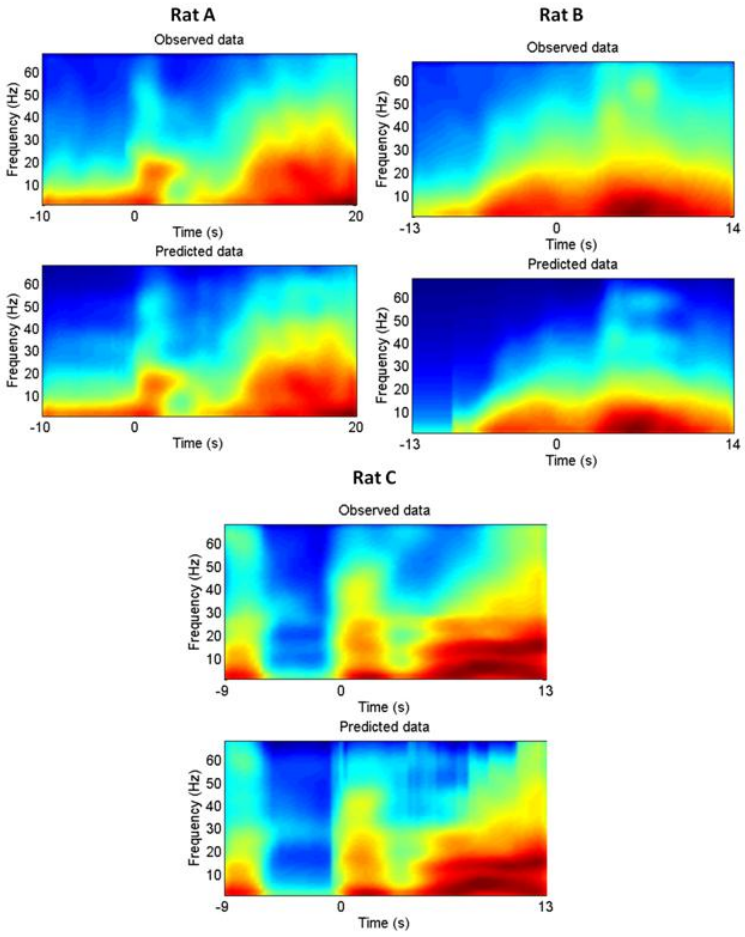

Figure 8. TF representation of observed and predicted seizure activity for the winning models as depicted from the RH electrode, for each of the three rats. The electrographic seizure onset is marked at 0 seconds.

The effect of these changes on the four subpopulations of the CMC model used here for each rat can be seen in the TF plots below (Figures 9-11). Some more variability is seen here across the animals. However, for all the three rats A,B and C an overall increase of the spectral activity is observed for all four subpopulations at the onset (0 seconds).

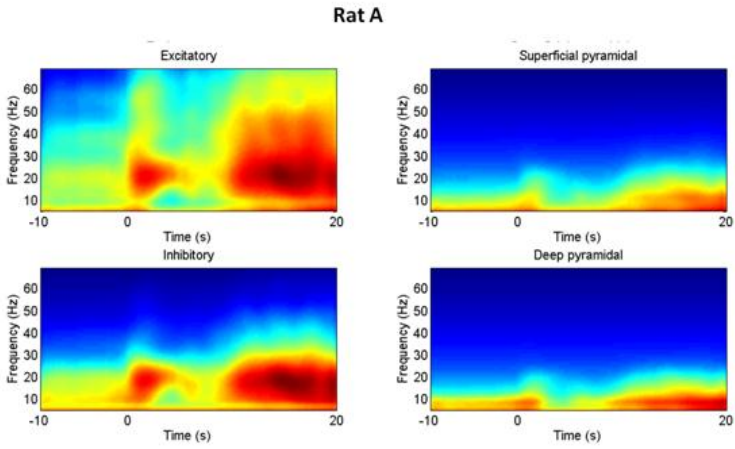

Figure 9. TF representation of the four subpopulations comprising the CMC model of the RH electrode.

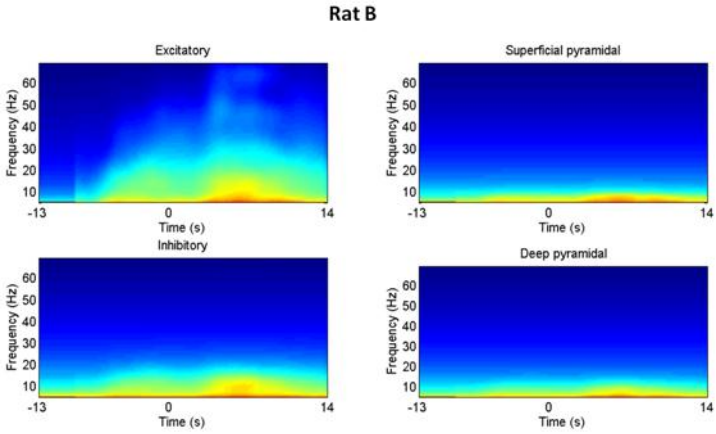

Figure 10 TF representation of the four subpopulations comprising the CMC model as depicted from RH electrode. There is a transient increase of the activity after the seizure onset.

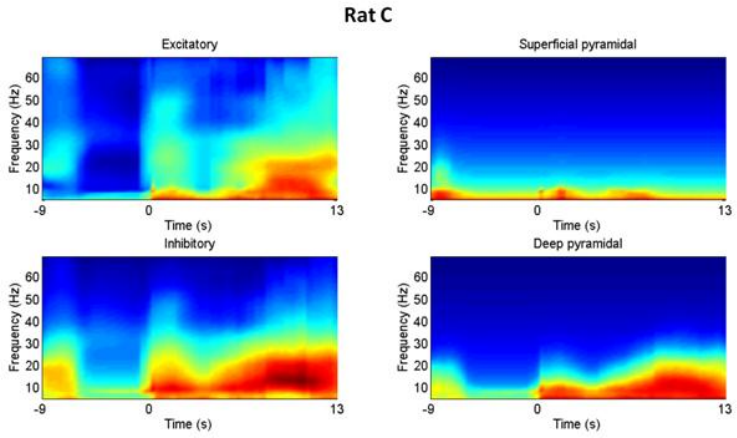

Figure 11. TF representation of the four subpopulations comprising the CMC model as depicted from the RH electrode. There is an overall increase in the activity at the seizure onset.

LH electrode
(Left Hippocampus)

The model with the highest evidence for the for the activity recorded from the LH electrode was different for each rat. For rat A it was the one allowing for variations of intrinsic inhibitory and excitatory connections while endogenous afferent activity from other areas was kept constant. For rat B it was the one allowing for variations of endogenous afferent activity from other areas while the intrinsic connections were kept constant. Finally, for rat C it was the one allowing for variations of both set of parameters. In (Figure 12) one can see the observed and the predicted seizure activity recorded at LH electrode for the three rats. The different winning models- each one revealing distinct underlying mechanisms- may reflect the different timing of the spreading of the lesion from the KA-treated right hippocampus to the left hippocampus for each rat.

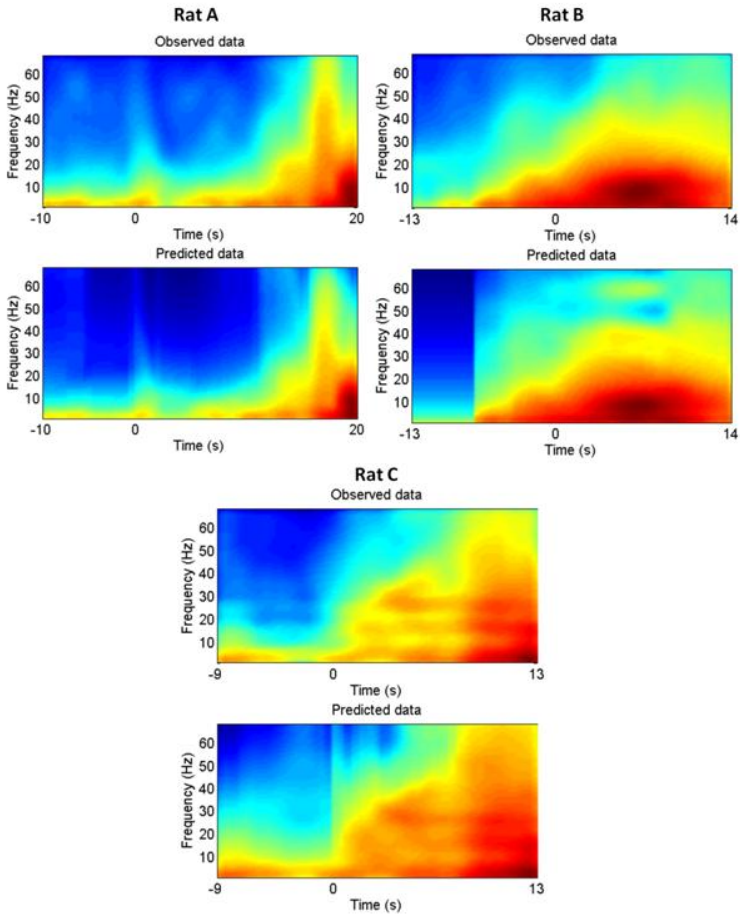

Figure 12. TF representation of observed and predicted seizure activity for the winning models as depicted from the LH electrode, for each of the 3 rats.

Discussion

In this work we have used dynamic causal modelling on a rat model of epilepsy to further investigate the pathophysiology of epilepsy by looking at changes in synaptic efficacy that may underlie the transient change from pre-ictal to ictal states. It has been discussed before that complex phenomena as epileptic seizures span different time scales

varying from milliseconds to days (Bernard et al. 2014). In our previous work we focused in tracking slow modulations to explain seizure onset (Papadopoulou et al. 2015). The methodological advance of this work was the incorporation of Bayesian upgrade scheme as seen in (Cooray 2015) which allowed for faster inversions of otherwise really computationally expensive models.

Our approach was always able to efficiently reproduce peri-ictal activity, albeit the winning model indicated by BMS was not always the same across the three rats.

The interpretation of these results will involve investigating whether these changes of parameters over time can be explained by different combinations of a few recurrent components, characteristic of the dynamic changes underlying seizure onset.

The second issue involves the possible interpretation of the differences in the pathophysiology and manifestations of epilepsy across animals in terms of these parameters. Such differentiation, stemming from the exact same protocol applied to all animals, is still unexplained. A working hypothesis in this sense can be that a clustering in the parameter space can separate the rats who developed more seizures from the rats that developed less seizures, or the rats which displayed more convulsive seizures and the rats that displayed more subclinical seizures.

If successful, this approach could easily be extended to the study of other pathophysiological and cognitive modulations of brain activity.

References

Bastos, A.M. et al., 2012. Canonical microcircuits for predictive coding. *Neuron*, 76(4), pp.695–711.

Bernard, C. et al., 2014. Modern concepts of seizure modeling. *International review of neurobiology*, 114, pp.121–53.

Cooray, G., 2015. Dynamic Causal Modelling of Electrographic Seizure Activity using Bayesian Belief Updating. *submitted*.

Cooray, G.K. et al., 2015. Characterising seizures in anti-NMDA-receptor encephalitis with Dynamic Causal Modelling. *NeuroImage*.

Friston, K.J. et al., 2012. DCM for complex-valued data: cross-spectra, coherence and phase-delays. *NeuroImage*, 59(1), pp.439–55.

Jansen, B.H. & Rit, V.G., 1995. Electroencephalogram and visual evoked potential generation in a mathematical model of coupled cortical columns. *Biological cybernetics*, 73(4), pp.357–66.

Moran, R., Pinotsis, D.A. & Friston, K., 2013. Neural masses and fields in dynamic causal modeling. *Frontiers in computational neuroscience*, 7, p.57.

Papadopoulou, M. et al., 2015. Tracking slow modulations in synaptic gain using dynamic causal modelling: validation in epilepsy. *NeuroImage*, 107, pp.117–26.

Raedt, R. et al., 2009. Seizures in the intrahippocampal kainic acid epilepsy model: characterization using long-term video-EEG monitoring in the rat. *Acta neurologica Scandinavica*, 119(5), pp.293–303.

Terry, J.R., Benjamin, O. & Richardson, M.P., 2012. Seizure generation: The role of nodes and networks. *Epilepsia*.

Chapter 5

Estimating directed connectivity from cortical recordings and reconstructed sources

Abstract

In cognitive neuroscience, electrical brain activity is most commonly recorded at the scalp. In order to infer the contributions and connectivity of underlying neuronal sources within the brain, it is necessary to reconstruct sensor data at the source level. Several approaches to this reconstruction have been developed, thereby solving the so-called implicit inverse problem (Michel et al. 2004). However, a unifying premise against which to validate these source reconstructions is seldom available. The dataset provided in this work, in which brain activity is simultaneously recorded on the scalp (non-invasively) by electroencephalography (EEG) and on the cortex (invasively) by electrocorticography (ECoG), can be of a great help in this direction. These multimodal recordings were obtained from a macaque monkey under wakefulness and sedation. Our primary goal was to establish the connectivity architecture between two sources of interest (frontal and parietal), and

to assess how their coupling changes over the conditions. We chose these sources because previous studies have shown that the connections between them are modified by anaesthesia (Boly et al. 2012). Our secondary goal was to evaluate the consistency of the connectivity results when analyzing sources recorded from invasive data (128 implanted ECoG sources) and source activity reconstructed from scalp recordings (19 EEG sensors) at the same locations as the ECoG sources. We conclude that the directed connectivity in the frequency domain between cortical sources reconstructed from scalp EEG is qualitatively similar to the connectivity inferred directly from cortical recordings, using both data-driven (directed transfer function; DTF) and biologically grounded (dynamic causal modelling; DCM) methods. Furthermore, the connectivity changes identified were consistent with previous findings (Boly et al. 2012). Our findings suggest that inferences about directed connectivity based upon non-invasive electrophysiological data have construct validity in relation to invasive recordings.

Introduction

Oscillatory synchronous activity of local or distributed neuronal populations is an ubiquitous phenomenon in neural systems and may represent a key neuronal mechanism underlying cognitive or perceptual processing (Buzsáki 2006). Neuronal oscillations are traditionally measured by EEG, recordings of local field potentials (LFP), or multi-unit recordings. Beyond the depiction of this neuronal synchronization, identifying driver-response relationships between interconnected brain sources and understanding their directed interactions and dynamics can also inform the functional architecture of sensory and cognitive processing, in both healthy and diseased brains (Bressler 1995). There are various measures that have been developed to identify

driven and driving interactions between brain sources. These measures vary from linear to nonlinear, bivariate to multivariate, and many rely on the Granger causality principle (Granger 1969). This approach quantifies improvement in the predictions of a time series, given its past, when information from the past of another time series is considered (Baccalá & Sameshima 2001; Kamiński & Blinowska 1991). These measures, which are based upon statistical dependencies in data over time, are thought to provide measures of directed functional connectivity. Another approach, DCM (David and Friston 2003), is used to infer (directed) effective connectivity, that is, how one source or neural system influences another. The main distinction between DCM (model-based) and Granger-based (data-based) methods is that DCM is based on biologically plausible neural mass models that are inherently causal in nature. In other words, the question is not whether there is (Granger) causality – but which (causal) models best accounts for data. This enables one to identify how a system of pre-specified neuronal populations generates the measured signal (Schoffelen and Gross 2009), and to compare different hypotheses or architectures in terms of their model evidence.

Measuring connectivity at the scalp level can be informative but one has to be careful about its interpretation in terms of brain dynamics. This is because scalp data sees neuronal sources through a specific 'lens' which distorts, mixes and loses information about the exact location of the underlying sources. A fundamental problem with scalp recordings is electrical conduction through the head volume. This means that instead of recording brain activity from one specific brain source, each sensor measures a linear superposition of signals from all over the brain. This mixing introduces instantaneous correlations in sensor data, so that the

interpretation of directed connectivity has to proceed with caution because spurious connectivity patterns can arise. In short, scalp recordings provide an indirect measure of source activity (with rather low signal to noise ratio), which is not easily interpretable. A critical assessment of directed connectivity measures based on EEG recordings can been found in Haufe et al. (2013). The authors report a series of simulations to assess the sensitivity of sensor-based functional connectivity when inferring source interactions from synthetic EEG recordings.

To make inferences about directed connectivity among brain sources one can either apply source reconstruction techniques to estimate source activity or use intracranial EEG (iEEG) data from electrodes implanted in human subjects (e.g., patients with brain tumours and epilepsy). Invasive iEEG recordings are difficult to obtain but they have been of great help, not only as a part of pre-surgical evaluation for patients, but also in the study of responses induced by cognitive tasks. These responses would be almost impossible to study with high precision on the scalp level. Finally, invasive (but rare) electrophysiological recordings can be used to validate the reconstruction and modelling of (readily available) sensor level data. This is one of the aims of our paper.

There are two prevalent approaches to measuring directed connectivity in the spectral domain. These are exemplified by (data-based) DTF (Kamiński and Blinowska 1991) and (model-based) biologically informed DCM (Friston et al. 2003). The first approach generalizes the concept of Granger causality to the spectral domain. It has been applied to iEEG recorded from patients with epilepsy: i) around the seizure onset, to identify the putative epileptogenic zone (van Mierlo et al. 2011; Papadopoulou et al. 2012) or ii) during

the performance of cognitive tasks, to investigate distributed neuronal processing (Brázdil et al. 2009; Flinker et al. 2015). DTF has also been used to infer directed functional connectivity between reconstructed sources (RS) in humans (Dai et al. 2012) and from intracranial recordings of monkeys (Liang et al. 2000). Similar approaches have addressed connectivity at the source level using Independent Component Analysis (Haufe et al. 2010), where DTFs have also been computed (Gómez-Herrero et al. 2008; Cantero et al. 2009).

In contrast to these data-based measures, DCM uses neurobiologically plausible models that are fitted to empirical observations, which are then subjected to Bayesian model comparison or selection (BMS). BMS allows one to evaluate competing hypotheses (or architectures) in terms of their Bayesian model evidence or marginal likelihood. In brief, DCM treats the brain as a nonlinear dynamical system that receives inputs and generates outputs. In this setting, an experiment is regarded as a perturbation (induced by the inputs) of coupled electromagnetic sources, which produces source-specific responses (Kiebel et al. 2009). The basic idea behind the method is to model the influence of each source on others – and identify the mechanisms that underlie distributed network responses. Dynamic causal modelling has been applied to both functional magnetic resonance imaging (fMRI) and magnetoencephalography (MEG)/EEG data.

DCM for MEG/EEG is based on a spatiotemporal generative model of electromagnetic brain activity, where the temporal dynamics are described by neural mass models of equivalent current dipole (ECD) sources, and their spatial expression at the sensor level is modelled by parameterized lead-field functions. Generally a DCM comprises a model of interacting

cortical sources, where each source corresponds to a canonical circuit of neural populations, and its electromagnetic output is generated by the modeled average depolarization of pyramidal cell populations. These electromagnetic outputs are then passed through an electromagnetic model of the head, accounting for volume conduction effects, to finally generate predictions at the M/EEG sensor level (Fastenrath et al. 2009). This process is called the forward problem, as opposite to the inverse problem which infers the activity in the brain starting from scalp recordings. Equipping neuronal models with a lead field effectively subsumes the source reconstruction problem into model inversion or fitting. In other words, DCM can estimate directed effective connectivity among sources using sensor data directly. DCM has been extensively applied to sensor space data to infer directed effective connectivity in healthy and diseased subjects (e.g., Garrido et al. 2008; Garrido et al. 2009; Herz et al. 2012; Herz et al. 2013; Herz et al. 2014). It has also been applied to LFP recordings in rodents (Moran et al. 2009; Moran et al. 2011; Moran et al. 2015) and intracranial electroencephalographic (iEEG) in humans (Papadopoulou et al. 2015). In some applications, DCM is applied to source reconstructed data in source space, as opposed to modelling responses in sensor space. This allows one to make inferences about connectivity among a predefined set of sources, without having to consider all the sources generating sensor data (e.g. Boly et al. 2012). This is the approach we adopt in the current paper, as we wanted to focus on a subset of sources for which we had invasive or direct recordings.

In this work we analyzed ECoG and source reconstructed data from one monkey during wakefulness and propofol anaesthesia. Our aims were twofold; first, we wanted to see whether directed connectivity in the frequency domain

between cortical sources reconstructed from scalp EEG is qualitatively similar to estimates based on ECoG recordings, using both DTF and DCM. Our second focus was on how the information flow between two pre-specified sources (frontal and parietal) was modulated in wakefulness and sedation.

It is worth mentioning that our aim is to compare the connectivity results obtained by reconstructed sources on one hand and the corresponding intracranial recordings on the other; a comparison of data-driven (DTF) and biophysical (DCM) models for directed dynamical connectivity is not the scope of the present work.

Methods

Data

These data are part of a dataset collected at a workshop titled “Controversies in EEG source imaging”, held in August 2014 at the University of Electronic Science and Technology in Chengdu, China, with the aim of discussing the major issues at stake when brain activity is recorded or modelled as electrical potentials. All the simulations and data are available from the following website http://neuroinformation.incf.org/ and will be described in detail in a technical report. Specifically for this study we used publicly available data (http://neurotycho.org/) that were originally analyzed and published in Yanagawa et al. (2013). ECoG and EEG signals were simultaneously recorded from the same monkey (*Macaca Mulatta*). The monkey was implanted with a 128 channel ECoG array that covered the lateral cortical surface of the left hemisphere with 5 millimeter spacing. EEG signals were recorded from 19 channels. The EEG electrodes locations conformed to the 10-20 system without Cz (to avoid interference with an ECoG

connector). ECoG and EEG data were sampled at 1000Hz. The monkey was seated in a primate chair with eyes closed and both arms constrained – and injected with an anaesthetic drug (propofol) during the recording to induce loss of consciousness.

In the following we report the steps for the leadfield reconstruction. Using BrainSuite2, a T1 MRI was corrected for intensity bias and segmented into tissues (i.e. grey and white matter) and cerebrospinal fluid. The white/grey matter interface was chosen as the source space model for EEG/ECoG, i.e., each node of the mesh was a potential source. The head was then divided into brain (enclosed by the pial surface), brain plus surrounding cerebrospinal fluid, skull and skin. This segmentation was checked and adjusted manually by an expert. The volume conductor model was based on the above segmentation, assuming constant electrical conductivities within each compartment. The skull-to-other conductivity ratio was set to 1/25. 1mm-thick silicone strips (housing the ECoG electrodes) were also included in the model because silicone has very low conductivity and can influence EEG signals. An X-ray 2D image was spatially registered to the pial surface. The transformed electrode positions were then projected onto the 3D pial surface. The silicone stripes were modelled according to Figure 1 in Nagasaka et al. (2011). These were modelled as a grid of 1-mm thick silicone rings of 3.5 mm radius, each surrounding an electrode of 2.0 mm radius. The conductivity of the silicone was set to a negligible value relative to the other compartments. The EEG electrodes were manually located on the monkey's scalp using IMAGIC (www.neuronicsa.com) and projected onto their corresponding mesh faces.

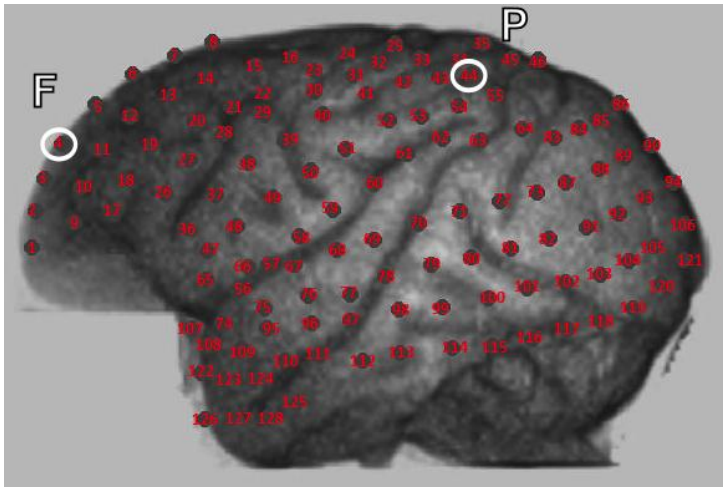

Figure 1. Layout of the ECoG contact locations. The frontal (F) and parietal (P) channels used in this study are indicated by white circles.

Tetrahedral meshes were created from the surfaces of the head model using Tetgen 2.0 (open source). Both EEG and ECoG lead fields were calculated using NeuroFEM, a program for computing lead fields using the Finite Element Method, which is part of the SimBio software package (*SimBio Development Group. "SimBio: A generic environment for bio-numericalsimulations",*https://www.mrt.uni-jena.de/simbio). Source reconstruction in the time domain (for the EEG data) was performed by LORETA (free academic software for source localization of EEG data: http://www.uzh.ch/keyinst/loreta)(Pascual-Marqui et al. 1994). The estimated current sources were constrained to be perpendicular to the cortical surface. No absolute value or norm was taken for the dipole or the resulting data, so no period doubling effects are to be expected. EEG sources were reconstructed in both hemispheres. For this study we only retained the RS nearest to the ECoG channels considered in the connectivity analyses. The correspondence between cortical and reconstructed activity was assessed by

means of canonical correlation analysis to provide a goodness of fit measure (results not shown here).

The pre-processing steps for both ECoG and RS included average reference removal, notch filtering at 50Hz, artefact removal by visual inspection and local detrending with the L1 norm technique (Kim et al. 2009). In the current validation study we restrict our analysis to a single pair of sources, a frontal source (**F**) and a parietal source (**P**), as indicated in Figure 1. This choice was motivated by a previous study using RS from scalp EEG recordings in humans that measured directed connectivity between cortical sources in these areas (Boly et al. 2012), and functional connectivity in anesthetized macaque monkeys (Moeller et al. 2009; Barttfeld et al. 2015). 30 seconds of brain activity were used for each condition (wakefulness and anaesthesia).

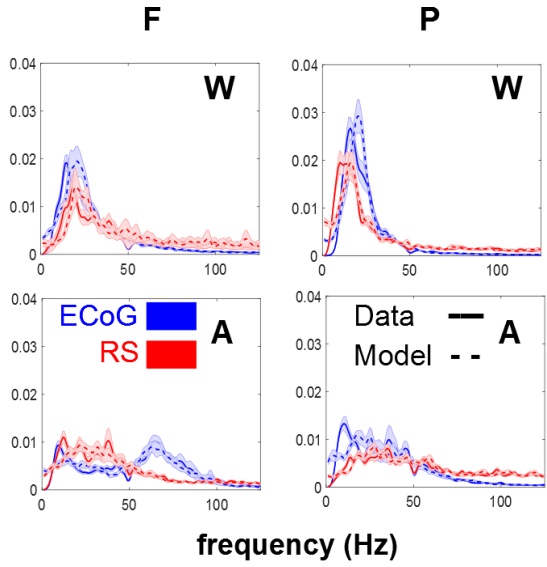

Figure 2. Power spectral densities of real data (full line) and data simulated with the coefficient of an autoregressive model of order 7 of the real data (dashed line) for ECoG (blue) and reconstructed sources (red). Left column: frontal source (F). Right column: parietal source (P). Top panels: wakefulness (W). Bottom panels: anaesthesia (A).

The spectra of the two channels in the two conditions are reported in Figure 2, together with the spectra of the data modelled with an autoregressive model of the composite system of the two sources, of order 7, as the one used for DTF.

Asshown in http://wiki.neurotycho.org/EEG-ECoG_recording EEG signals don't include high frequency (> 60Hz) components of the ECoG signal.

Directed Transfer Function

The DTF is a multivariate directed functional connectivity measure, usually based on an autoregressive model (AR) in the frequency domain (Kamiński and Blinowska 1991). The AR model is of the form

$$\sum_{j=0}^{p} \hat{A}_j x_{t-j} = e_t \qquad (1)$$

where $x_t = (x_{1,t}, x_{2,t}, ..., x_{k,t})$ is a vector of k-channel multivariate processes, $e_t = (e_{1,t}, e_{2,t}, ..., e_{k,t})$ is a vector of multivariate uncorrelated white innovations or noise processes and $\hat{A}_1, \hat{A}_2, ...\hat{A}_p$ are the $k \times k$ matrices of model coefficients. Multiplying both sides of (1) by x_{t-s}^T and taking the expectation returns the coefficients $\hat{A}_i$, as follows

$$\hat{R}(-s) + \hat{A}_1 \hat{R}(1-s) + ... + \hat{A}_p \hat{R}(p-s) = 0 \qquad (2)$$

where $\hat{R}(s) = E[x_t, x_{t+s}^T]$ is the covariance matrix for time lag s. To characterize Granger causal coupling between signals in the spectral domain, the Fourier transformation of

equation (1) is calculated, where the transform functions are of the form $\hat{X}(z) = \hat{H}(z)\hat{E}(z)$ where

$$\hat{H}(z) = (\sum_{j=0}^{p} \hat{A}_j e^{-2\pi f \Delta t})^{-1} .$$

The DTF then is derived from the transfer matrix and can be expressed as

$$DTF_{ij}(f) = \left|H_{ij}(f)\right|^2 \quad (3)$$

Usually, the DTF is normalized with respect to the incoming to the incoming information flow so that it takes the form

$$DTF_{ij}(f) = \frac{\left|H_{ij}(f)^2\right|}{\sum_{m=1}^{K}\left|H_{im}(f)\right|^2} \quad (4)$$

Consequently, the element $H_{ij}(f)$ of the matrix describes the connection between the *j*-th input and the *i*-th output at each frequency. The values of the normalized DTF are located in the range [0, 1] where a high value indicates a greater information transfer in the direction $j \rightarrow i$ and a low value indicates little or no transfer. For the present study we used 7 as the autoregressive model order, as determined by the Bayesian Information Criterion.

In a recent Opinion paper, Kaminski and Blinowska (2014), the inventors of DTF, postulated that this measure is not sensitive to volume conduction, since it is insensitive to phase shifts. However, while it is true that a phase shift in sensor data indicates information transfer, no inference can be made about where the implicit sources are located, except in special cases in which the experimental protocol or

the anatomy ensure that the activity of a single source is expressed at a single sensor (Plomp et al. 2014).

As mentioned above, DTF is applied to two sources, a frontal and a posterior one, for each level of consciousness, using 15 non-overlapping segments of 2 seconds.

Dynamic Causal Modelling

For this study we used DCM for cross-spectral density (CSD), which is a generalization of DCM for steady state responses. All our analyses used the standard procedures described in (Friston et al. 2012). CSD is the Fourier transform of the cross-correlation function and can be thought of as reporting the correlations at each frequency. CSD therefore describes the similarity between two signals, that is, how much power is shared for each frequency.

The neural mass model used here was the LFP variant. This particular neural mass model has been used previously in modelling intracortical local field potentials from rats, to assess changes in directed effective connectivity under pharmacological manipulations (Moran et al. 2009; Moran et al. 2015). It has also been used as a generative model for non-invasive EEG studies, in source-reconstructed data from frontal and parietal cortices during normal wakefulness, propofol-induced mild sedation and loss of consciousness in humans (Boly et al. 2012).

One can regard each neural mass as a cortical source, where each source comprises three subpopulations that contribute to the ongoing dynamics. These subpopulations include spiny stellate cells in the granular layer and pyramidal cells and inhibitory interneurons in supragranular layers.

Each of the subpopulations is modelled with pairs of first order differential equations of the following form :

$$\begin{aligned} \dot{x}_\nu &= x_1 \\ \dot{x}_1 &= \kappa H(E(x)+C(u)) - 2\kappa x_1 - \kappa^2 x_\nu \end{aligned} \tag{5}$$

The column vectors x_ν and x_1, correspond to the mean voltages and currents where $E(x)$ and $C(u)$ correspond to endogenous and exogenous inputs respectively that the presynaptic input to each subpopulation comprises (see Moran et al., 2009).

The nodes (sources) of DCM model sources in the brain are connected by (extrinsic) forward and backward connections according to anatomical connectivity rules established in (Felleman and Van Essen 1991). Feedforward connections target the granular layer, while feedback connections target the superficial and deep layers (Bastos et al. 2012). More details about the different models that can be used within the DCM framework can be found in (Moran et al. 2013).

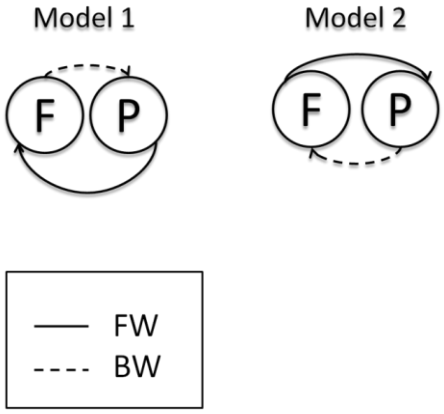

Figure 3. The two architectures for connections between the sources of interest tested with DCM.

Here, we first use DCM to test hypotheses about the connectivity architecture between the two sources of interest in frontal and parietal regions. We tested two physiologically plausible models. Our first model connects the parietal to the frontal source by forward connections and frontal to parietal with backward connections, while the second model constitutes the reverse architecture (Figure 3).

The designation of fronto-parietal and parieto-frontal connections as backward and forward is based on the functional asymmetries in the anatomy and physiology of projections – extrapolating from the visual system. A brief review of this evidence, from the point of view of the extended motor system can be found in (Shipp et al. 2013).

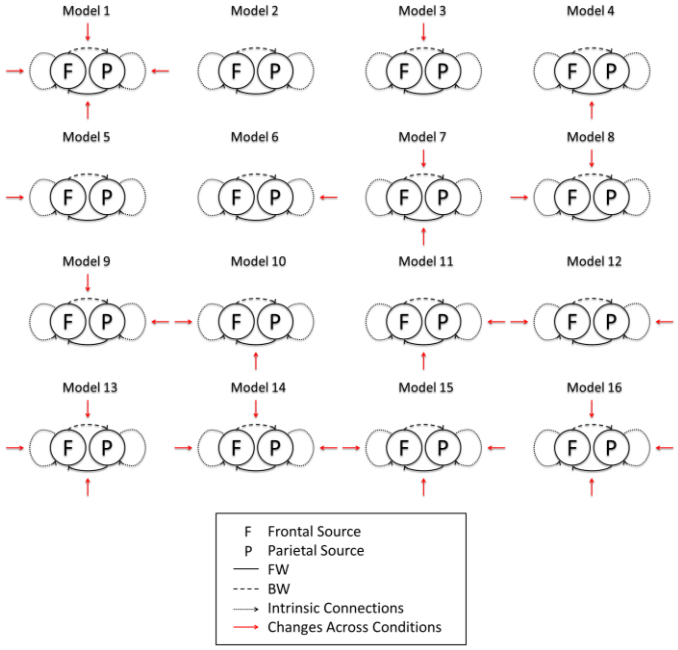

Figure 4. The sixteen possible models tested by DCM to explain changes in connectivity from wakefulness to anaesthesia.

We inverted the two models using both sets of empirical data and then performed (fixed effects) Bayesian model selection (BMS) to identify the most likely model. We then modelled the condition-specific effects under the best model, corresponding to wakefulness and anaesthesia. These effects were modelled in terms of changes in intrinsic and extrinsic connections relative to the first condition (wakefulness) (Figure 4).

Results

In this study we evaluated directed connectivity in the frequency domain between two sources located in frontal and posterior brain regions, and determined how the information flow between the two sources is modulated by anaesthesia. This evaluation used both ECoG and reconstructed source activity, enabling us to assess the validity of connectivity estimates based upon non-invasive EEG signals.

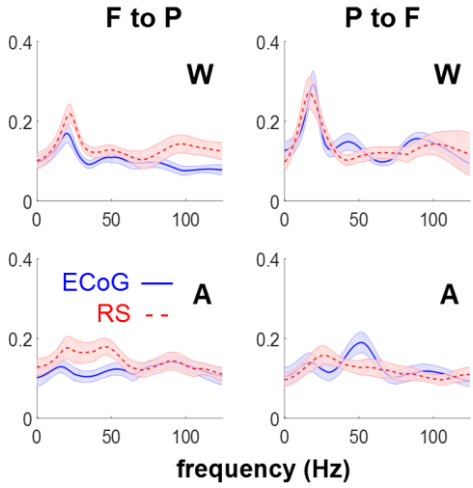

Figure 5. DTF plotted against frequency in the two directions in Wakefulness (W) and Anaesthesia (A) for ECoG and RS. Shaded areas indicate standard errors.

DTF quantifies information flow across brain areas for each frequency bin. The curves for each condition and modality are reported in (Figure 5). We have assessed the significance of the modulations corresponding to the spectral interval [3 40] Hz with a nonparametric Wilcoxon Rank Sum test. Significant decrease during loss of consciousness is reported in the connectivity from the parietal to the frontal source, for both the ECoG and reconstructed EEG source activity ($P<0.02$, FDR corrected). The other modulations, tested across consciousness state and across imaging modalities, were not significant.

DCM and BMS of the directed effective connectivity between the same sources identified model 1 as the most plausible, with a forward connection from the parietal to frontal region and backward connections from the frontal to the parietal region (Figure 3). The difference between the best and next best model was much greater than three reflecting strong evidence in favour of the first model over competing hypotheses. The same winning model was identified for ECoG and reconstructed EEG source activity.

For the second part of our DCM analysis, we modelled condition-specific effects in terms of all the possible combinations of condition-specific changes in the forward connections, the backward connections, neither or both. BMS identified model 1 as the winning model (Figure 4). This model allows for changes all the connections. As before, the same winning model was identified for both ECoG and reconstructed EEG sources. The differences in log evidence among the four models were comparable for the invasive data and to the reconstructed EEG data. This suggests that there is roughly the same amount of information in both modalities when it comes to disambiguate the models or hypotheses. This is reflected also the posterior probabilities

(left panel of Figure 6) over models, which are also comparable.

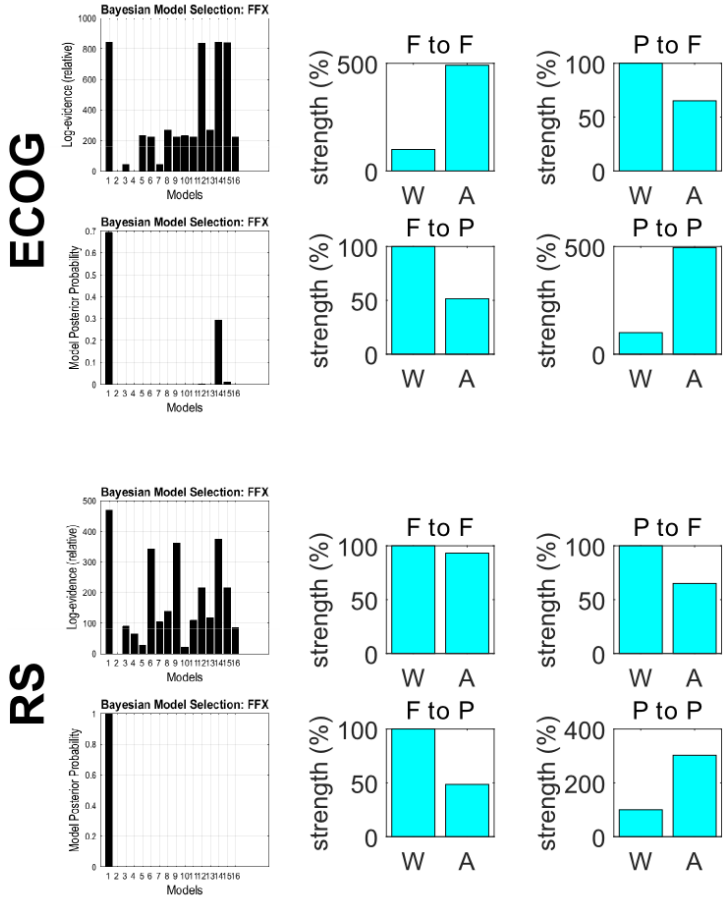

Figure 6. Log evidences and posterior probabilities (left) and changes in connectivity in the winning model (model 1, right) for ECoG sources (top) and reconstructed sources (bottom) across the two conditions: Wakefulness (W) and Anaesthesia (A), as estimated by DCM.

Looking at the condition-specific effects on the extrinsic connectivity (Figure 6, right panel), the parameter estimates based upon the ECoG data concur with the changes in DTF; namely, a decrease is seen in both forward connectivity from the parietal to the frontal source, and in backward

connectivity from the frontal to the parietal source. At the same time a strong increase in self connections in anaesthesia is reported in both sources for ECoG; a slight decrease in the frontal source and a moderate increase in the parietal source for reconstructed activity. These changes are relative to the 100% connectivity strength in the wakefulness condition.

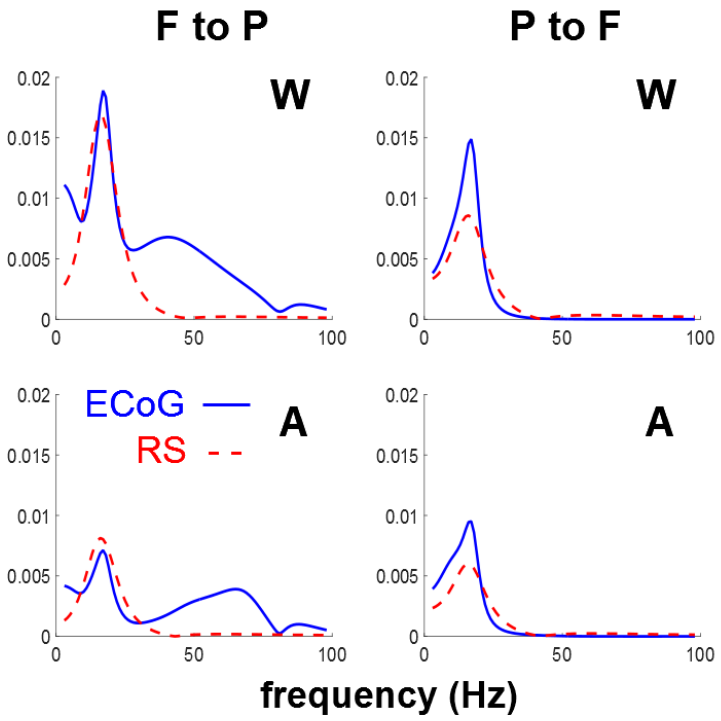

Figure 7. Directed Transfer functions obtained from DCM under the winning model in the two conditions: Wakefulness (W) and Anaesthesia (A) for ECoG and RS.

One interesting aspect of DCM is that we can estimate the DTF implicitly from the condition-specific effects on the parameters. In other words, given the model parameters, we can compute the associated directed transfer functions between the sources, as shown in Figure 7. This figure uses the same format as Figure 5. The fact that directed transfer

functions (and Granger causality) can be derived from the DCM results speaks to the fact that Granger causality and directed transfer functions are essentially data features (hence data-led measures), and not the model attributes responsible for directed information flow. It is pleasing to note that, qualitatively, the data-based DTFs and those based upon DCM parameter estimates show the same dependency on experimental condition. Higher DTF values at frequencies higher than the main peak are observed in from the frontal to the parietal source for electrocorticogram but not for the reconstructed sources. The forms of the DTFs are more constrained under DCM, because they have to be produced by a biologically plausible mechanism. Furthermore, the DCM transfer functions have been modulated by the spectral power of the innovations (which is also estimated). Note that the autoregressive evaluations of DTFs do not estimate the spectral density of the innovations, which are assumed to be white (see equation 1).

Discussion

In a previous study that analyzed these data with directed functional connectivity, all possible pairs of ECoG sources (with a bipolar montage) were considered (Yanagawa et al. 2013). Functional connectivity differed significantly between conscious and unconscious states in all combinations of cortical sources, with the most dramatic change occurring for the transfer functions that fell into a specific spectral domain across conditions. This motivated the authors to look for large-scale inter-region interactions over the entire cortex by grouping the bipolar channels in 8 cortical regions, after which spectral Granger causality was computed for each pairwise combination. The changes in connectivity patterns after this grouping confirmed that the spectral

changes due to modulations of consciousness affected large-scale communications across the entire cortex.

Here we focused on a pair of sources since in many experiments, in particular event-related ones, only a few sources are considered, and in order to apply DCM between two regions known to play a distinct joint role in wakefulness versus anaesthesia.

In this study, we have shown that the directed connectivity in the frequency domain between cortical sources reconstructed from scalp EEG is qualitatively similar to, and statistically undistinguishable from, the connectivity inferred directly from cortical recordings. The modulations of DTFs across frequency are qualitatively the same (although in a few cases the peaks differ slightly in position or width). Concerning the effects of the anaesthesia, the same pattern emerged from electrocorticographic and reconstructed sources, with a decrease in the information flow from the parietal to the frontal source. This modulation is in general agreement with previous literature (Lee et al. 2009; Ku et al. 2011; Boly et al. 2012). This comparison must stay qualitative since the studies mentioned above consider human subjects and scalp EEG.

Dynamic causal modelling produced Bayesian model comparisons that were consistent between electrocorticograms and reconstructed sources. These models explained the decrease in coupling from parietal to frontal sources in terms of condition-specific changes in extrinsic (forward and backward) connectivity with the frontal source as well to changes in intrinsic connectivity at both sources. In these analyses, Bayesian model selection based on the invasive and non-invasive data was again consistent; however, quantitative connectivity changes

following inversion of the EEG and ECoG data showed opposite changes in extrinsic and intrinsic connectivity but similar directed transfer functions. We mention this discrepancy to illustrate that the quantitative estimates of effective connectivity can, in some instances, depend upon the nature of the data, especially when there is a conditional dependency among parameter estimates. In principle, one would base their inferences on all the data at hand and model both the ECoG and EEG data together. In this setting, the most precise or informative data would supervene in terms of model comparison and parameter estimates (the model comparison results in Figure 5 would suggest that the ECoG data were more precise). In more realistic DCM analyses, one generally includes several sources to disambiguate between explanations based upon reciprocal changes in intrinsic and extrinsic connectivity. One of the characteristics of DCM is that it can also model hidden sources; for example the thalamic sources in Boly et al. (2012). The inclusion of hidden sources is sometimes required to adjudicate among different hypothetical architectures, using Bayesian model selection in the usual way. Crucially, this is not an option with data-led measures of directed functional connectivity. Further discussion of the relationship between data-driven functional connectivity in the spectral domain and DCM based measures of effective connectivity can be found in Friston et al. (2014).

The adequacy or quality of any model is generally established through Bayesian model comparison. Good models have a high evidence and entail a level of complexity that is suitable for the data at hand. The DCM of source activity has been refined over many years and provides the appropriate level of detail – in terms of the number of sources and parameters. These parameters include not just aspects of the underlying neuronal (connectivity and

synaptic) architecture but how neuronal activity is measured. For example, the contribution of different neuronal populations to different sorts of sensors is accommodated through free parameters, that scale the relative contributions (with a prior bias towards superficial populations).

Being aware of the limitations of single-subject studies, we do not infer any pathophysiological explanations from our results. Also, a task protocol with more localized sources would definitely provide additional insight. Nonetheless this unprecedented recording setup provides a valid support for the exploratory analysis that we performed with the sole protocol available at the moment, which allowed us to explore modulations in steady-state activity. It is worth to recall that whenever activity has to be estimated or disambiguated with a fine spatial resolution, a large number of scalp electrodes is recommended.

Our provisional results suggest that directed connectivity in the frequency domain between cortical sources reconstructed from scalp EEG is qualitatively similar to the connectivity inferred directly from cortical recordings, using both functional and effective connectivity measures. These findings advocate that inferences about directed connectivity based upon non-invasive electrophysiological data can have construct validity in relation to invasive constructs.

References

Baccalá, L.A. & Sameshima, K., 2001. Partial directed coherence: a new concept in neural structure determination. *Biological cybernetics*, 84(6), pp.463–74.

Barttfeld, P. et al., 2015. Signature of consciousness in the dynamics of resting-state brain activity. *Proceedings of the National Academy of Sciences*, p.201418031.

Bastos, A.M. et al., 2012. Canonical microcircuits for predictive coding. *Neuron*, 76(4), pp.695–711.

Boly, M. et al., 2012. Connectivity changes underlying spectral EEG changes during propofol-induced loss of consciousness. *The Journal of neuroscience : the official journal of the Society for Neuroscience*, 32(20), pp.7082–90.

Brázdil, M. et al., 2009. Directional functional coupling of cerebral rhythms between anterior cingulate and dorsolateral prefrontal areas during rare stimuli: A directed transfer function analysis of human depth EEG signal. *Human Brain Mapping*, 30(1), pp.138–146.

Bressler, S.L., 1995. Large-scale cortical networks and cognition. *Brain Research Reviews*, 20(3), pp.288–304.

Buzsáki, G., 2006. *Rhythms of the brain*, OXFORD UNIV PRESS INC.

Cantero, J.L. et al., 2009. Functional integrity of thalamocortical circuits differentiates normal aging from mild cognitive impairment. *Human Brain Mapping*, 30(12), pp.3944–3957.

Dai, Y. et al., 2012. Source connectivity analysis from MEG and its application to epilepsy source localization. *Brain topography*, 25(2), pp.157–66.

David, O. & Friston, K.J., 2003. A neural mass model for MEG/EEG: *NeuroImage*, 20(3), pp.1743–1755.

Fastenrath, M., Friston, K.J. & Kiebel, S.J., 2009. Dynamical causal modelling for M/EEG: spatial and temporal symmetry constraints. *NeuroImage*, 44(1), pp.154–63.

Felleman, D.J. & Van Essen, D.C., 1991. Distributed Hierarchical Processing in the Primate Cerebral Cortex. *Cerebral Cortex*, 1(1), pp.1–47.

Flinker, A. et al., 2015. Redefining the role of Broca's area in speech. *Proceedings of the National Academy of Sciences*, 112(9), p.201414491.

Friston, K.J. et al., 2012. DCM for complex-valued data: cross-spectra, coherence and phase-delays. *NeuroImage*, 59(1), pp.439–55.

Friston, K.J. et al., 2014. Granger causality revisited. *NeuroImage*, 101, pp.796–808.

Friston, K.J., Harrison, L. & Penny, W., 2003. Dynamic causal modelling. *NeuroImage*, 19(4), pp.1273–1302.

Garrido, M.I. et al., 2009. Dynamic causal modeling of the response to frequency deviants. *Journal of neurophysiology*, 101(5), pp.2620–31.

Garrido, M.I. et al., 2008. The functional anatomy of the MMN: a DCM study of the roving paradigm. *NeuroImage*, 42(2), pp.936–44.

Gómez-Herrero, G. et al., 2008. Measuring directional coupling between EEG sources. *NeuroImage*, 43(3), pp.497–508.

Granger, C.W.J., 1969. Investigating Causal Relations by Econometric Models and Cross-Spectral Methods. *Econometrica*, 37(3), pp.424–38.

Haufe, S. et al., 2013. A critical assessment of connectivity measures for EEG data: a simulation study. *NeuroImage*, 64, pp.120–33.

Haufe, S. et al., 2010. Modeling sparse connectivity between underlying brain sources for EEG/MEG. *IEEE transactions on bio-medical engineering*, 57(8), pp.1954–63.

Herz, D.M. et al., 2013. Dopamine Replacement Modulates Oscillatory Coupling Between Premotor and Motor Cortical Areas in Parkinson's Disease. *Cerebral cortex (New York, N.Y. : 1991)*, 24(11), pp.2873–2883.

Herz, D.M. et al., 2014. Levodopa reinstates connectivity from prefrontal to premotor cortex during externally paced movement in Parkinson's disease. *NeuroImage*, 90, pp.15–23.

Herz, D.M. et al., 2012. Task-specific modulation of effective connectivity during two simple unimanual motor tasks: a 122-channel EEG study. *NeuroImage*, 59(4), pp.3187–93.

Kaminski, M. & Blinowska, K.J., 2014. Directed Transfer Function is not influenced by volume conduction-inexpedient pre-processing should be avoided. *Frontiers in computational neuroscience*, 8, p.61.

Kamiński, M.J. & Blinowska, K.J., 1991. A new method of the description of the information flow in the brain structures. *Biological cybernetics*, 65(3), pp.203–10.

Kiebel, S.J. et al., 2009. Dynamic causal modeling for EEG and MEG. *Human brain mapping*, 30(6), pp.1866–76.

Kim, S.-J. et al., 2009. ℓ_1 Trend Filtering. *SIAM Review*, 51(2), pp.339–360.

Ku, S.-W. et al., 2011. Preferential inhibition of frontal-to-parietal feedback connectivity is a neurophysiologic correlate of general anesthesia in surgical patients. *PloS one*, 6(10), p.e25155.

Lee, U. et al., 2009. The directionality and functional organization of frontoparietal connectivity during consciousness and anesthesia in humans. *Consciousness and cognition*, 18(4), pp.1069–78.

Liang, H. et al., 2000. Causal influences in primate cerebral cortex during visual pattern discrimination. *Neuroreport*, 11(13), pp.2875–80.

Michel, C.M. et al., 2004. EEG source imaging. *Clinical neurophysiology : official journal of the International Federation of Clinical Neurophysiology*, 115(10), pp.2195–222.

Van Mierlo, P. et al., 2011. Accurate epileptogenic focus localization through time-variant functional connectivity analysis of intracranial electroencephalographic signals. *NeuroImage*, 56(3), pp.1122–33.

Van Mierlo, P. et al., 2013. Ictal-onset localization through connectivity analysis of intracranial EEG signals in patients with refractory epilepsy. *Epilepsia*, 54(8), pp.1409–18.

Moeller, S. et al., 2009. Functional connectivity of the macaque brain across stimulus and arousal states. *The Journal of neuroscience : the official journal of the Society for Neuroscience*, 29(18), pp.5897–909.

Moran, R., Pinotsis, D.A. & Friston, K., 2013. Neural masses and fields in dynamic causal modeling. *Frontiers in computational neuroscience*, 7, p.57.

Moran, R.J. et al., 2011. Dynamic causal models and physiological inference: a validation study using isoflurane anaesthesia in rodents. *PloS one*, 6(8), p.e22790.

Moran, R.J. et al., 2009. Dynamic causal models of steady-state responses. *NeuroImage*, 44(3), pp.796–811.

Moran, R.J. et al., 2015a. Losing control under ketamine: suppressed cortico-hippocampal drive following acute ketamine in rats. *Neuropsychopharmacology : official publication of the American College of Neuropsychopharmacology*, 40(2), pp.268–77.

Moran, R.J. et al., 2015b. Losing control under ketamine: suppressed cortico-hippocampal drive following acute ketamine in rats. *Neuropsychopharmacology : official publication of the American College of Neuropsychopharmacology*, 40(2), pp.268–77.

Nagasaka, Y., Shimoda, K. & Fujii, N., 2011. Multidimensional Recording (MDR) and Data Sharing : An Ecological Open Research and Educational Platform for Neuroscience. , 6(7).

Papadopoulou, M. et al., 2012. Mapping the epileptic brain with EEG dynamical connectivity: Established methods and novel approaches. *The European Physical Journal Plus*, 127(11), p.144.

Papadopoulou, M. et al., 2015. Tracking slow modulations in synaptic gain using dynamic causal modelling: validation in epilepsy. *NeuroImage*, 107, pp.117–26.

Pascual-Marqui, R.D., Michel, C.M. & Lehmann, D., 1994. Low resolution electromagnetic tomography: a new method for localizing electrical activity in the brain. *International Journal of Psychophysiology*, 18(1), pp.49–65.

Plomp, G. et al., 2014. The physiological plausibility of time-varying Granger-causal modeling: normalization and weighting by spectral power. *NeuroImage*, 97, pp.206–16.

Schoffelen, J.-M. & Gross, J., 2009. Source connectivity analysis with MEG and EEG. *Human brain mapping*, 30(6), pp.1857–65.

Shipp, S., Adams, R.A. & Friston, K.J., 2013. Reflections on agranular architecture: predictive coding in the motor cortex. *Trends in Neurosciences*, 36(12), pp.706–716.

Yanagawa, T. et al., 2013. Large-scale information flow in conscious and unconscious states: an ECoG study in monkeys. *PloS one*, 8(11), p.e80845.

Chapter 6
General Discussion

In this thesis we have investigated the modulations of various dynamical networks as a tool to understand brain function. We achieved that by using various data driven (autoregressive) and biologically inspired (DCM) models and by investigating both healthy and diseased brain networks in humans or animals (rats, monkeys).

In Chapter 2 we have analysed scalp and invasive iEEG data recorded from a patient with epilepsy. The fact that epileptic seizures are characterized by an increase in accumulated energy in specific frequency bands motivated us to use methods operating in the frequency domain able to reveal the direction of information flow (e.g. DTF, PDC) or not (e.g. coherence). We showed how by tracking the rank of the connectivity matrices, helps us to detect the transition to a more organized state and how such a spatiotemporal approach can be valuable for seizure detection and localisation.

In Chapters 3 and 4 we zoomed into the brain network and we focused on investigating which are the slow modulations in synaptic gain that they adequately explain the transition

from one state of the a network to another (e.g. pre-ictal to ictal). We have achieved this by using a biologically informed method, the dynamic causal modelling (DCM) and as convenient benchmark for our analysis we used again data recorded either from patients with epilepsy or from animals with induced seizures (rats). More specifically, in Chapter 3 we showed that changes in intrinsic (within-source) connectivity were sufficient to explain seizure onset and that these slow changes mediated a transient loss of excitatory-inhibitory balance. In Chapter 4 we adopted a similar policy but now applied on a rat model. Our main focus was again to investigate the pathophysiology of epilepsy shortly after lesion, in terms of physiologically plausible variables such as changes in synaptic efficacy. The methodological advance was involving a Bayesian update scheme in the inversions DCMs which allowed for updating schemes which were computationally less expensive in comparison to the standard inversion scheme used in Chapter 3. This work reflects only a small part on the questions one could ask when using DCM in this framework. One may be interested for example, what are the differences between the lesioned and perilesional hippocampi, are there systematic changes in pathophysiology over the weeks following lesion and is the pathophysiology restricted to the lesion site or is it more distributed? We aim to answer some of these questions in subsequent studies.

Furthermore, in both chapters (3 and 4) we stretched the importance of identifying plausible mechanisms at the synaptic level underlying brain state changes over a timescale of seconds (slow changes in synaptic efficacy). Extending this idea we think that it is important not only to pinpoint the mechanisms responsible for the brain state change, but also to know the exact number of latent variables which are necessary to explain seizure activity in a

physiologically plausible way. This allows us to build hierarchical dynamic causal models that are explicitly parameterised in terms of a small number of latent variables. In this direction our ongoing work involves the use of Bayesian model comparison (BMS) to compare models in which one or more mixtures of parameters are sufficient to explain the data.

This framework can be used beyond the epilepsy research, in studies of synaptic plasticity, in studies of short or long-term potentiation or associative learning etc.

In Chapter 5 our focus changed from what we discussed in Chapters 3 and 4. In this chapter we wanted to present a detailed comparison of two different methods to estimate effective connectivity from invasive and non-invasive electrophysiological data. The multimodal recordings used in this chapter were obtained from a macaque monkey under three different levels of consciousness – wakefulness, anesthesia and recovery. Our work addressed the assumption that effective connectivity between cortical areas as obtained from scalp EEG recordings corresponds to the 'true' connectivity between them. We test this by comparing the results obtained by scalp EEG data to the 'ground truth' as depicted from the reconstructed sources. We are confident that our results will help to further anchor connectivity measures in physiology.

Overall, we hope that our findings will not only provide relevant implications on how one can investigate the modulations of dynamical networks as a tool to understand brain function but that they will also lay the ground for future research.

Chapter 7
Nederlandstalige samenvatting

In de laatste tien jaar zijn concepten en methodieken die oorspronkelijk ontwikkeld werden binnen de informatietechnologie en wiskundige fysica in sterke mate toepasbaar geworden voor het modelleren en interpreteren van data afkomstig van neuro-imaging die gekenmerkt worden door complexe dynamieken en een hoge mate van connectiviteit. Wanneer men de relatie tussen de hersenanatomie en -functie bestudeert vanuit een netwerkperspectief, kan dit leiden tot fundamentele inzichten over de manier waarop eenvoudige elementen georganiseerd worden in dynamische patronen. Recente studies met betrekking tot functionele en structurele hersenconnectiviteit tonen aan dat specifieke eigenschappen van complexe hersennetwerken informatiesegregatie en –integratie tijdens intensieve cognitieve processen ondersteunen. Wijzigingen in deze netwerkeigenschappen die optreden tijdens de ontwikkeling, het verouderingsproces of ten gevolge van neurologische ziekten, hebben belangrijke klinische gevolgen. Daarnaast maakt het onderzoek van de paden en richting van informatiedoorstroming het mogelijk om een hiërarchische

organisatie af te leiden, zoals een top-down controle en een bottom-up aanpassing en dit op verschillende schalen in de hersenen. De laatste tien jaar zien we een systematische groei in het aantal studies rond complexe netwerken. We stellen vast dat de studie van complexe systemen vandaag een gevestigd paradigma geworden is. Waar vroeger de focus lag op het ontrafelen van de ingewikkelde topologische eigenschappen van complexe netwerken, concentreert men zich vandaag op de studie van de dynamische processen op temporele en ruimtelijke schalen en op de co-evolutie van netwerkstructuren en dynamische processen. Eén van de grote uitdagingen van vandaag bestaat erin de niet-triviale topologische organisatie van de hersenen op het structureel/anatomische en het functionele niveau te begrijpen. Naast de structurele connectiviteit, die kenmerkend is voor de witte stof-banen, gebruikt men verschillende andere methoden om hersenconnectiviteit op te sporen. Functionele connectiviteit infereert men meestal op basis van correlaties tussen neurale activiteit en definieert men als statistische afhankelijkheden tussen **externe** neurofysiologische gebeurtenissen. Een tweede familie van onderzoeksmethodieken focust op het blootleggen van de gerichte informatietransfer tussen de verschillende hersengebieden (effectieve connectiviteit). De laatste jaren zijn verschillende benaderingen voorgesteld, waaronder structurele vergelijkingsmodellen, dynamisch causale modellen, de Granger Causality of entropie-transfer. Uiteraard verschillen de netwerken die bekomen worden op basis van deze benaderingen intrinsiek van elkaar, zowel onderling als ten aanzien van de structurele netwerken. Daarnaast is er sprake van een sterke variabiliteit onder de proefpersonen en is de reproduceerbaarheid van de netwerkstructuur niet uitgebreid onderzocht. Om de informatie die we uit de beschikbare data kunnen halen met

betrekking tot de hersenfuncties te maximaliseren, is het belangrijk om zowel de verschillen tussen deze netwerken als de gemeenschappelijke kenmerken in detail te bestuderen. Dit alles in aanmerking genomen, is de belangrijkste doelstelling van deze thesis te onderzoeken hoe de aanpassing van dynamische netwerken een instrument kan zijn om tot een beter begrip te komen van de hersenfuncties. Binnen deze opzet is epilepsie, een chronische neurologische stoornis waarbij men geconfronteerd wordt met terugkerende aanvallen en waaraan 1% van de wereldbevolking lijdt, een geschikte benchmark en dit om twee redenen: het netwerkperspectief dat we hanteren om de hersenen te bestuderen en de wijzigingen binnen de dynamiek van dit netwerk. Tijdens een aanval zien we een abnormaal hoge neuronale activiteit in de hersenen. Dit abnormaal verschijnsel geeft aanleiding tot dynamieken die een invloed hebben op verschillende temporele en ruimtelijke schalen. Om de mechanismes te begrijpen die aan de basis liggen van deze dynamieken dienen we enerzijds de relaties tussen de elementen van de aanvallen te identificeren en dit binnen en over de verschillende schalen heen en anderzijds hun dynamisch repertoire te analyseren.

De thesis is als volgt opgebouwd:

In **Hoofdstuk 1** maakt de lezer kennis met de terminologie, de metingen en methoden die we doorheen de verschillende hoofdstukken gebruiken.

We beginnen met een korte beschrijving van de verschillende componenten van het menselijk brein, gaande van de kleinste deelcomponenten, met name de neuronen en hun fysiologie tot de verschillende grote corticale regio's. Vervolgens geven we een korte samenvatting van de meest

gebruikte technieken voor het bestuderen van hersenactiviteit en leggen daarbij de nadruk op elektrofysiologie en elektrofysiologische data (EEG). Deze thesis focust uitsluitend op deze twee technieken. We geven eveneens een beknopte beschrijving van de netwerken en hun eigenschappen en beschrijven hoe deze worden toegepast in de studie van het menselijk brein. Tot slot geven we een korte inleiding over de methoden die we in deze thesis hanteren om de dynamische connectiviteit in de hersenen op te sporen en te modelleren. Deze methoden brengen we onder in 2 groepen; de data-gestuurde of model-vrije methoden (voorbeeld: de 'directed transfer function' - DTF) en de model-gestuurde methoden (voorbeeld: dynamisch causale modellen – DCM).

Hoofdstuk 2 is opgedeeld in twee stukken. In het eerste deel vindt de lezer een beknopt overzicht van de belangrijkste methoden met betrekking tot functionele connectiviteit die in de literatuur gebruikt worden om de informatiedoorstroming in een aangetast hersennetwerk te bestuderen (zoals in het geval bij epilepsie).

Het tweede deel bevat onze toepassing van onze theorie op zowel invasieve als schedelhuid EEG-registraties van een patiënt met epilepsie. We beperken ons tot frequentiedomeinmetingen, zoals coherentie, directed transfer function, partial directed coherence. Onze belangrijkste doelstelling is deze instrumenten te gebruiken om de dynamische verbindingen tussen de hersenregio's te verkennen en een waardevolle vergelijking te maken tussen de verschillende gehanteerde instrumenten. Uiteindelijk willen we onderzoeken of deze instrumenten geschikt zijn om veranderingen op te sporen in de dynamieken en de informatiedoorstroming tijdens de overgang van de pre-ictale fase naar het begin van een epileptische aanval.

In **Hoofdstuk 3** willen we op synaptisch niveau de aanpassingen in een aangetast hersennetwerk onderzoeken en dit voor fenomenen die variëren op een schaal in seconden. Voor dit onderzoek gebruiken we een op biologie gebaseerde methode, met name de methode van het dynamisch-causaal modelleren (DCM). De basisprincipes van deze methode zijn uitgelegd in het inleidende Hoofdstuk 1. Onze belangrijkste doelstelling is het identificeren van synaptische sleutelparameters of verbindingen die aanleiding geven tot geobserveerde signalen. Hiervoor gebruiken we invasieve metingen van drie aanvallen van één epilepsiepatiënt. We focussen op een netwerk van twee oorzaken die twee regio's beslaan die van belang zijn.

In **Hoofdstuk 4** breiden we de studie die we in Hoofdstuk 3 voorstellen uit door de gebruikte methodieken verder te ontwikkelen. Door gebruik te maken van dynamisch causale modellen (DCM) kunnen we nu het Bayesiaans update-model toepassen. Dit laat ons toe een goed begrip te krijgen van hoe een neuronale variabele fluctueert binnen verschillende tijdsschalen. Voor deze studie gebruiken we 'local field potentials' (LFPs) die opgetekend zijn bij drie ratten waarbij epileptische aanvallen zijn uitgelokt. Het doel is om de pathofysiologie van het begin van een aanval - kort na de laesie - te beschrijven en dit in termen van fysiologisch plausibele variabelen, zoals wijzigingen in de synaptische doeltreffendheid en de snelheidsconstante. Door gebruik te maken van het Bayesiaans vergelijkingsmodel onderzoeken we of de parametrische wijzigingen beperkt blijven tot de intrinsieke connectiviteit tussen de neuronale populaties (en hun tijdsconstante), de spectrale vorm van de endogene (afferente) neuronale input, of een weerslag hebben op beide.

In **Hoofdstuk 5** vergelijken we DTF-metingen en metingen van de effectieve connectiviteit (DCM-metingen) die gebaseerd zijn op (invasieve) elektrocortiografische (ECoG) activiteit met gereconstrueerde reacties op dezelfde locaties die gebaseerd zijn op gelijktijdige (niet-invasieve) schedelhuid-data (EEG). Deze multimodale data zijn het resultaat van testen die in drie verschillende omstandigheden uitgevoerd werden op een makaak, met name in rust, onder verdoving en tijdens het herstelproces. Onze doelstelling is tweeledig. In eerste instantie leggen we de connectiviteitsstructuur vast tussen twee oorzaken die van belang zijn – een frontale en pariëtale oorzaak – en onderzoeken hoe de combinatie van beiden wijzigt onder veranderende omstandigheden. In tweede instantie evalueren we de consistentie van de connectiviteitsresultaten en dit op basis van een analyse van bronnen afgeleid uit invasieve data (128 geïmplanteerde ECoG-bronnen) en van bronactiviteit zoals gereconstrueerd op basis van schedelhuid-registraties (19 EEG-sensoren).

Tot slot vatten we in **Hoofdstuk 6** de bevindingen uit de verschillende hoofdstukken samen en bespreken we de implicaties ervan voor toekomstig onderzoek.

% Data Storage Fact Sheet

% Name/identifier study Brain mapping of an epileptic brain using EEG functional and effective connectivity
% Author: Margarita Papadopoulou, Marco Leite, Alfred Meurs, Evelien Carrette, Robrecht Raedt, Kristl Vonck, Paul Boon and Daniele Marinazzo
% Date: 2012

1. Contact details
==========

1a. Main researcher

- name: Margarita Papadopoulou
- address: Department of Data Analysis, 1 Henri Dunantlaan. B 9000 Gent
- e-mail: margarita.papadopoulou@ugent.be

1b. Responsible Staff Member (ZAP)

- name: Daniele Marinazzo
- address: Department of Data Analysis, 1, Henri Dunantlaan. B 9000 Gent
- e-mail: daniele.marinazzo@ugent.be

If a response is not received when using the above contact details, please send an email to data.pp@ugent.be or contact Data Management, Faculty of Psychology and Educational Sciences, Henri Dunantlaan 2, 9000 Ghent, Belgium.

2. Information about the datasets to which this sheet applies
==========
* Reference of the publication in which the datasets are reported:

* Which datasets in that publication does this sheet apply to?:

3. Information about the files that have been stored
==========

3a. Raw data
---

* Have the raw data been stored by the main researcher? [X] YES / [ ] NO
If NO, please justify:

* On which platform are the raw data stored?
  - [X] researcher PC
  - [ ] research group file server
  - [ ] other (specify): ...

* Who has direct access to the raw data (i.e., without intervention of another person)?
  - [X] main researcher
  - [X] responsible ZAP
  - [ ] all members of the research group
  - [ ] all members of UGent
  - [X] other (specify): Owners of the data: laboratory of clinical and experimental neurophysiology http://www.ugent.be/ge/inwgen/en/research/neurology/lcen.htm

3b. Other files
---

* Which other files have been stored?
  - [X] file(s) describing the transition from raw data to reported results. Specify: ...
  - [X] file(s) containing processed data. Data after cleaning, bipolar montage and divided in the relevant segments used for the analyses.
  - [X] file(s) containing analyses. Specify: in-house software and public toolboxes
  - [X] files(s) containing information about informed consent (at LCEN)
  - [X] a file specifying legal and ethical provisions (at LCEN)
  - [ ] file(s) that describe the content of the stored files and how this content should be interpreted. Specify: ...
  - [ ] other files. Specify: ...

* On which platform are these other files stored?
  - [X] individual PC
  - [ ] research group file server
  - [X] other: PCs and archives of LCEN members (data owners)

* Who has direct access to these other files (i.e., without intervention of another person)?
  - [X] main researcher
  - [X] responsible ZAP
  - [ ] all members of the research group
  - [ ] all members of UGent
  - [ ] other (specify): ...

4. Reproduction
===
* Have the results been reproduced independently?: [ ] YES / [X] NO

* If yes, by whom (add if multiple):
   - name:
   - address:
   - affiliation:
   - e-mail:

v0.2

% Data Storage Fact Sheet

% Name/identifier study Mapping the epileptic brain with EEG dynamical connectivity: established methods and novel approaches
% Author:Margarita Papadopoulou, Kristl Vonck, Paul Boon and Daniele Marinazzo
% Date: 2012

1. Contact details
==========

1a. Main researcher

- name: Margarita Papadopoulou
- address: Department of Data Analysis, 1 Henri Dunantlaan. B 9000 Gent
- e-mail: margarita.papadopoulou@ugent.be

1b. Responsible Staff Member (ZAP)

- name: Daniele Marinazzo
- address: Department of Data Analysis, 1, Henri Dunantlaan. B 9000 Gent
- e-mail: daniele.marinazzo@ugent.be

If a response is not received when using the above contact details, please send an email to data.pp@ugent.be or contact Data Management, Faculty of Psychology and Educational Sciences, Henri Dunantlaan 2, 9000 Ghent, Belgium.

2. Information about the datasets to which this sheet applies
==========
* Reference of the publication in which the datasets are reported:

* Which datasets in that publication does this sheet apply to?:

3. Information about the files that have been stored
==========

3a. Raw data
---

* Have the raw data been stored by the main researcher? [X] YES / [ ] NO
If NO, please justify:

* On which platform are the raw data stored?
 - [X] researcher PC
 - [ ] research group file server
 - [ ] other (specify): ...

* Who has direct access to the raw data (i.e., without intervention of another person)?
 - [X] main researcher
 - [X] responsible ZAP
 - [ ] all members of the research group
 - [ ] all members of UGent
 - [X] other (specify): Owners of the data: laboratory of clinical and experimental neurophysiology http://www.ugent.be/ge/inwgen/en/research/neurology/lcen.htm

3b. Other files
---

* Which other files have been stored?
 - [X] file(s) describing the transition from raw data to reported results. Specify: ...
 - [X] file(s) containing processed data. Data after cleaning, bipolar montage and divided in the relevant segments used for the analyses.
 - [X] file(s) containing analyses. Specify: in-house software and public toolboxes
 - [X] files(s) containing information about informed consent (at LCEN)
 - [X] a file specifying legal and ethical provisions (at LCEN)
 - [ ] file(s) that describe the content of the stored files and how this content should be interpreted. Specify: ...
 - [ ] other files. Specify: ...

* On which platform are these other files stored?
 - [X] individual PC
 - [ ] research group file server
 - [X] other: PCs and archives of LCEN members (data owners)

* Who has direct access to these other files (i.e., without intervention of another person)?
 - [X] main researcher
 - [X] responsible ZAP
 - [ ] all members of the research group
 - [ ] all members of UGent
 - [ ] other (specify): ...

4. Reproduction
==
* Have the results been reproduced independently?: [ ] YES / [X] NO

* If yes, by whom (add if multiple):
  - name:
  - address:
  - affiliation:
  - e-mail:

v0.2

% Data Storage Fact Sheet

% Name/identifier study Tracking slow modulations in synaptic gain using Dynamic Causal Modelling: Validation in epilepsy
% Author: Margarita Papadopoulou, Marco Leite, Pieter van Mierlo, Kristl Vonck, Louis Lemieux, Karl Friston and Daniele Marinazzo
% Date: 2015

1. Contact details
==========

1a. Main researcher

- name: Margarita Papadopoulou
- address: Department of Data Analysis, 1 Henri Dunantlaan. B 9000 Gent
- e-mail: margarita.papadopoulou@ugent.be

1b. Responsible Staff Member (ZAP)

- name: Daniele Marinazzo
- address: Department of Data Analysis, 1, Henri Dunantlaan. B 9000 Gent
- e-mail: daniele.marinazzo@ugent.be

If a response is not received when using the above contact details, please send an email to data.pp@ugent.be or contact Data Management, Faculty of Psychology and Educational Sciences, Henri Dunantlaan 2, 9000 Ghent, Belgium.

2. Information about the datasets to which this sheet applies
==========
* Reference of the publication in which the datasets are reported:

* Which datasets in that publication does this sheet apply to?:

3. Information about the files that have been stored
==========

3a. Raw data
---

* Have the raw data been stored by the main researcher? [X] YES / [ ] NO
If NO, please justify:

* On which platform are the raw data stored?
  - [X] researcher PC
  - [ ] research group file server
  - [ ] other (specify): ...

* Who has direct access to the raw data (i.e., without intervention of another person)?
  - [X] main researcher
  - [X] responsible ZAP
  - [ ] all members of the research group
  - [ ] all members of UGent
  - [X] other (specify): Owners of the data: laboratory of clinical and experimental neurophysiology http://www.ugent.be/ge/inwgen/en/research/neurology/lcen.htm

3b. Other files

---

* Which other files have been stored?
 - [X] file(s) describing the transition from raw data to reported results. Specify: ...
 - [X] file(s) containing processed data. Data after cleaning, bipolar montage and divided in the relevant segments used for the analyses.
 - [X] file(s) containing analyses. Specify: in-house software and public toolboxes
 - [X] files(s) containing information about informed consent (at LCEN)
 - [X] a file specifying legal and ethical provisions (at LCEN)
 - [ ] file(s) that describe the content of the stored files and how this content should be interpreted. Specify: ...
 - [ ] other files. Specify: ...

* On which platform are these other files stored?
 - [X] individual PC
 - [ ] research group file server
 - [X] other: PCs and archives of LCEN members (data owners)

* Who has direct access to these other files (i.e., without intervention of another person)?
 - [X] main researcher
 - [X] responsible ZAP
 - [ ] all members of the research group
 - [ ] all members of UGent
 - [ ] other (specify): ...

4. Reproduction
==========
* Have the results been reproduced independently?: [ ] YES / [X] NO

* If yes, by whom (add if multiple):
  - name:
  - address:
  - affiliation:
  - e-mail:

v0.2